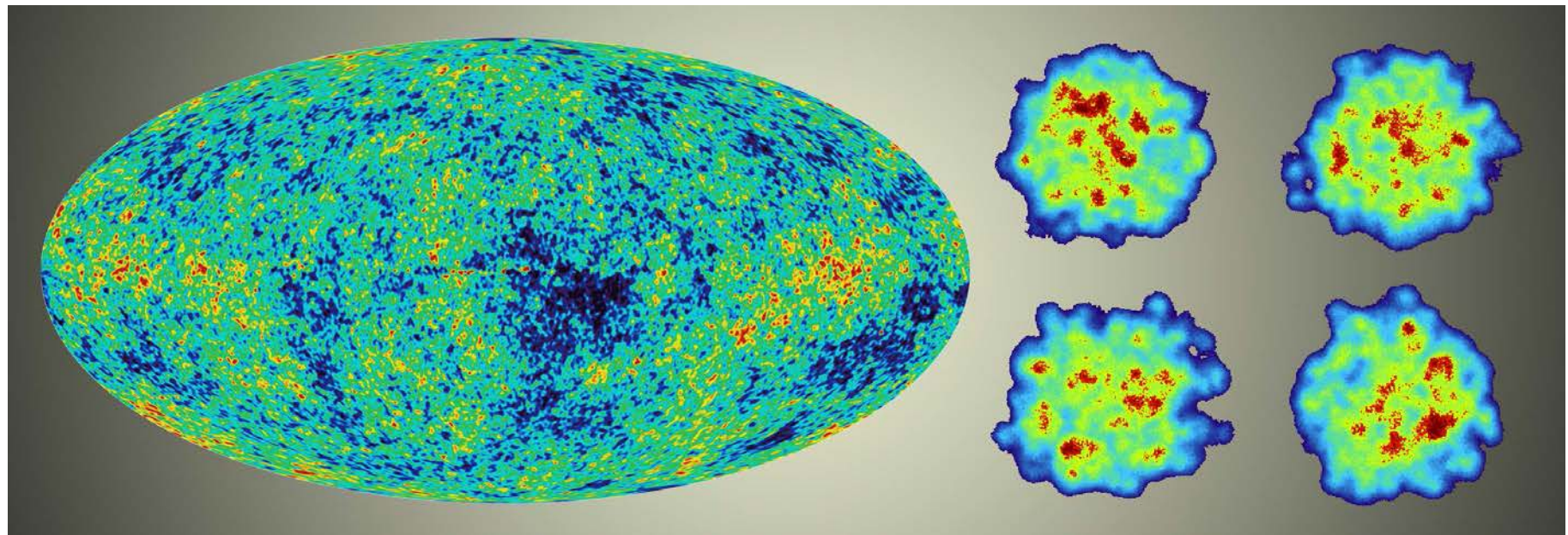
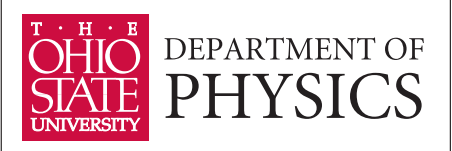


The Little Bang Standard Model*

Ulrich Heinz (The Ohio State University)



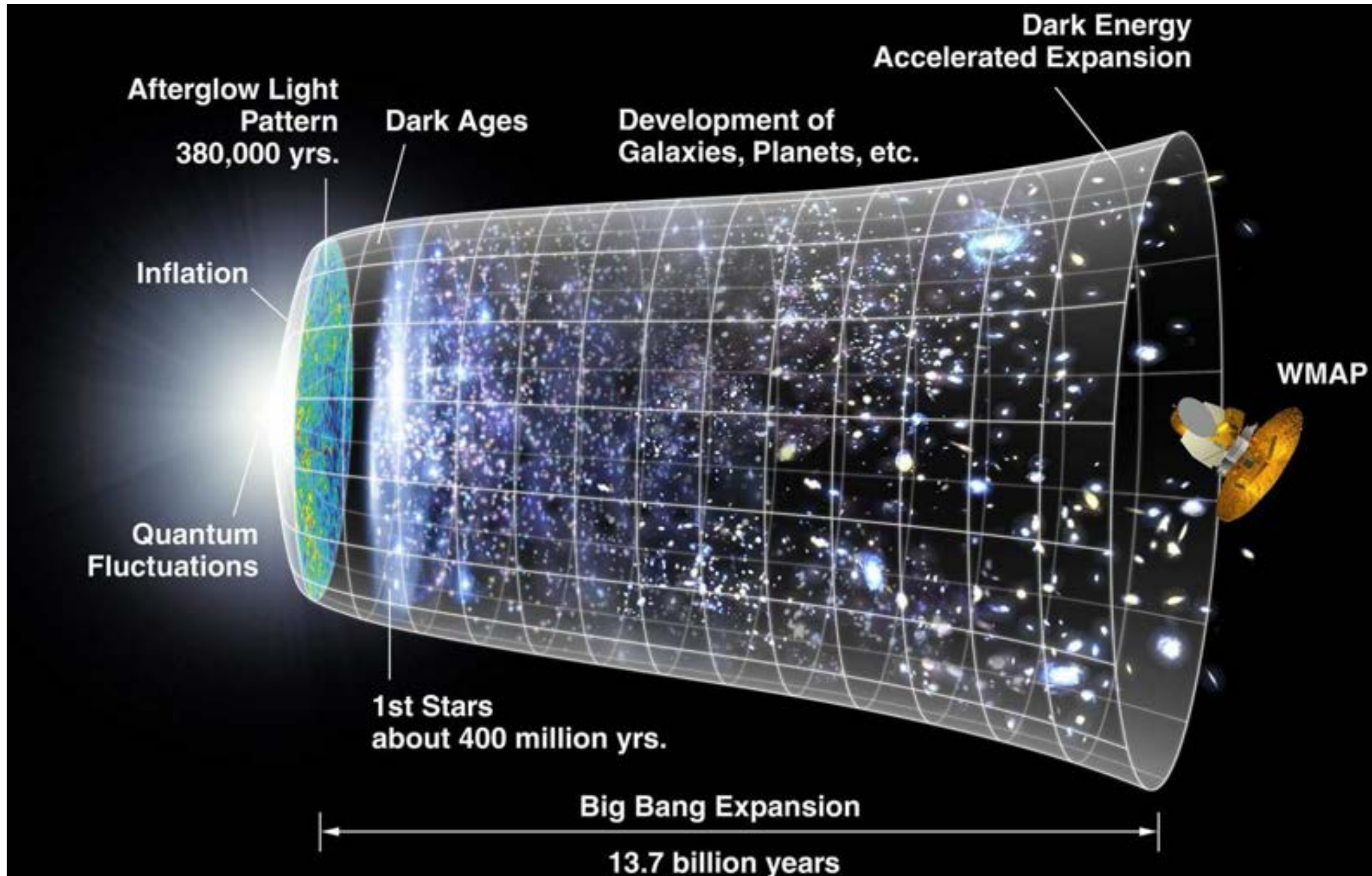
Kavli Institute for the Physics and Mathematics of the Universe
University of Tokyo, 13 December 2013



*Supported by the U.S. Department of Energy

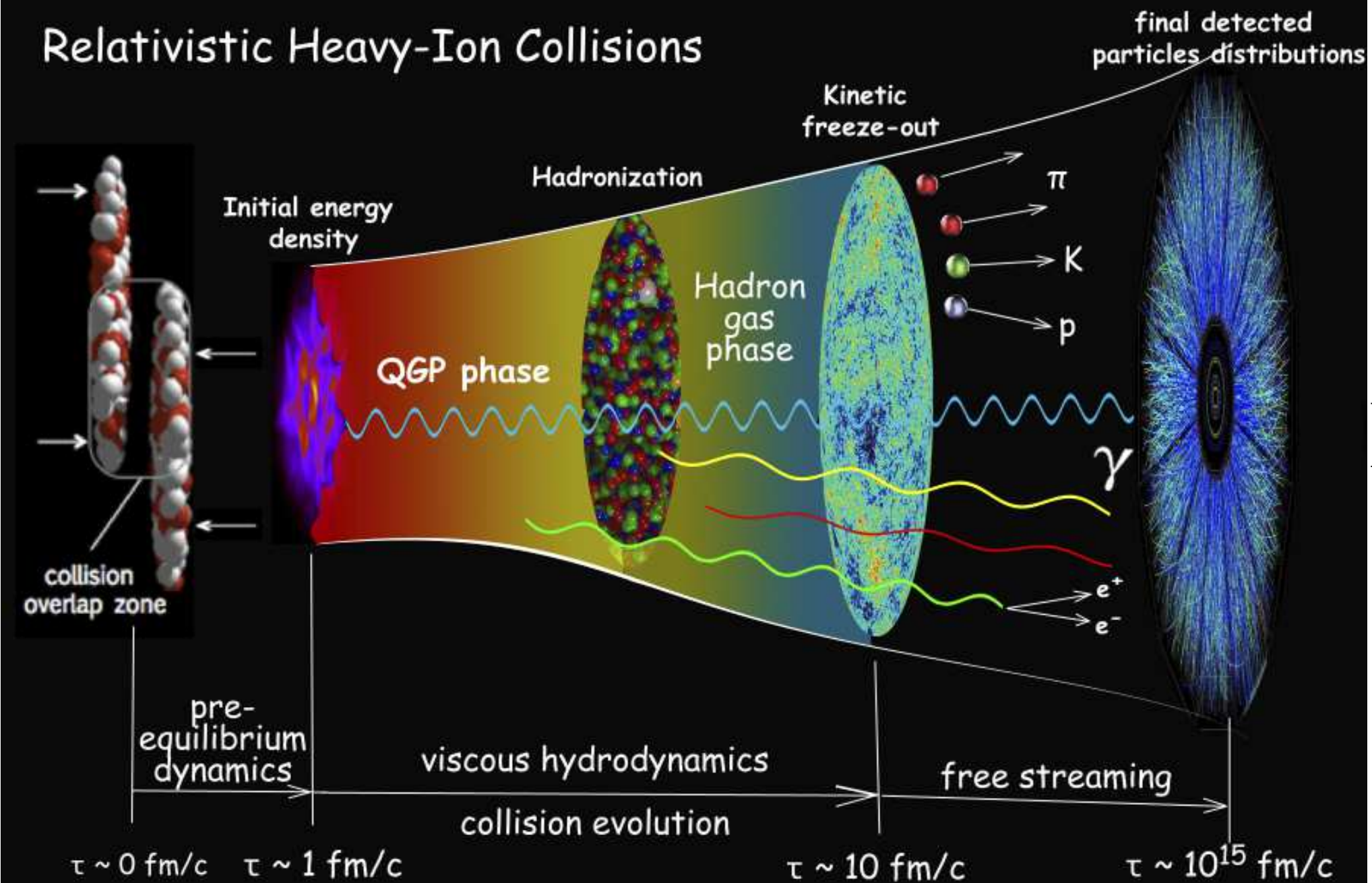


The Big Bang

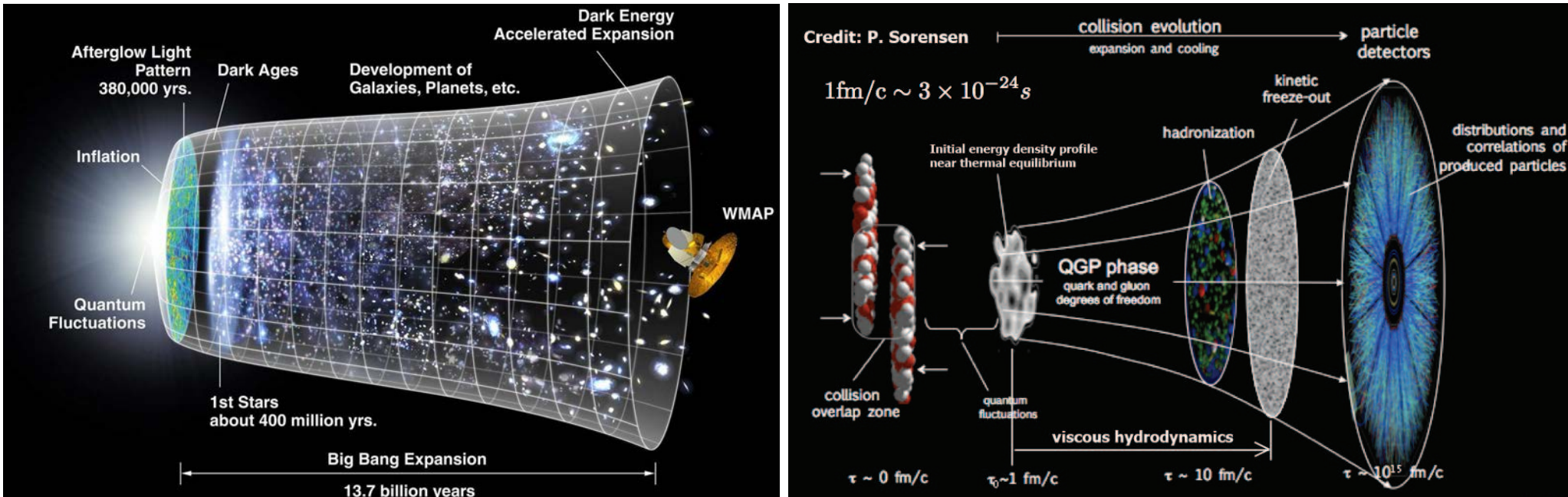


The Little Bang

Relativistic Heavy-Ion Collisions



Big Bang vs. Little Bang

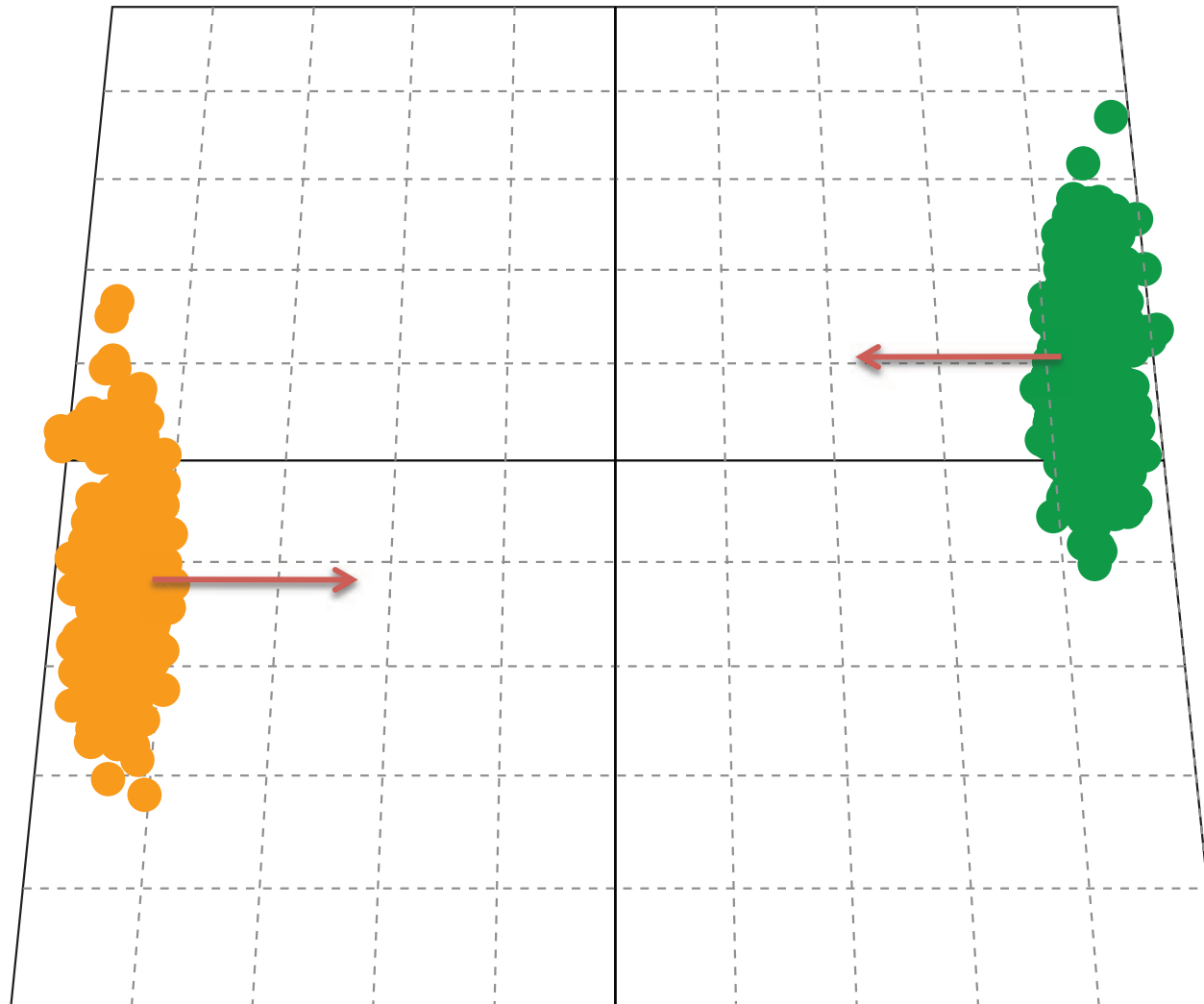


Similarities: Hubble-like expansion, expansion-driven dynamical freeze-out
 chemical freeze-out (nucleo-/hadrosynthesis) before thermal freeze-out (CMB, hadron p_T -spectra)
 initial-state quantum fluctuations imprinted on final state

Differences: Expansion rates differ by 18 orders of magnitude
 Expansion in 3d, not 4d; driven by pressure gradients, not gravity
 Time scales measured in fm/c rather than billions of years
 Distances measured in fm rather than light years
 “Heavy-Ion Standard Model” still under construction \implies **this talk**

Relativistic Nucleus-Nucleus Collisions

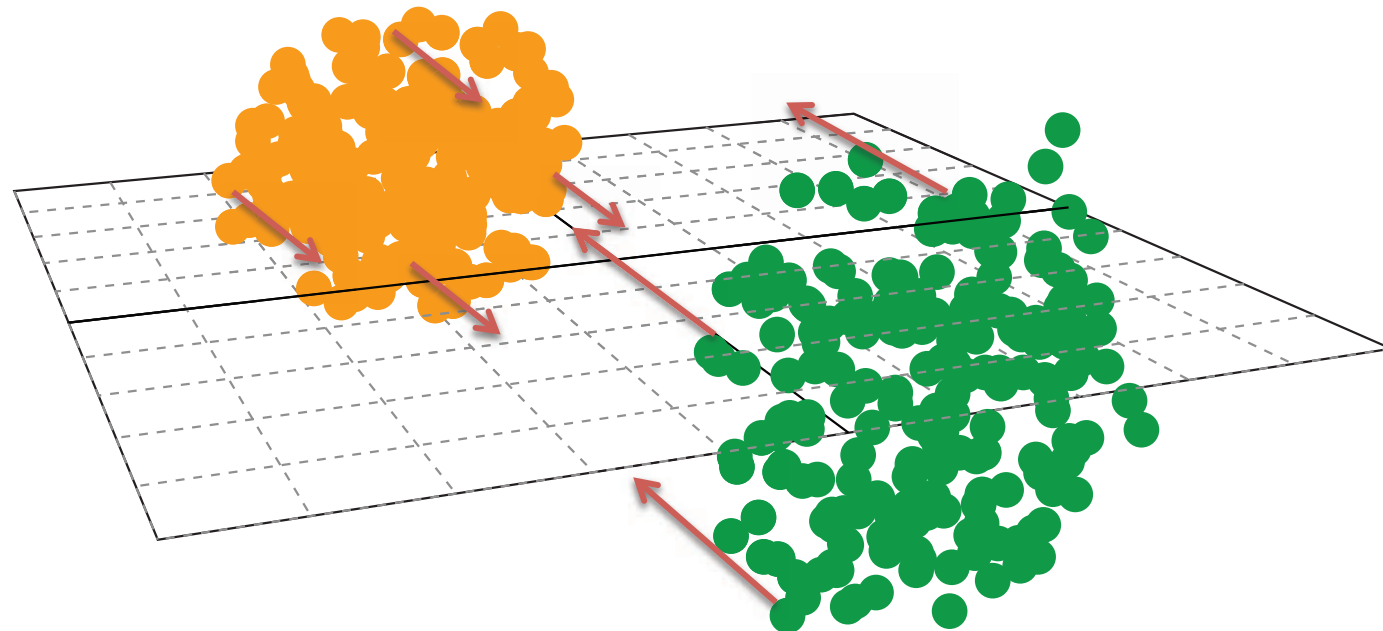
Animation: P. Sorensen



Collision of two Lorentz contracted gold nuclei

Relativistic Nucleus-Nucleus Collisions

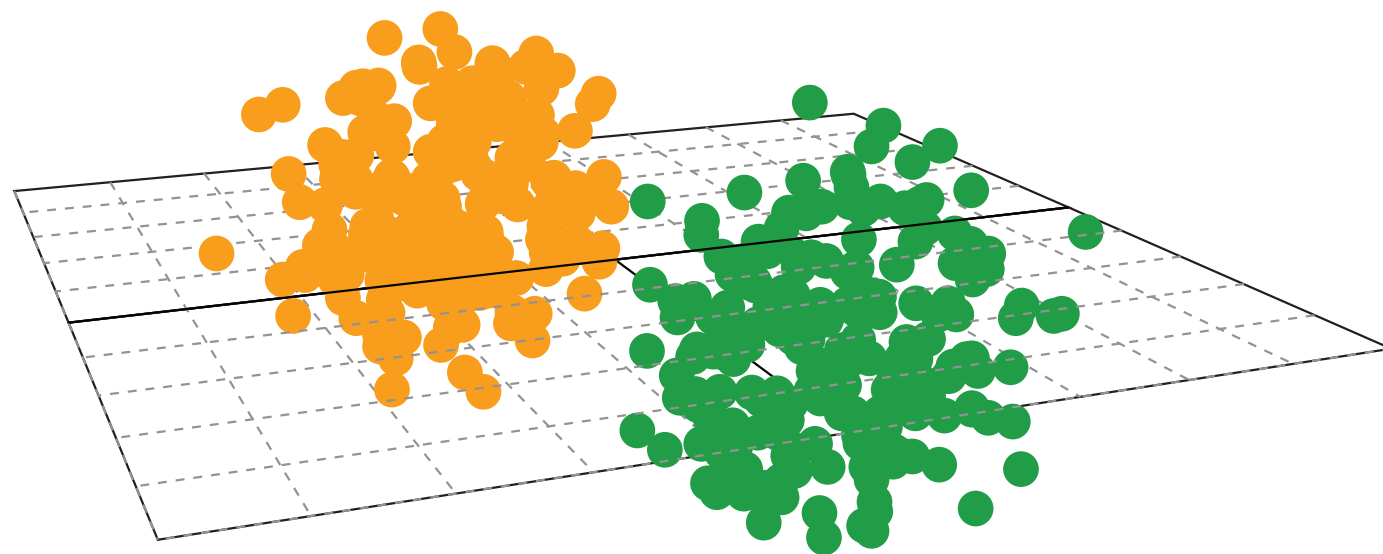
Animation: P. Sorensen



Collision of two Lorentz contracted gold nuclei

Relativistic Nucleus-Nucleus Collisions

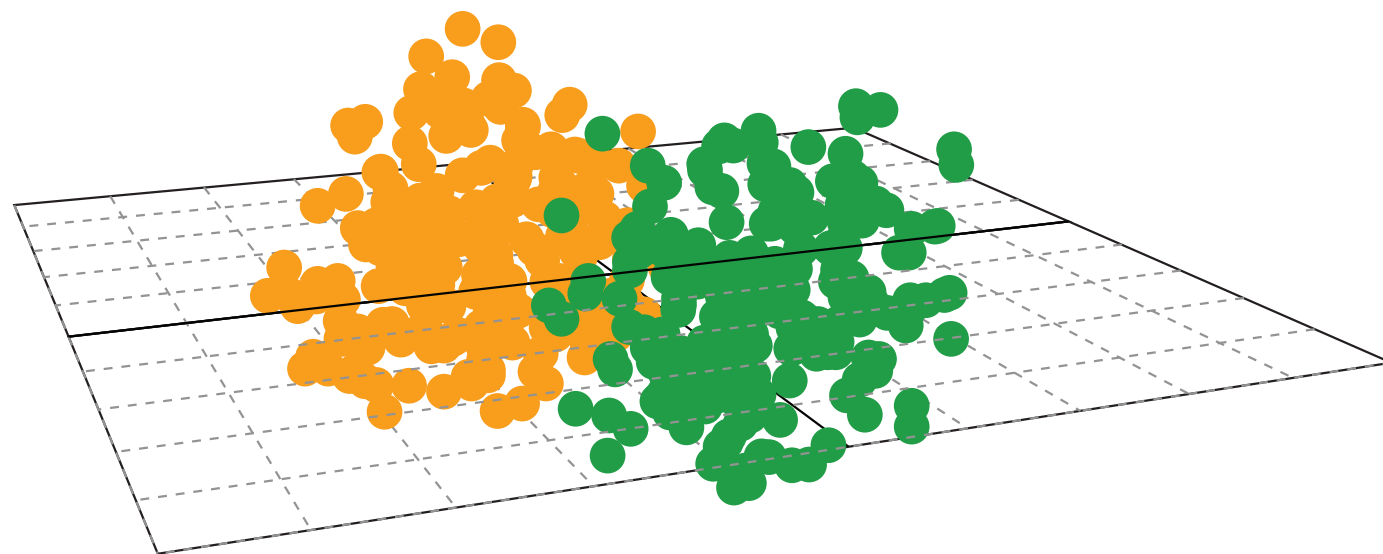
Animation: P. Sorensen



Collision of two Lorentz contracted gold nuclei

Relativistic Nucleus-Nucleus Collisions

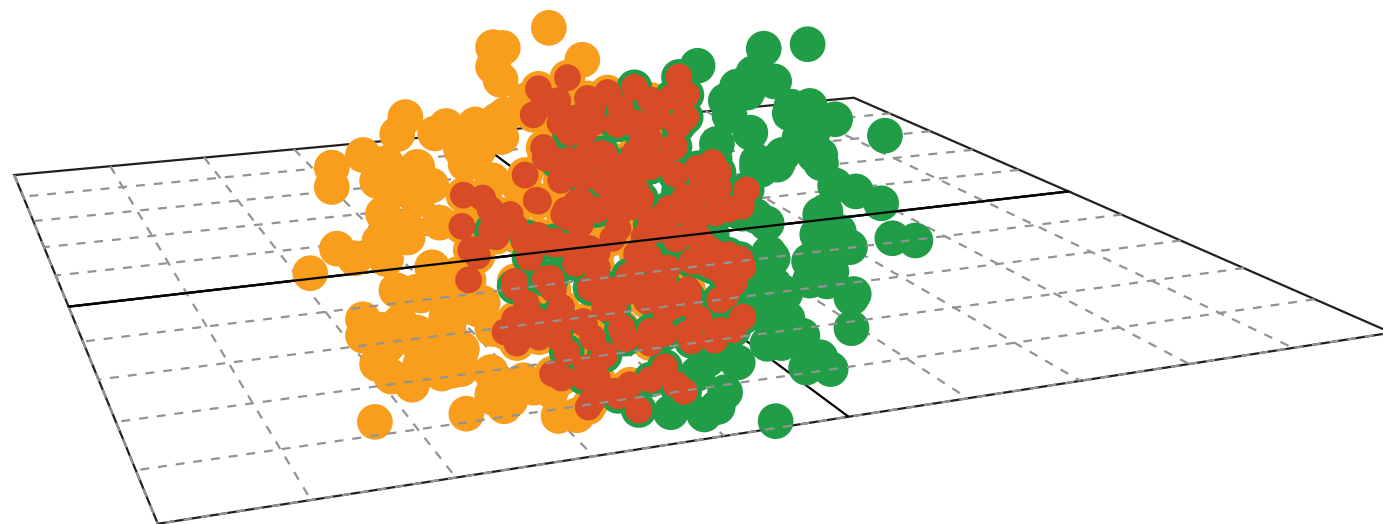
Animation: P. Sorensen



Collision of two Lorentz contracted gold nuclei

Relativistic Nucleus-Nucleus Collisions

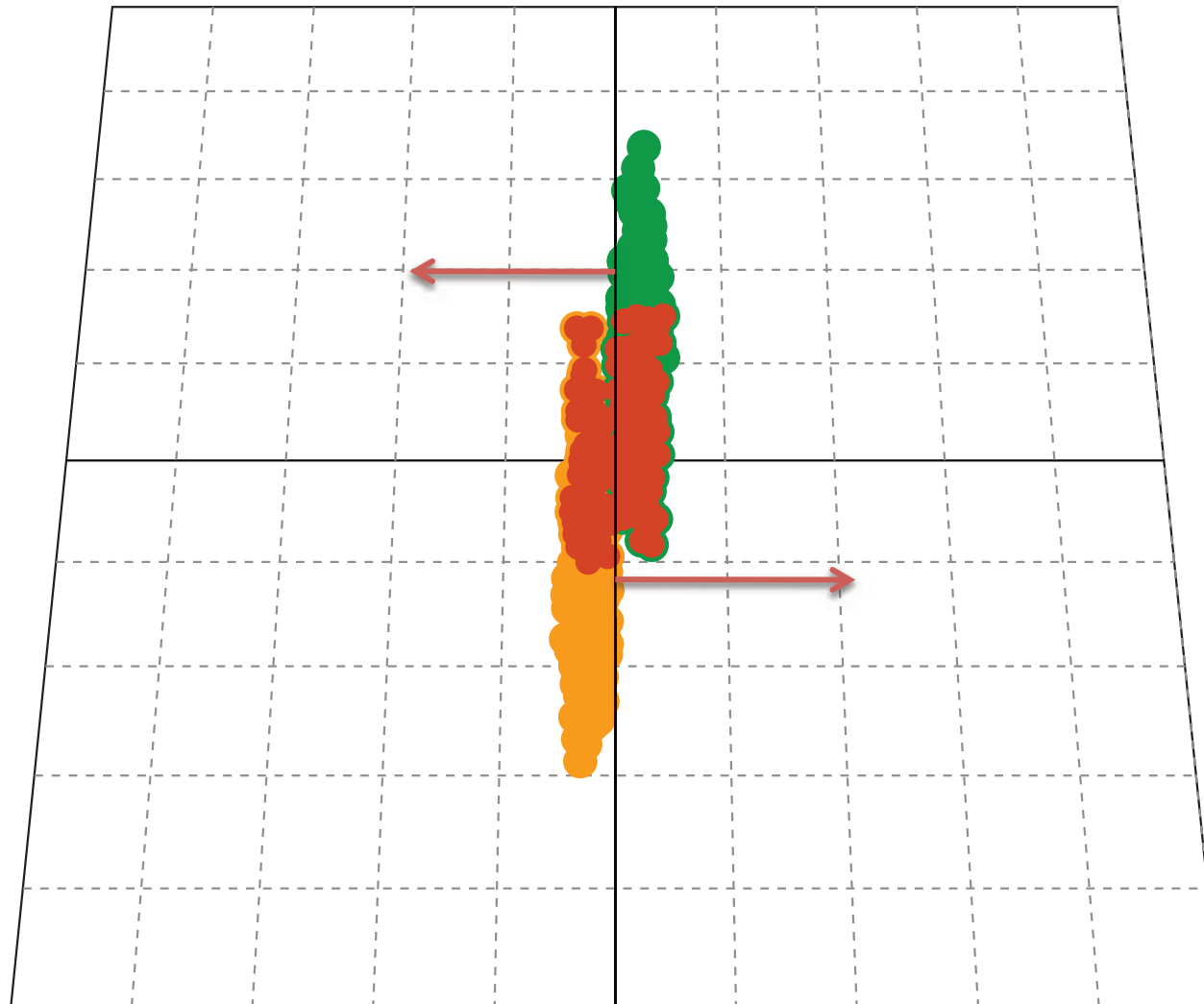
Animation: P. Sorensen



Collision of two Lorentz contracted gold nuclei

Relativistic Nucleus-Nucleus Collisions

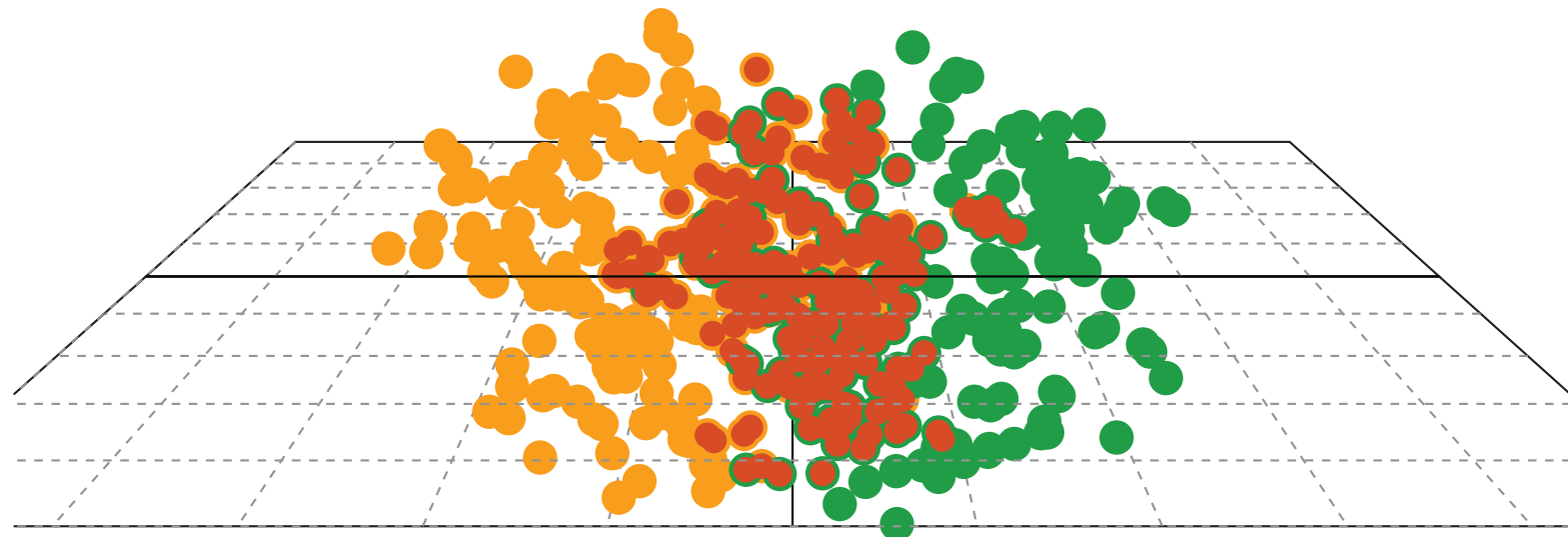
Animation: P. Sorensen



Collision of two Lorentz contracted gold nuclei

Relativistic Nucleus-Nucleus Collisions

Animation: P. Sorensen

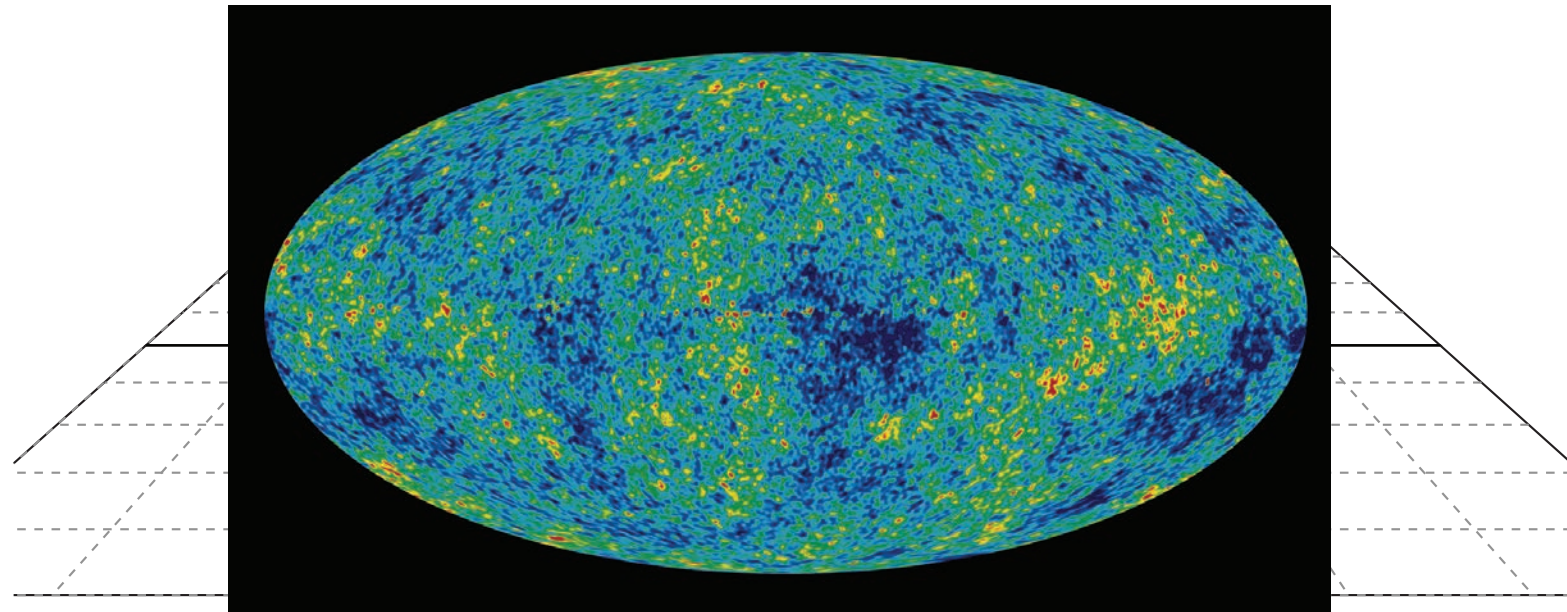


Produced fireball is $\sim 10^{-14}$ meters across
and lives for $\sim 5 \times 10^{-23}$ seconds

Collision of two Lorentz contracted gold nuclei

Relativistic Nucleus-Nucleus Collisions

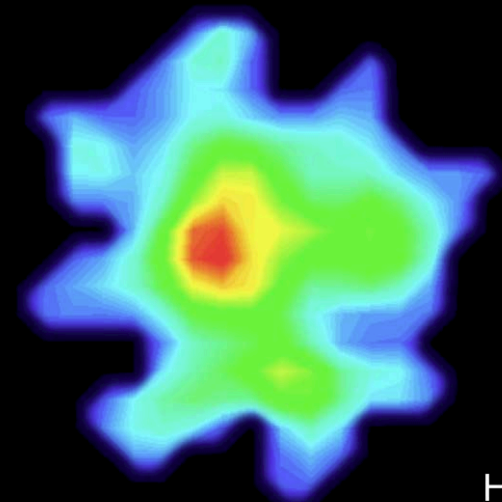
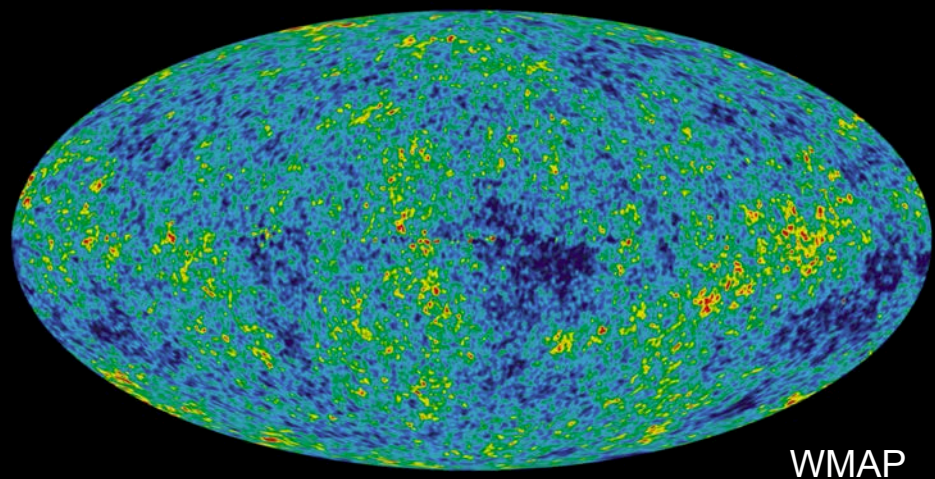
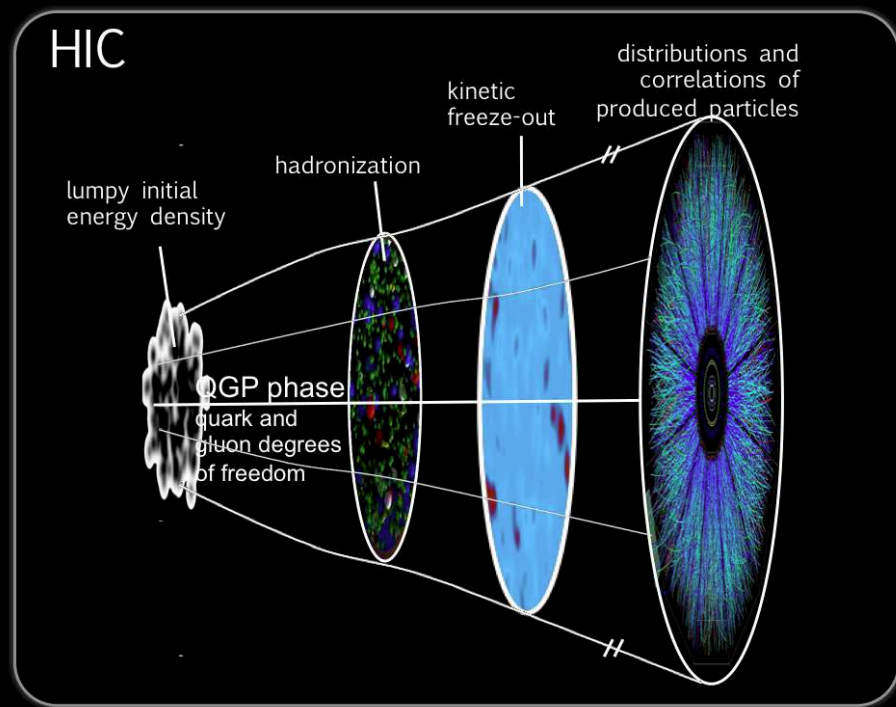
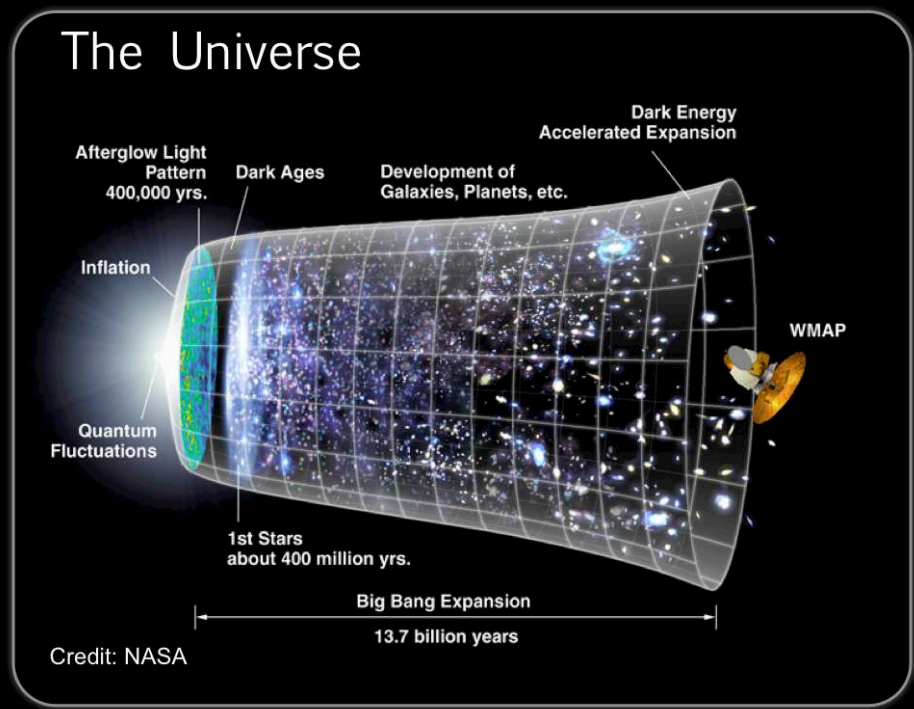
Animation: P. Sorensen



Produced fireball is $\sim 10^{-14}$ meters across
and lives for $\sim 5 \times 10^{-23}$ seconds

Collision of two Lorentz contracted gold nuclei

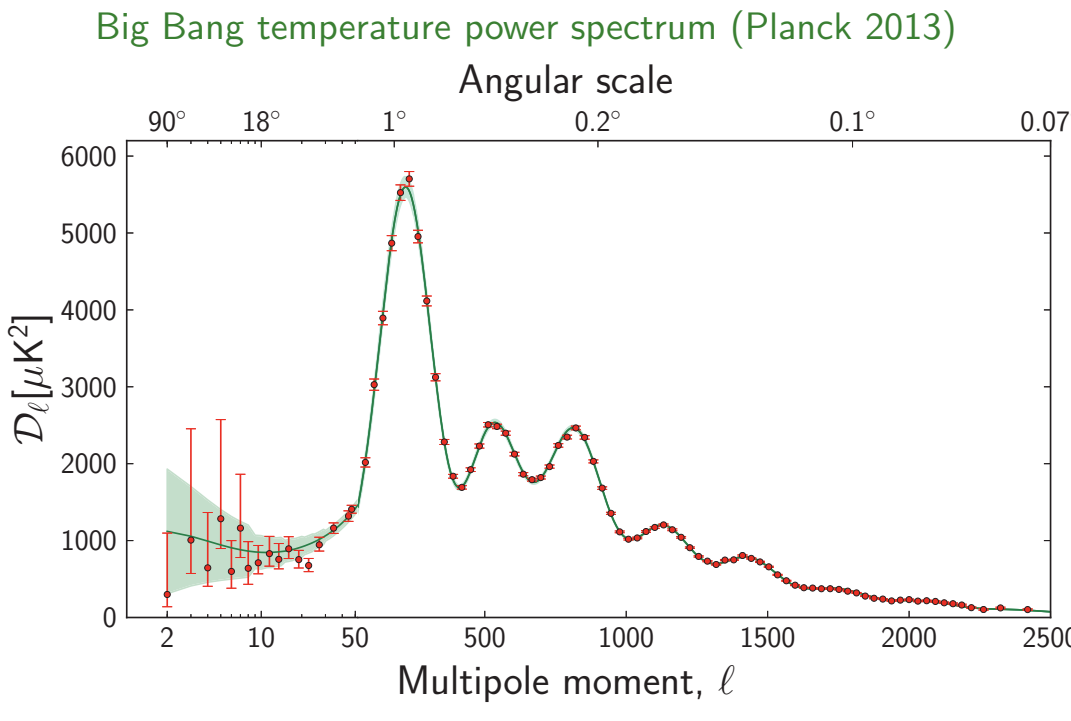
The Big Bang vs the Little Bangs



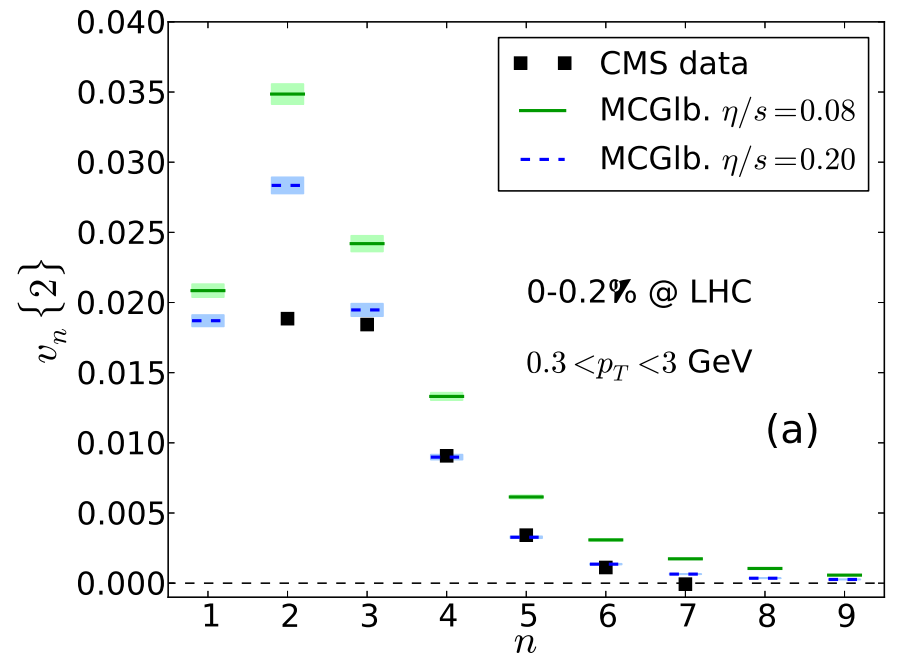
Big vs. Little Bang: The fluctuation power spectrum

Mishra, Mohapatra, Saumia, Srivastava, PRC77 (2008) 064902 and C81 (2010) 034903

Mocsy & Sorensen, NPA855 (2011) 241, PLB705 (2011) 71



Flow power spectrum for ultracentral PbPb Little Bangs
(Data: CMS, Quark Matter 2012; Theory: OSU 2013)



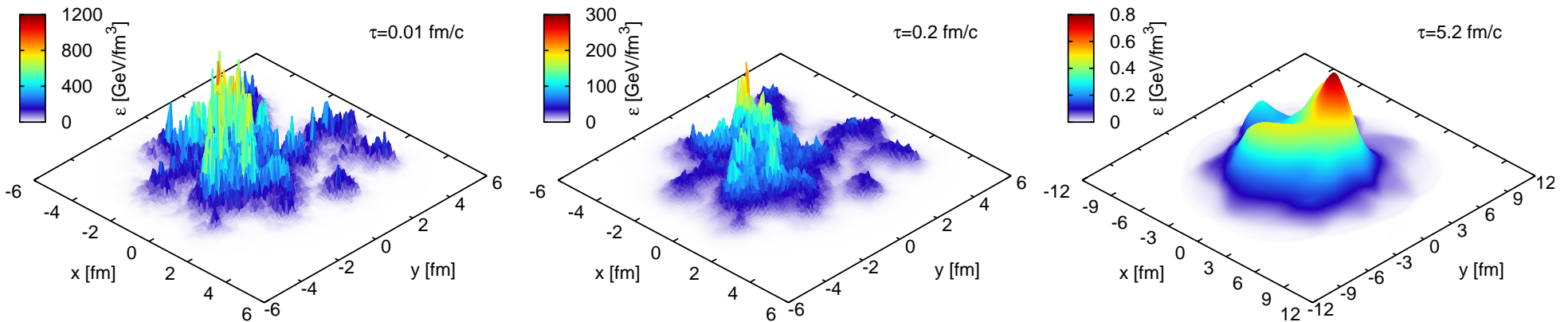
Higher flow harmonics get suppressed by shear viscosity

A detailed study of fluctuations is a powerful discriminator between models!

Each Little Bang evolves differently!

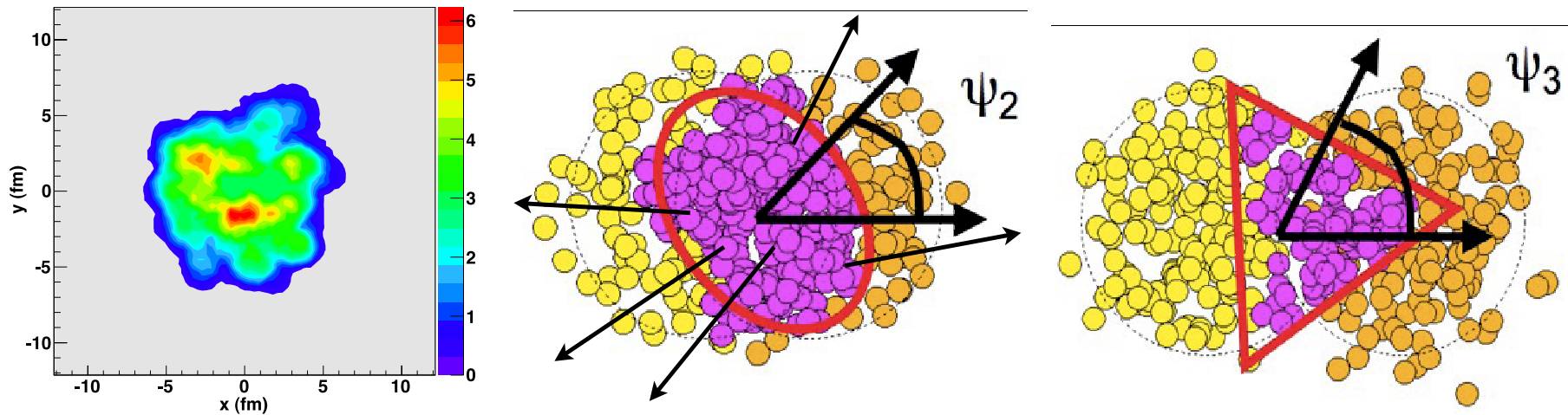
Density evolution of a single $b = 8$ fm Au+Au collision at RHIC, with IP-Gasma initial conditions, Gasma evolution to $\tau = 0.2$ fm/c followed by (3+1)-d viscous hydrodynamic evolution with MUSIC using $\eta/s = 0.12 = 1.5/(4\pi)$

Schenke, Tribedy, Venugopalan, PRL 108 (2012) 252301:



Event-by-event shape and flow fluctuations rule!

(Alver and Roland, PRC81 (2010) 054905)



- Each event has a different initial shape and density distribution, characterized by different set of harmonic eccentricity coefficients ε_n
- Each event develops its individual hydrodynamic flow, characterized by a set of harmonic flow coefficients v_n and flow angles ψ_n
- At small impact parameters fluctuations (“hot spots”) dominate over geometric overlap effects
(Alver & Roland, PRC81 (2010) 054905; Qin, Petersen, Bass, Müller, PRC82 (2010) 064903)

How anisotropic flow is measured:

Definition of flow coefficients:

$$\frac{dN^{(i)}}{dy p_T dp_T d\phi_p}(b) = \frac{dN^{(i)}}{dy p_T dp_T}(b) \left(1 + 2 \sum_{n=1}^{\infty} v_n^{(i)}(y, p_T; b) \cos(n(\phi_p - \Psi_n^{(i)})) \right).$$

Define event average $\{\dots\}$, ensemble average $\langle\dots\rangle$

Flow coefficients v_n typically extracted from azimuthal correlations (k -particle cumulants). E.g. $k = 2, 4$:

$$c_n\{2\} = \langle \{e^{ni(\phi_1-\phi_2)}\} \rangle = \langle \{e^{ni(\phi_1-\psi_n)}\} \{e^{-ni(\phi_2-\psi_n)}\} + \delta_2 \rangle = \langle v_n^2 + \delta_2 \rangle$$
$$c_n\{4\} = \langle \{e^{ni(\phi_1+\phi_2-\phi_3-\phi_4)}\} \rangle - 2\langle \{e^{ni(\phi_1-\phi_2)}\} \rangle = \langle -v_n^4 + \delta_4 \rangle$$

v_n is correlated with the event plane while δ_n is not (“non-flow”). $\delta_2 \sim 1/M$, $\delta_4 \sim 1/M^3$.
4th-order cumulant is free of 2-particle non-flow correlations.

These measures are affected by event-by-event flow fluctuations:

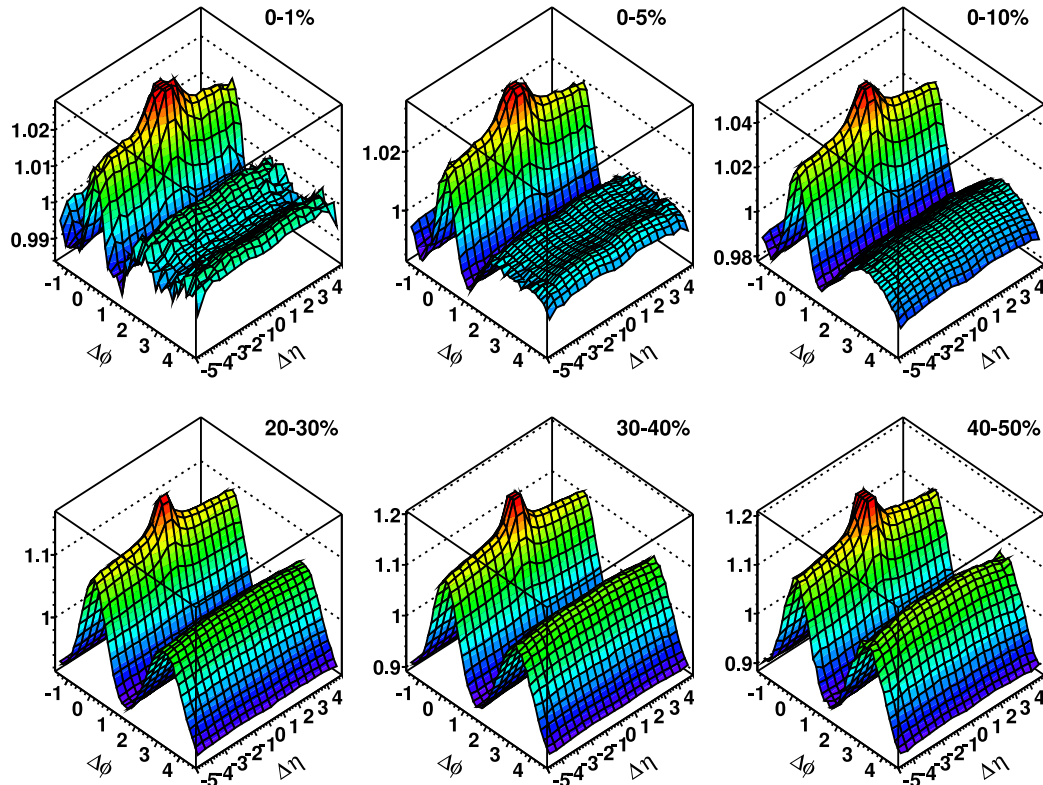
$$\langle v_2^2 \rangle = \langle v_2 \rangle^2 + \sigma^2, \quad \langle v_2^4 \rangle = \langle v_2 \rangle^4 + 6\sigma^2 \langle v_2 \rangle^2$$

$v_n\{k\}$ denotes the value of v_n extracted from the k^{th} -order cumulant:

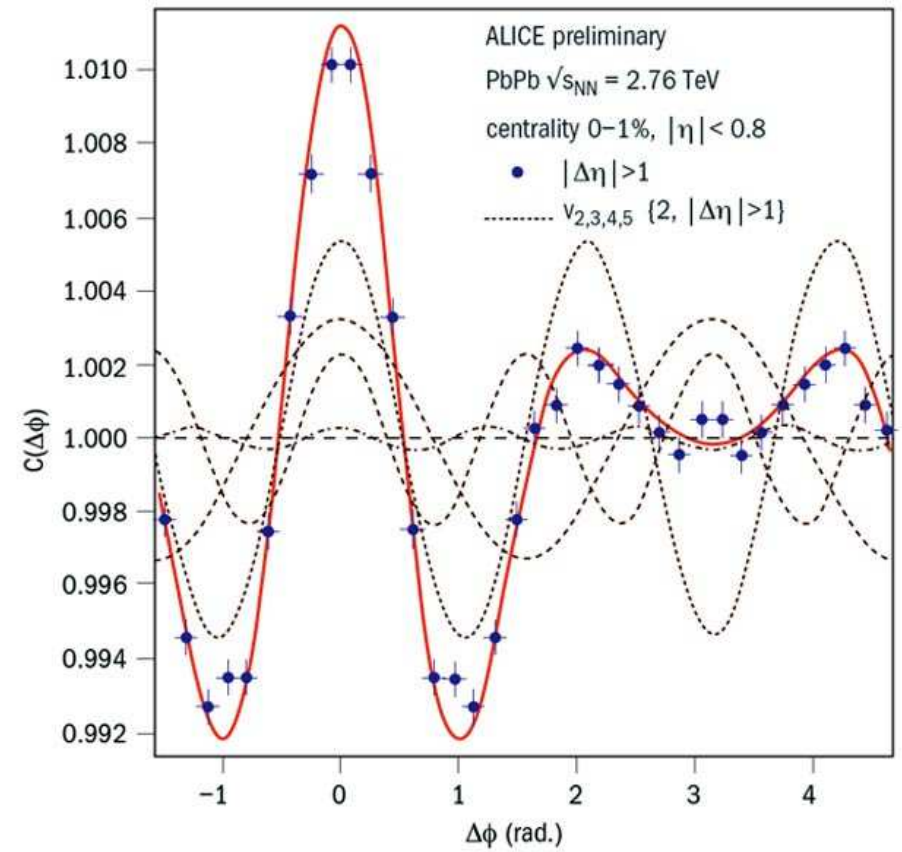
$$v_2\{2\} = \sqrt{\langle v_2^2 \rangle}, \quad v_2\{4\} = \sqrt[4]{2\langle v_2^2 \rangle^2 - \langle v_2^4 \rangle}$$

Panta rhei: “soft ridge”=“Mach cone”=flow!

ATLAS (J. Jia), Quark Matter 2011



ALICE (J. Grosse-Oetringhaus), QM11

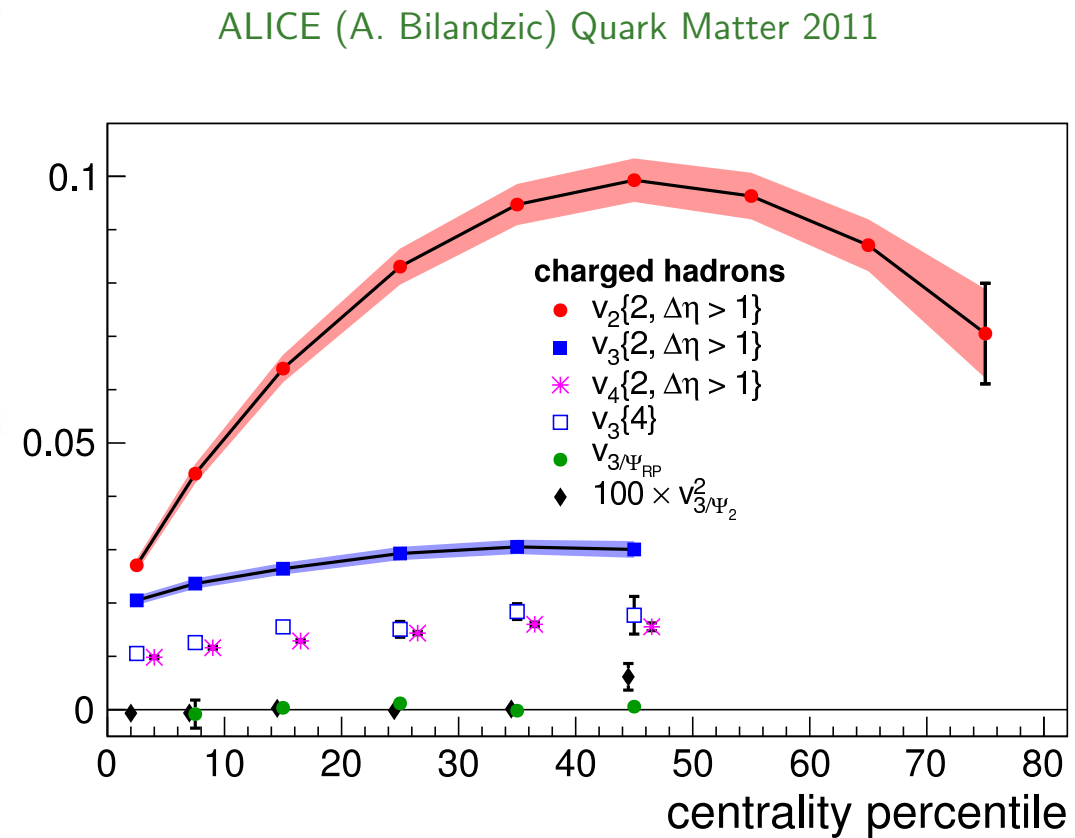
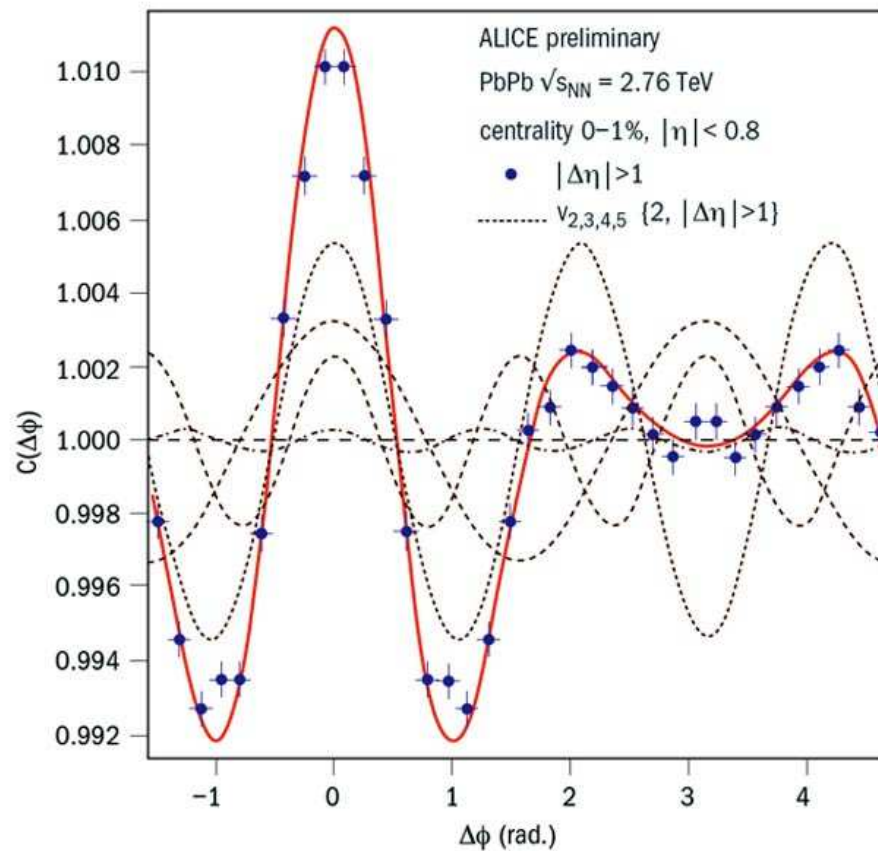


- anisotropic flow coefficients v_n and flow angles ψ_n correlated over large rapidity range!

M. Luzum, PLB 696 (2011) 499: All long-range rapidity correlations seen at RHIC are consistent with being entirely generated by hydrodynamic flow.

- in the 1% most central collisions $v_3 > v_2$
 - ⇒ prominent “Mach cone”-like structure!
 - ⇒ event-by-event eccentricity fluctuations dominate!

Event-by-event shape and flow fluctuations rule!



- in the 1% most central collisions $v_3 > v_2 \implies$ prominent “Mach cone”-like structure!
- triangular flow angle uncorrelated with reaction plane and elliptic flow angles
 \implies due to event-by-event eccentricity fluctuations which dominate the anisotropic flows in the most central collisions

Viscous relativistic hydrodynamics (Israel & Stewart 1979)

Include shear viscosity η , neglect bulk viscosity (massless partons) and heat conduction ($\mu_B \approx 0$); solve

$$\partial_\mu T^{\mu\nu} = 0$$

with modified energy momentum tensor

$$T^{\mu\nu}(x) = (e(x)+p(x))u^\mu(x)u^\nu(x) - g^{\mu\nu}p(x) + \pi^{\mu\nu}.$$

$\pi^{\mu\nu}$ = traceless viscous pressure tensor which relaxes locally to 2η times the shear tensor $\nabla^{\langle\mu} u^{\nu\rangle}$ on a microscopic kinetic time scale τ_π :

$$D\pi^{\mu\nu} = -\frac{1}{\tau_\pi} (\pi^{\mu\nu} - 2\eta \nabla^{\langle\mu} u^{\nu\rangle}) + \dots$$

where $D \equiv u^\mu \partial_\mu$ is the time derivative in the local rest frame.

Kinetic theory relates η and τ_π , but for a strongly coupled QGP neither η nor this relation are known \Rightarrow treat η and τ_π as independent phenomenological parameters.

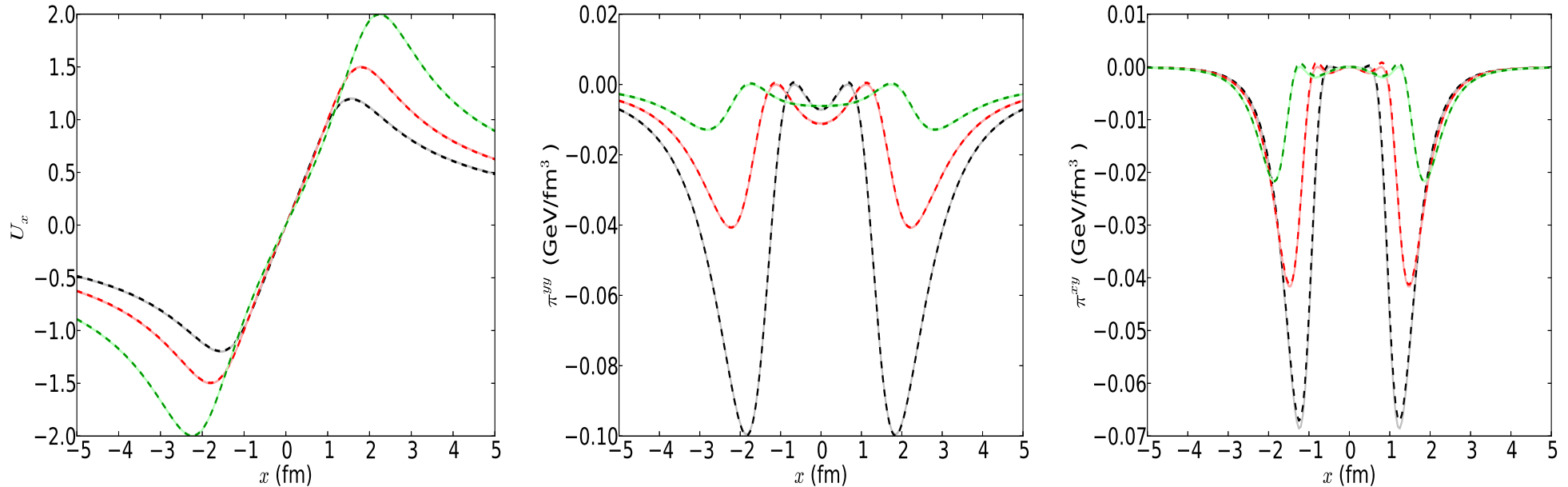
For consistency: $\tau_\pi \theta \ll 1$ ($\theta = \partial^\mu u_\mu$ = local expansion rate).

Numerical precision: “Gubser-Test”

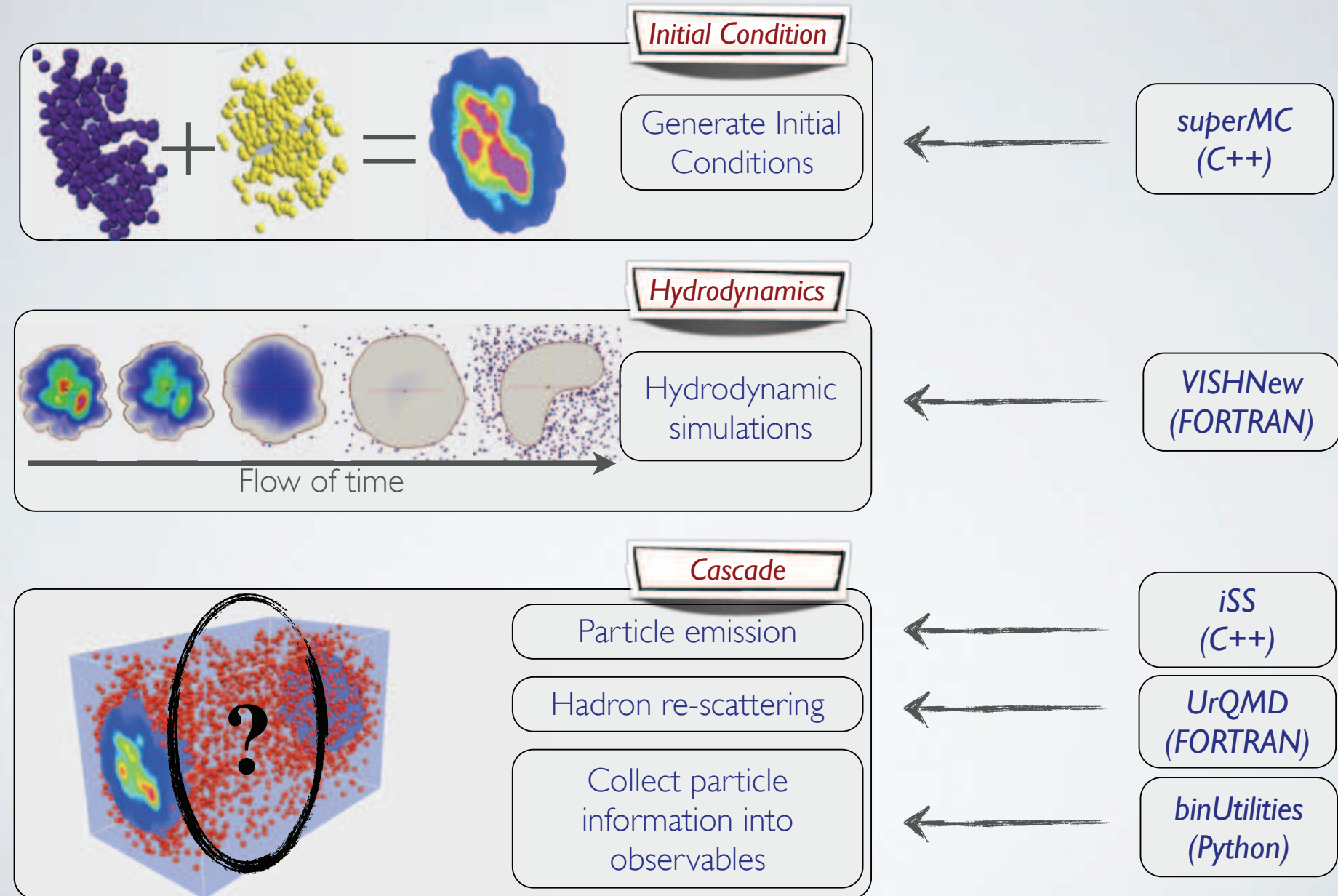
Gubser (PRD82 (2010) 085027) found analytical solution for relativistic Navier-Stokes equation with conformal EOS, boost-invariant longitudinal and non-zero transverse flow, corresponding to a specific transverse temperature profile.

Marrochio, Noronha *et al.* (arXiv:1307.6130) found semianalytical generalization of this solution for Israel-Stewart theory. This solution provides a stringent test for numerical Israel-Stewart codes (very rapid and non-trivial transverse expansion!)

VISH2+1 (C. Shen, 2013)

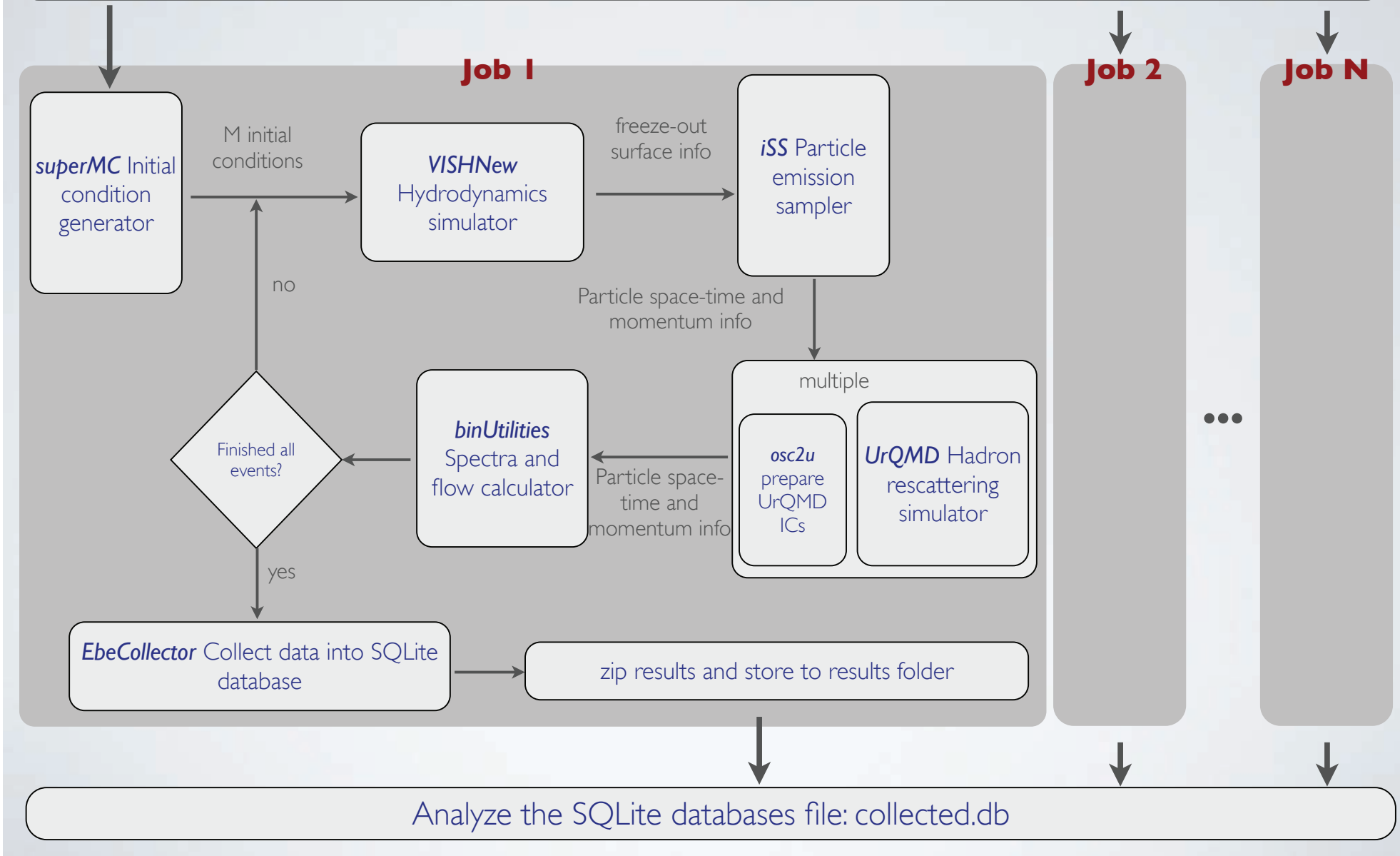


iEBE: e-by-e hydro on demand



iEBE package structure

generateJobs.py & submitJobs_xxx.py Generate jobs and run them in parallel



iEBE available through JET Collaboration web site

Converting initial shape

fluctuations into

final flow anisotropies –

the QGP shear viscosity

$$(\eta/s)_{\text{QGP}}$$

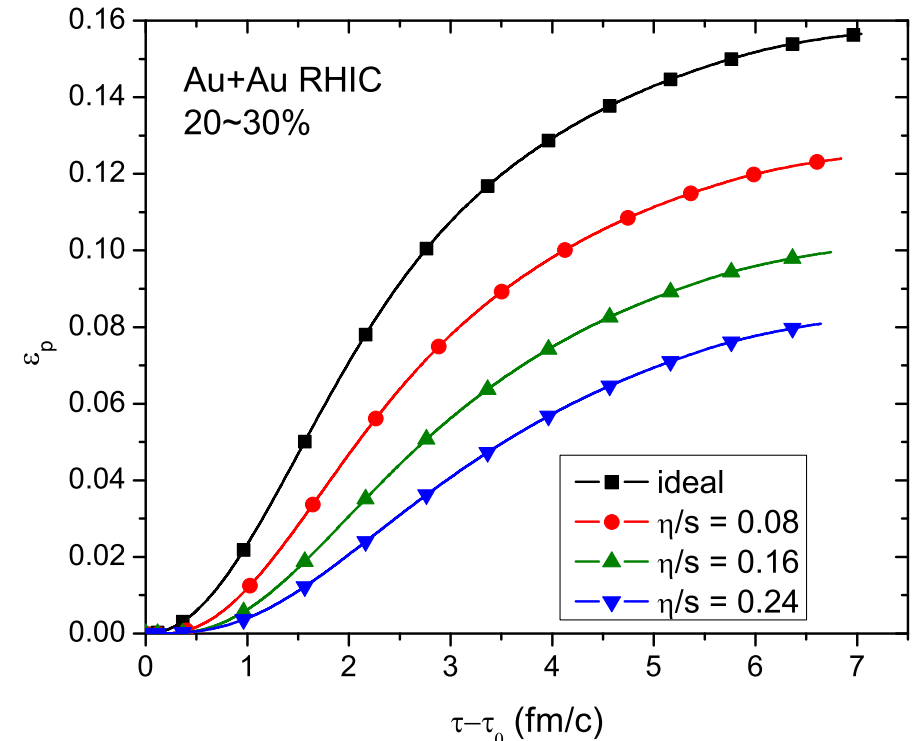
How to use elliptic flow for measuring $(\eta/s)_{\text{QGP}}$

Hydrodynamics converts
spatial deformation of initial state \Rightarrow
momentum anisotropy of final state,
through anisotropic pressure gradients

Shear viscosity degrades conversion efficiency

$$\varepsilon_x = \frac{\langle\langle y^2 - x^2 \rangle\rangle}{\langle\langle y^2 + x^2 \rangle\rangle} \implies \varepsilon_p = \frac{\langle T^{xx} - T^{yy} \rangle}{\langle T^{xx} + T^{yy} \rangle}$$

of the fluid; the suppression of ε_p is monotonically related to η/s .



The observable that is most directly related to the total hydrodynamic momentum anisotropy ε_p is the **total (p_T -integrated) charged hadron elliptic flow v_2^{ch}** :

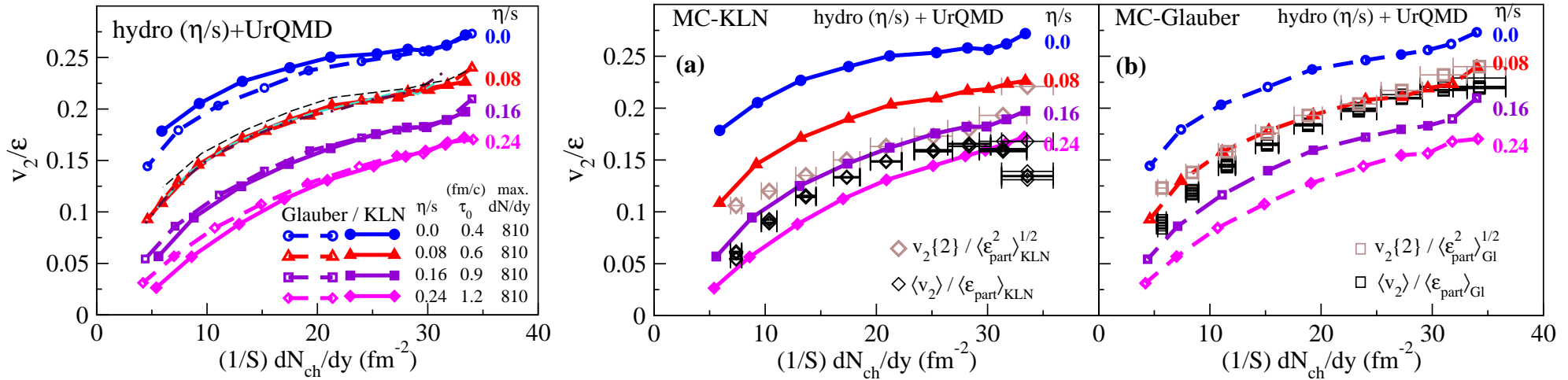
$$\varepsilon_p = \frac{\langle T^{xx} - T^{yy} \rangle}{\langle T^{xx} + T^{yy} \rangle} \iff \frac{\sum_i \int p_T dp_T \int d\phi_p p_T^2 \cos(2\phi_p) \frac{dN_i}{dy p_T dp_T d\phi_p}}{\sum_i \int p_T dp_T \int d\phi_p p_T^2 \frac{dN_i}{dy p_T dp_T d\phi_p}} \iff v_2^{\text{ch}}$$

How to use elliptic flow for measuring $(\eta/s)_{\text{QGP}}$ (ctd.)

- If ε_p **saturates** before hadronization (e.g. in PbPb@LHC (?))
 - ⇒ $v_2^{\text{ch}} \approx$ not affected by details of hadronic rescattering below T_c
but: $v_2^{(i)}(p_T)$, $\frac{dN_i}{dy d^2 p_T}$ change during hadronic phase (addl. radial flow!), and these changes depend on details of the hadronic dynamics (chemical composition etc.)
 - ⇒ $v_2(p_T)$ of a single particle species **not** a good starting point for extracting η/s
- If ε_p **does not saturate** before hadronization (e.g. AuAu@RHIC), dissipative hadronic dynamics affects not only the distribution of ε_p over hadronic species and in p_T , but even the final value of ε_p itself (from which we want to get η/s)
 - ⇒ need hybrid code that couples viscous hydrodynamic evolution of QGP to **realistic microscopic dynamics** of late-stage hadron gas phase
 - ⇒ **VISHNU** ("Viscous Israel-Stewart Hydrodynamics 'n' UrQMD")
(Song, Bass, UH, PRC83 (2011) 024912) Note: this paper shows that UrQMD \neq viscous hydro!

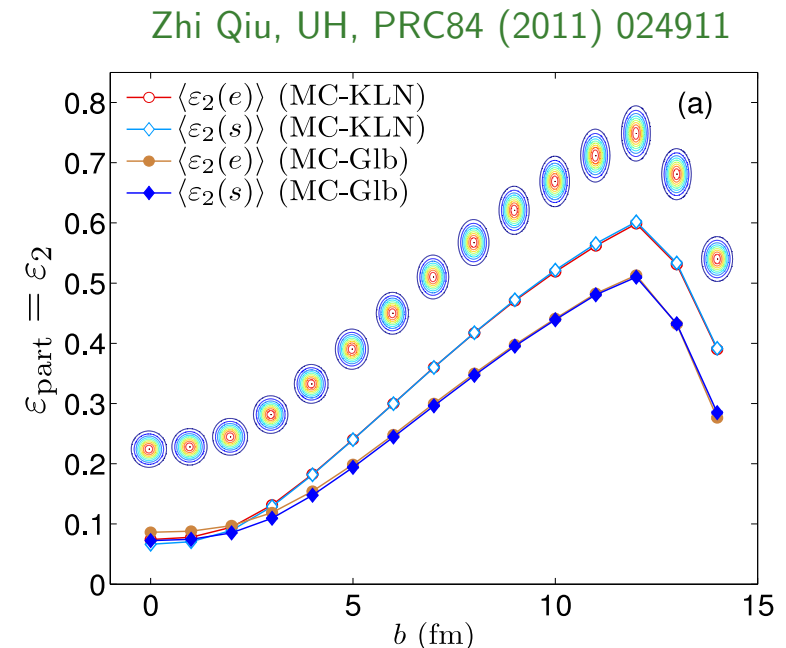
Extraction of $(\eta/s)_{\text{QGP}}$ from AuAu@RHIC

H. Song, S.A. Bass, UH, T. Hirano, C. Shen, PRL106 (2011) 192301



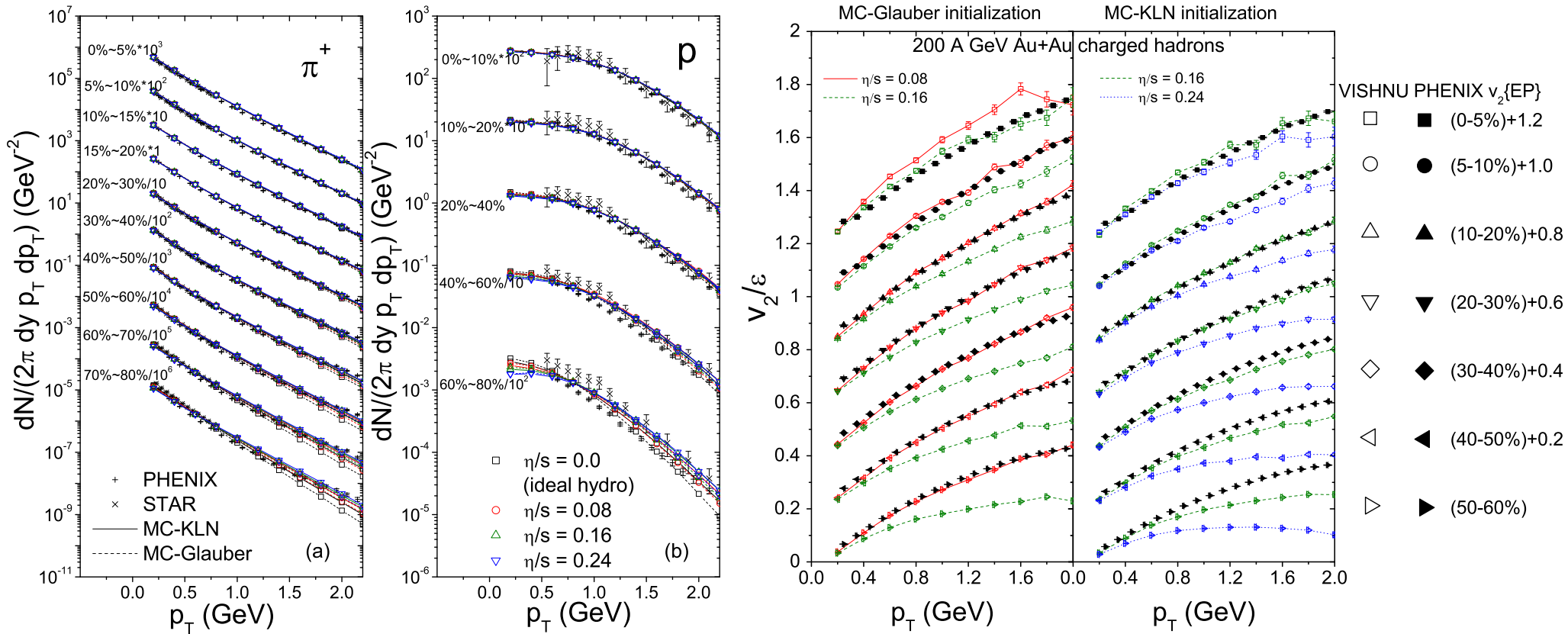
$$1 < 4\pi(\eta/s)_{\text{QGP}} < 2.5$$

- All shown theoretical curves correspond to parameter sets that correctly describe centrality dependence of charged hadron production as well as p_T -spectra of charged hadrons, pions and protons at all centralities
 - $v_2^{\text{ch}}/\varepsilon_x$ vs. $(1/S)(dN_{\text{ch}}/dy)$ is “universal”, i.e. depends **only on** η/s but (in good approximation) not on initial-state model (Glauber vs. KLN, optical vs. MC, RP vs. PP average, etc.)
 - dominant source of uncertainty: $\varepsilon_x^{\text{Gl}}$ vs. $\varepsilon_x^{\text{KLN}}$ →
 - smaller effects: *early flow* → increases $\frac{v_2}{\varepsilon}$ by \sim few % → larger η/s
bulk viscosity → affects $v_2^{\text{ch}}(p_T)$, but \approx not v_2^{ch}



Global description of AuAu@RHIC spectra and v_2

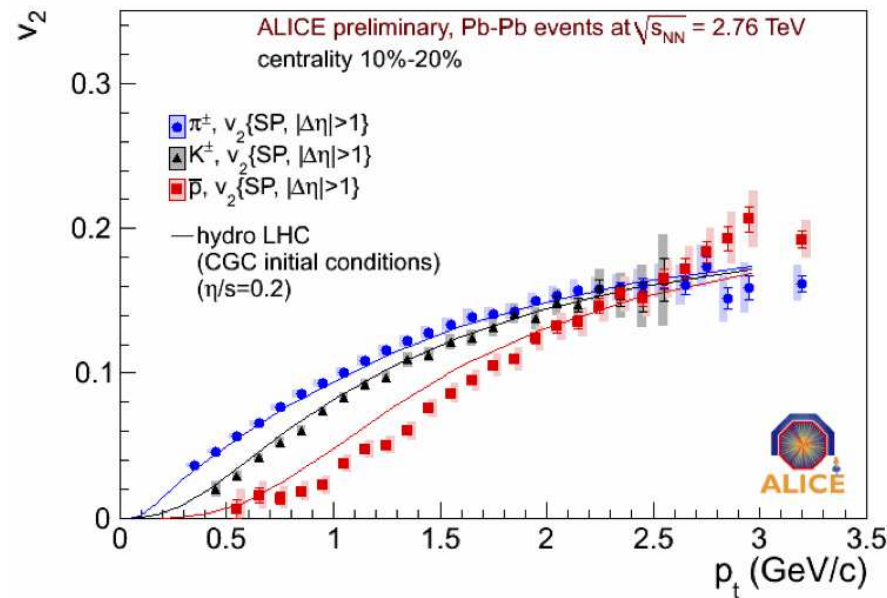
VISHNU (H. Song, S.A. Bass, UH, T. Hirano, C. Shen, PRC83 (2011) 054910)



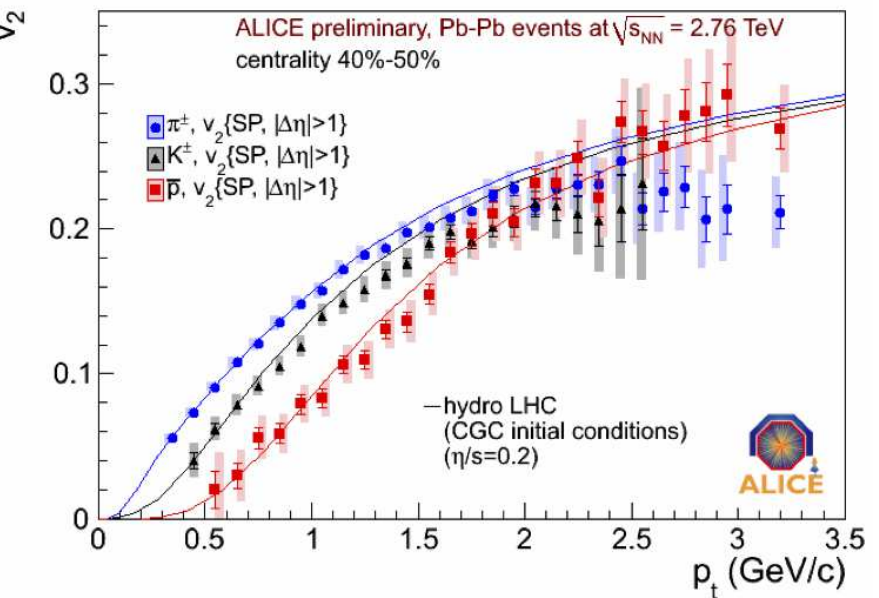
$(\eta/s)_{\text{QGP}} = 0.08$ for MC-Glauber and $(\eta/s)_{\text{QGP}} = 0.16$ for MC-KLN work well for charged hadron, pion and proton spectra and $v_2(p_T)$ at all collision centralities

Successful prediction of $v_2(p_T)$ for identified hadrons in PbPb@LHC

Data: ALICE, Quark Matter 2011



Prediction: Shen et al., PRC84 (2011) 044903 (VISH2+1)



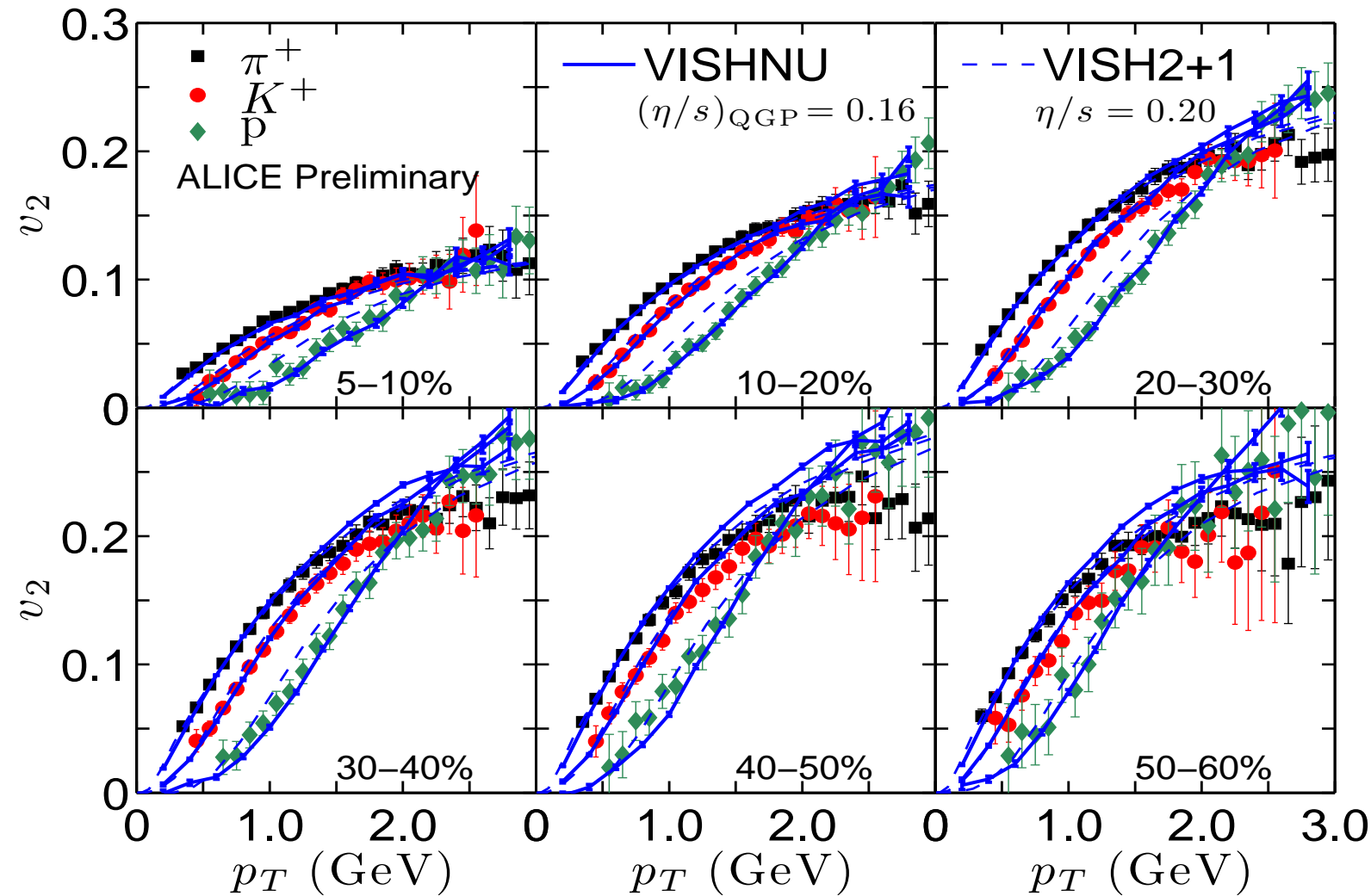
Perfect fit in semi-peripheral collisions!

The problem with insufficient proton radial flow exists only in more central collisions

Adding the hadronic cascade (VISHNU) helps:

$v_2(p_T)$ in PbPb@LHC: ALICE vs. VISHNU

Data: ALICE, preliminary (Snellings, Krzewicki, Quark Matter 2011)
 Dashed lines: Shen et al., PRC84 (2011) 044903 (VISH2+1, MC-KLN, $(\eta/s)_{QGP}=0.2$)
 Solid lines: Song, Shen, UH 2011 (VISHNU, MC-KLN, $(\eta/s)_{QGP}=0.16$)



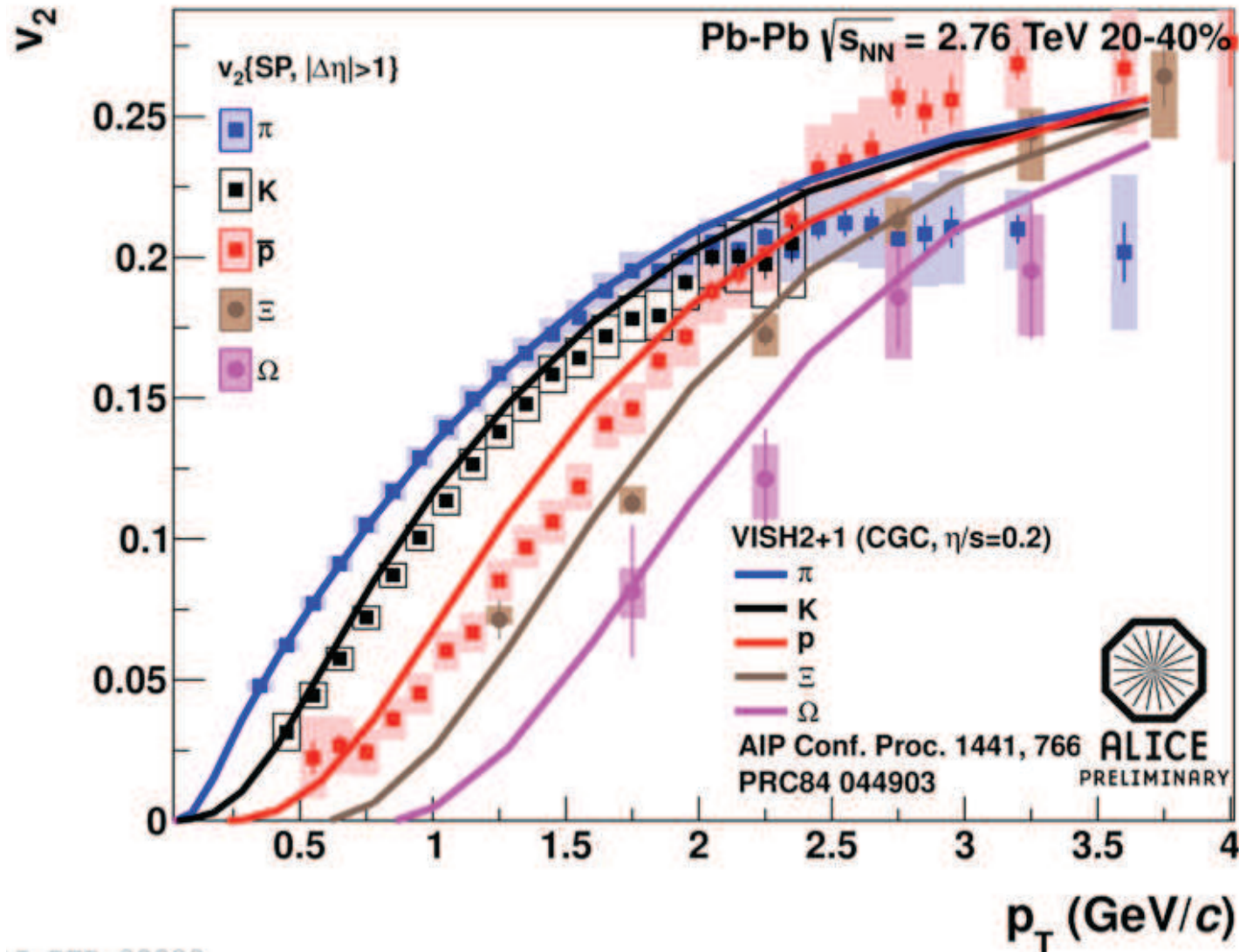
VISHNU yields correct magnitude and centrality dependence of $v_2(p_T)$ for pions, kaons **and protons!**

Same $(\eta/s)_{QGP} = 0.16$ (for MC-KLN) at RHIC and LHC!

Successful prediction of $v_2(p_T)$ for identified hadrons in PbPb@LHC (II)

Data: ALICE, Quark Matter 2012

Prediction: Shen et al., PRC84 (2011) 044903 (VISH2+1)



Radial flow pushes v_2 for heavier hadrons to larger p_T

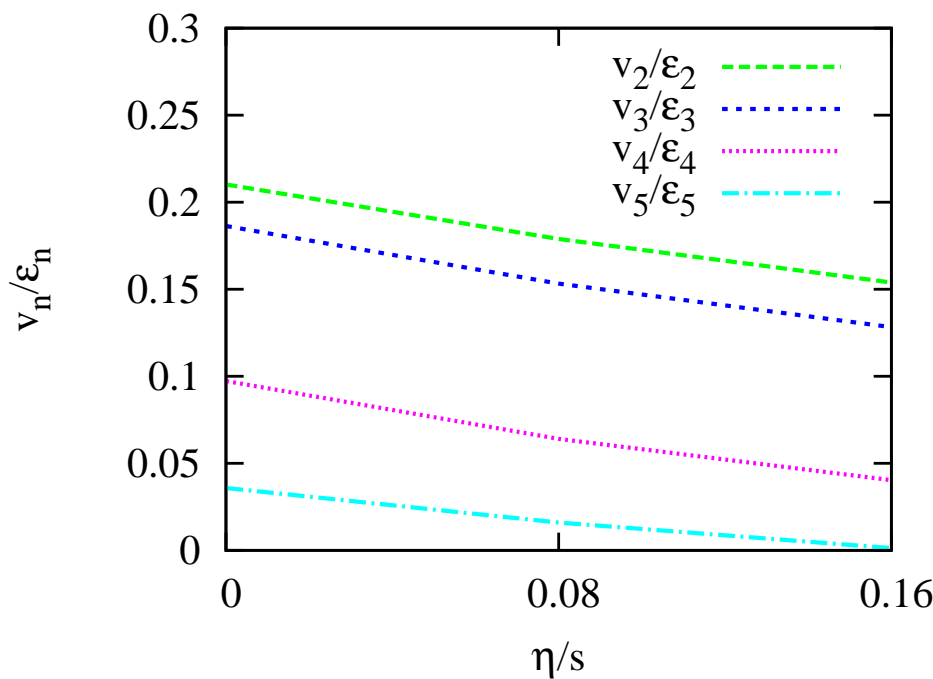
Theory curves are true predictions, without any parameter adjustment

Back to the “elephant in the room”: How to eliminate the large model uncertainty in the initial eccentricity?

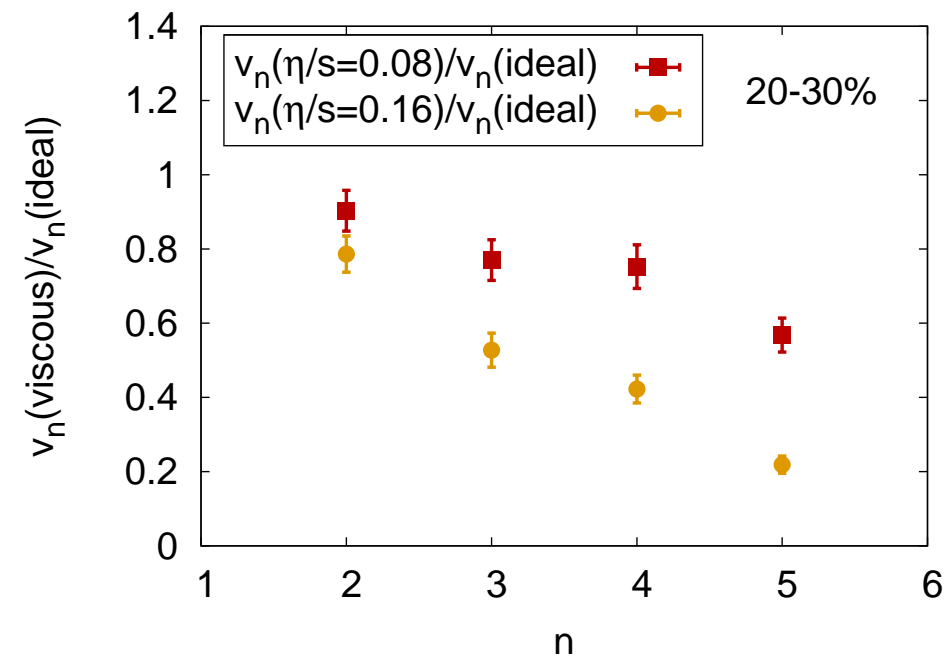
Two observations:

I. Shear viscosity suppresses higher flow harmonics more strongly

Alver et al., PRC82 (2010) 034913
(averaged initial conditions)



Schenke et al., arXiv:1109.6289
(event-by-event hydro)

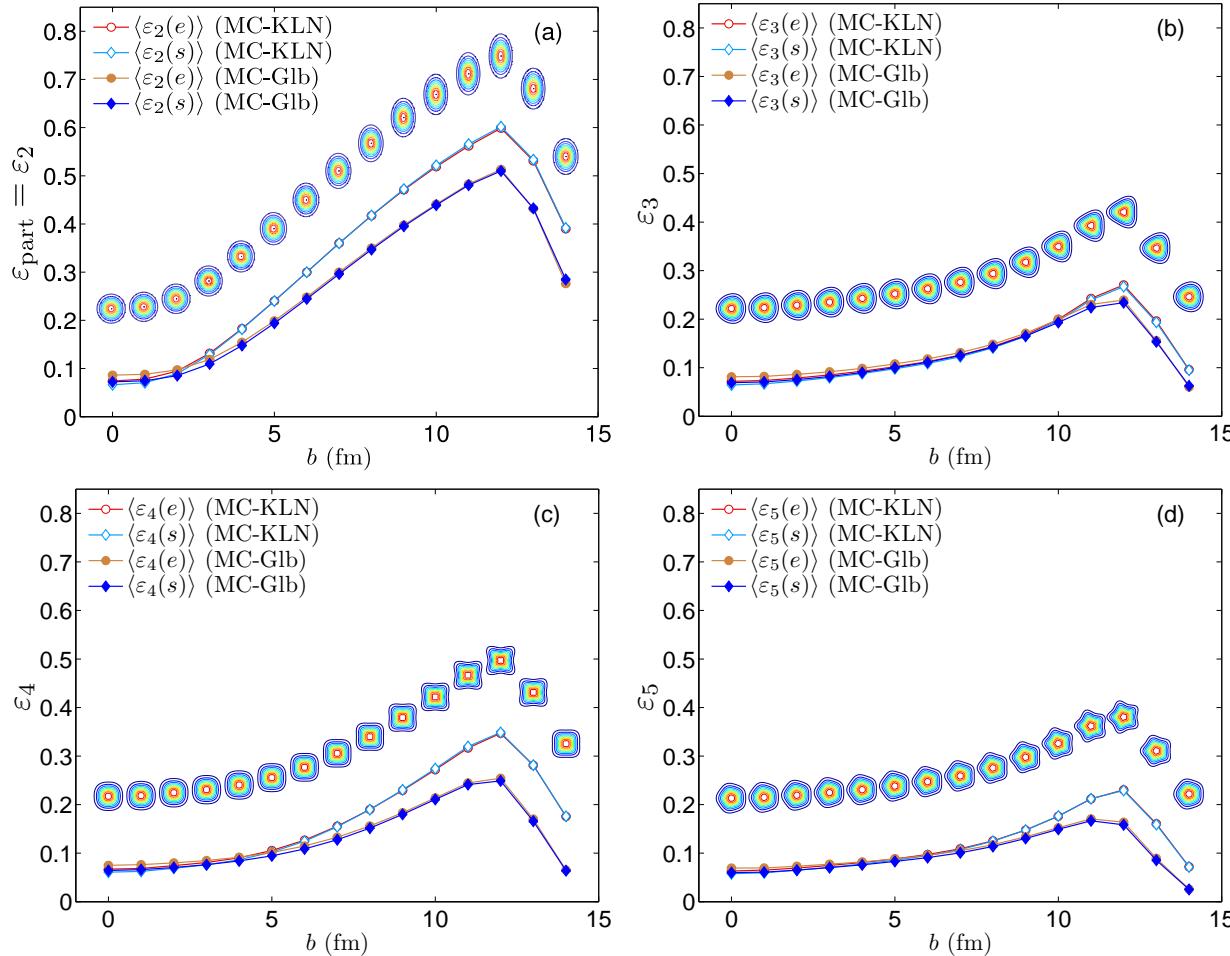


➡ **Idea:** Use simultaneous analysis of elliptic and triangular flow to constrain initial state models
(see also Bhalerao, Luzum Ollitrault, PRC 84 (2011) 034910)

Two observations:

II. ε_3 is \approx model independent

Zhi Qiu, UH, PRC84 (2011) 024911



Initial eccentricities ε_n and angles ψ_n :

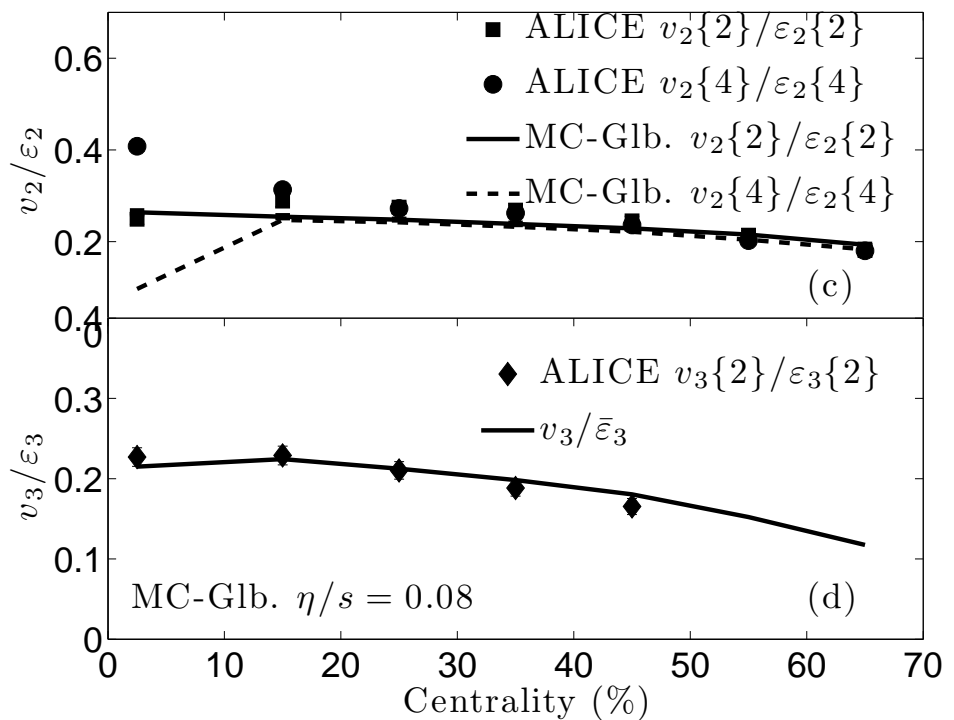
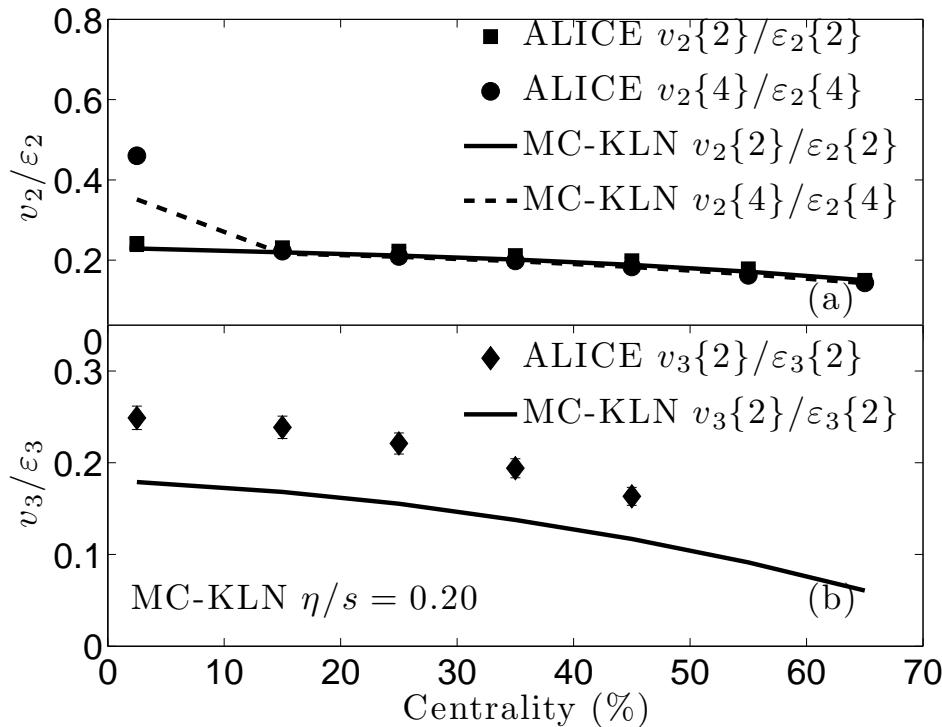
$$\varepsilon_n e^{in\psi_n} = -\frac{\int r dr d\phi r^2 e^{in\phi} e(r,\phi)}{\int r dr d\phi r^2 e(r,\phi)}$$

- MC-KLN has larger ε_2 and ε_4 , but similar ε_5 and almost identical ε_3 as MC-Glauber
- Angles of ε_2 and ε_4 are correlated with reaction plane by geometry, whereas those of ε_3 and ε_5 are random (purely fluctuation-driven)
- While v_4 and v_5 have mode-coupling contributions from ε_2 , v_3 is almost pure response to ε_3 and $v_3/\varepsilon_3 \approx \text{const.}$ over a wide range of centralities

⇒ Idea: Use total charged hadron v_3^{ch} to determine $(\eta/s)_{\text{QGP}}$,
 then check v_2^{ch} to distinguish between MC-KLN and MC-Glauber!

Combined v_2 & v_3 analysis: η/s is small!

Zhi Qiu, C. Shen, UH, PLB707 (2012) 151 and QM2012 (e-by-e VISH2+1)

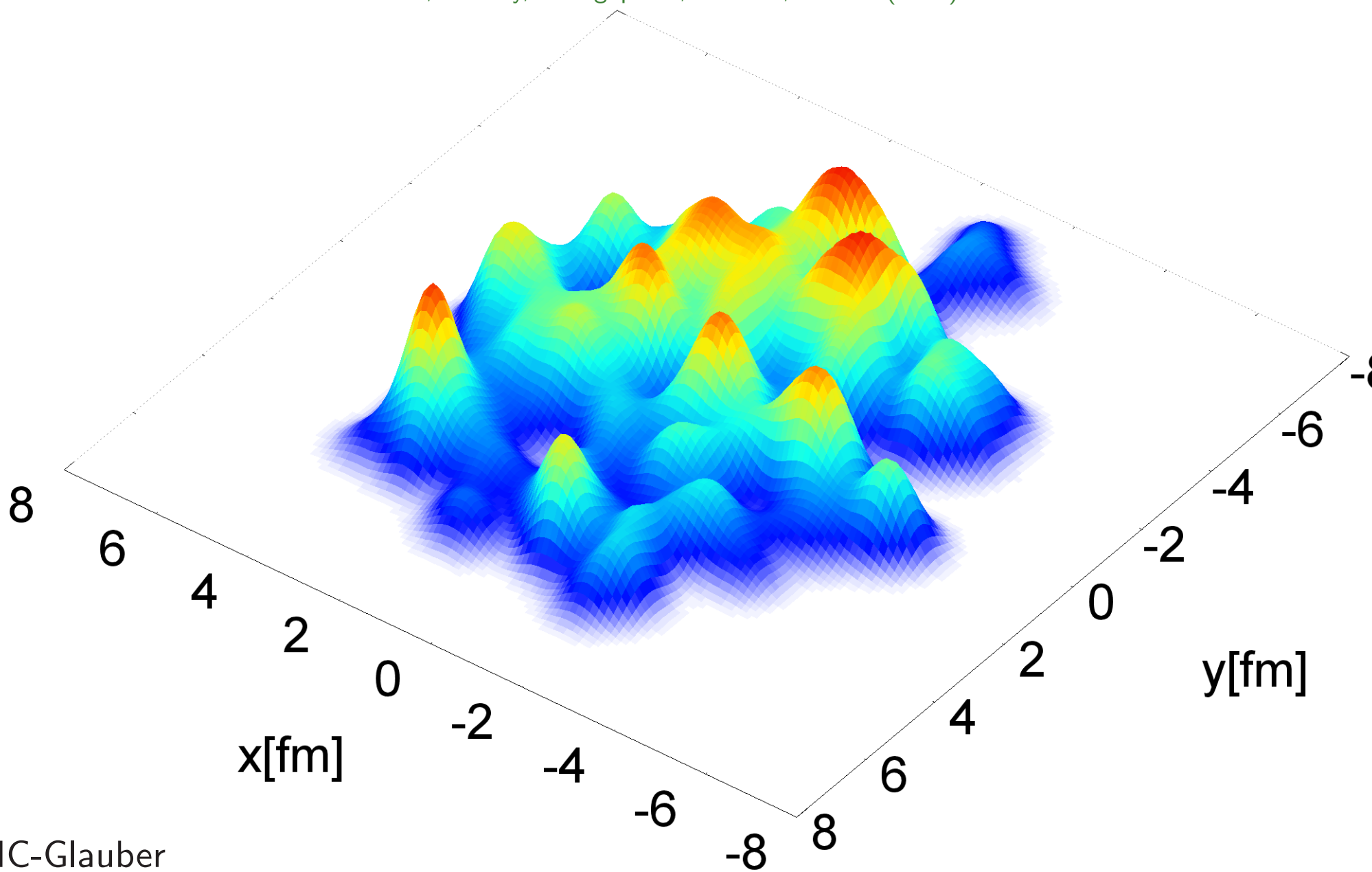


- Both MC-KLN with $\eta/s = 0.2$ and MC-Glauber with $\eta/s = 0.08$ give very good description of v_2/ε_2 at all centralities.
- **Only $\eta/s = 0.08$ (with MC-Glauber initial conditions) describes v_3/ε_3 !**
- PHENIX, comparing to calculations by Alver et al. (PRC82 (2010) 034913), come to similar conclusions at RHIC energies (Adare et al., arXiv:1105.3928, and Lacey et al., arXiv:1108.0457)
- **Large v_3 measured at RHIC and LHC requires small $(\eta/s)_{QGP} \simeq 1/(4\pi)$** unless the fluctuations in these models are completely wrong and ε_3 is really 50% larger than these models predict!

Sub-nucleonic fluctuations

Adding sub-nucleonic quantum fluctuations

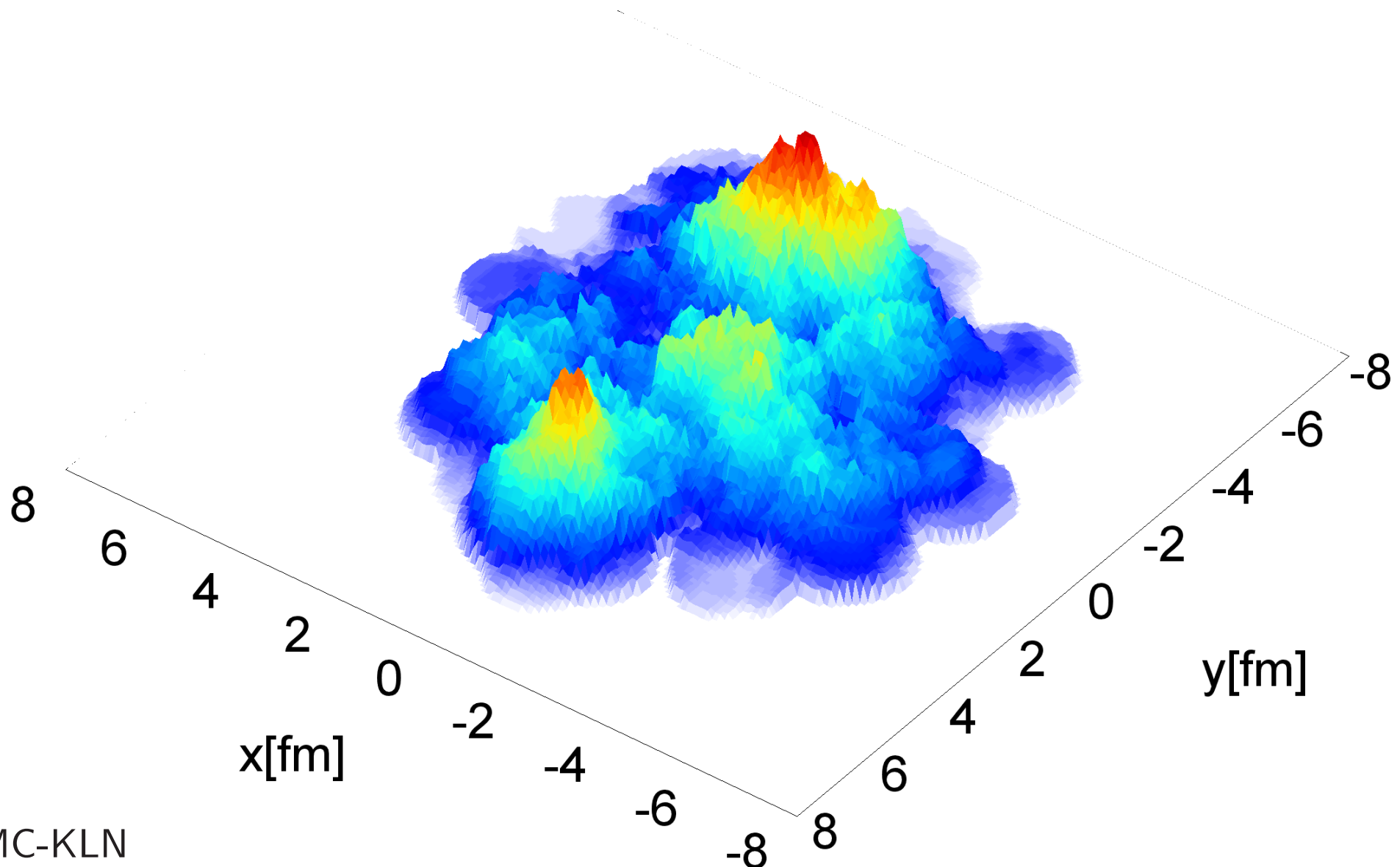
Schenke, Tribedy, Venugopalan, PRL108, 252301 (2012)



MC-Glauber

Adding sub-nucleonic quantum fluctuations

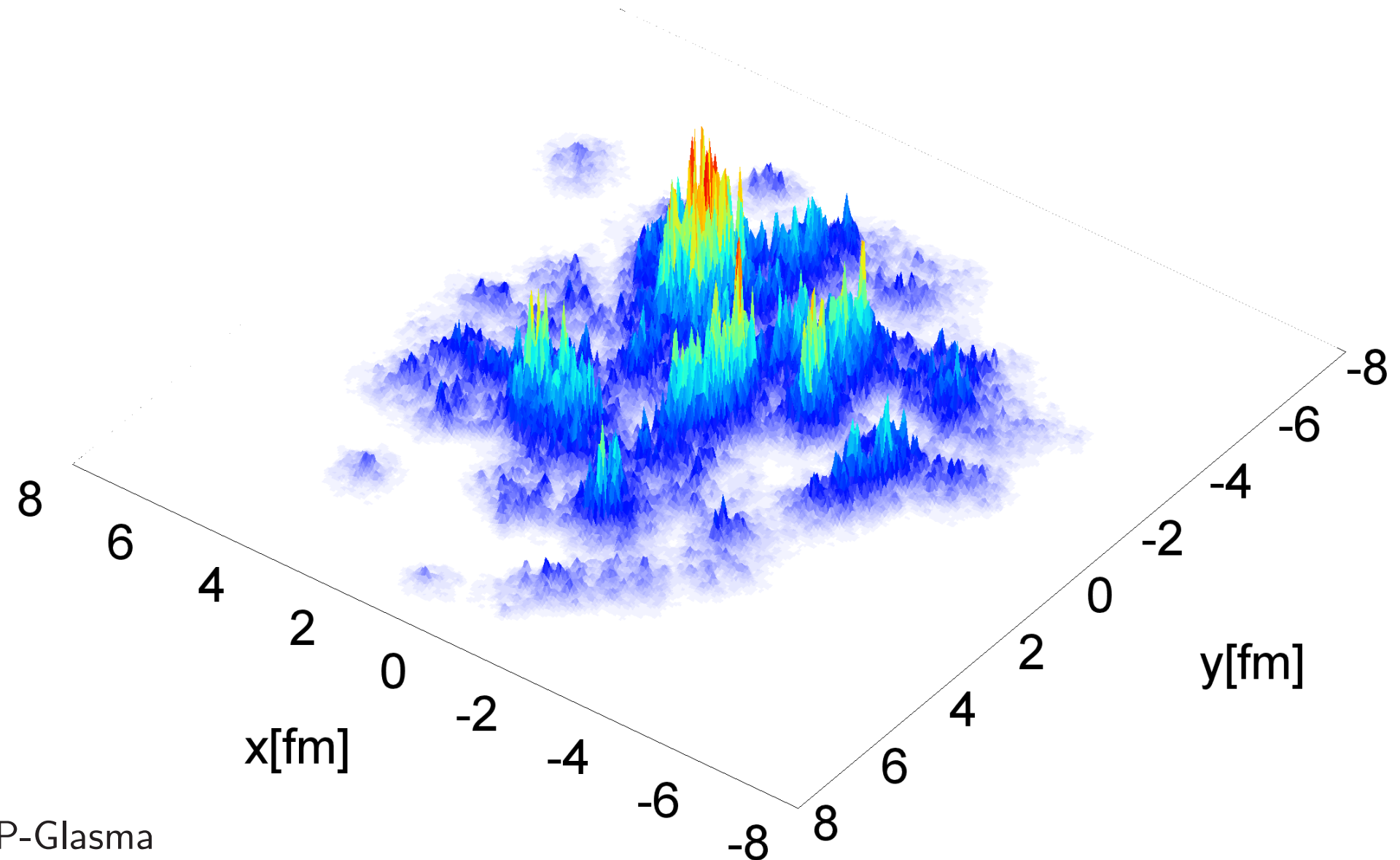
Schenke, Tribedy, Venugopalan, PRL108, 252301 (2012)



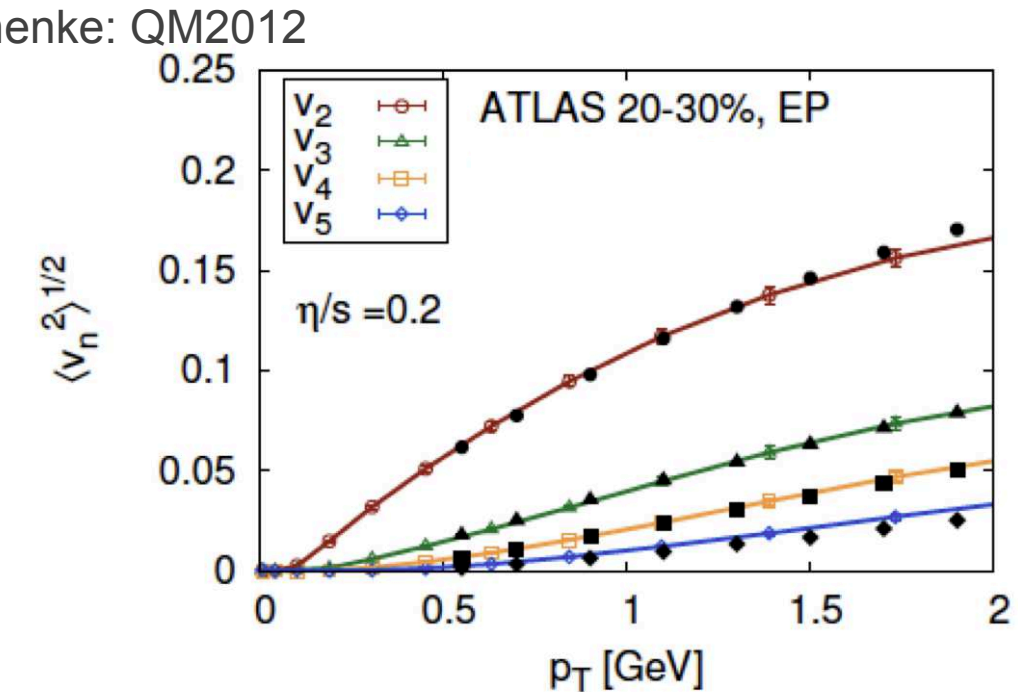
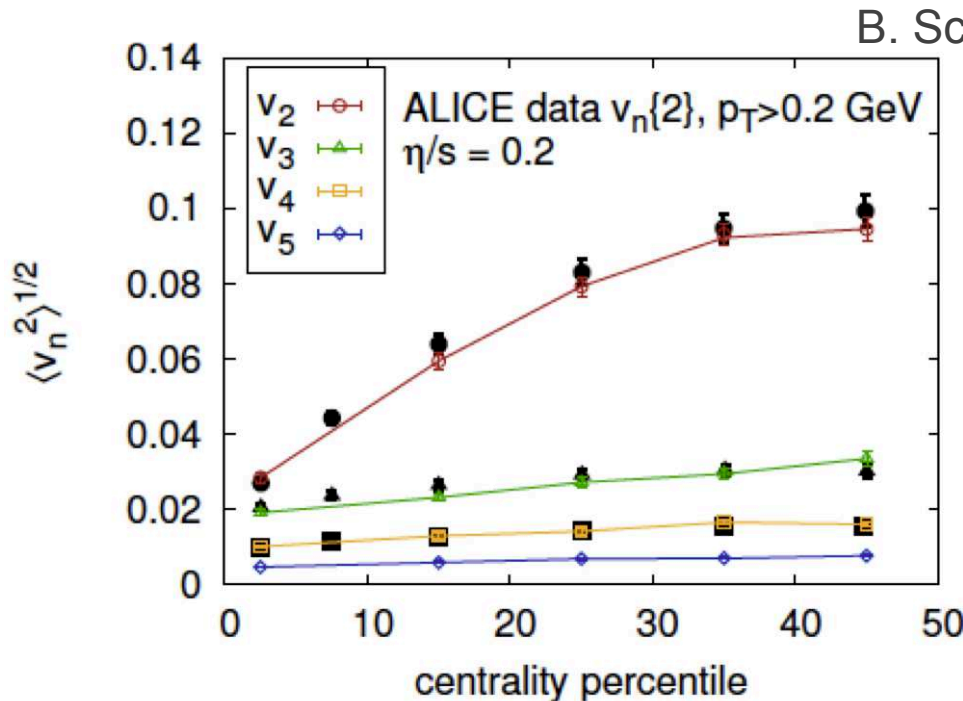
MC-KLN

Adding sub-nucleonic quantum fluctuations

Schenke, Tribedy, Venugopalan, PRL108, 252301 (2012)



Towards a Standard Model of the Little Bang



With inclusion of sub-nucleonic quantum fluctuations
and pre-equilibrium dynamics of gluon fields:

→ outstanding agreement between data and model

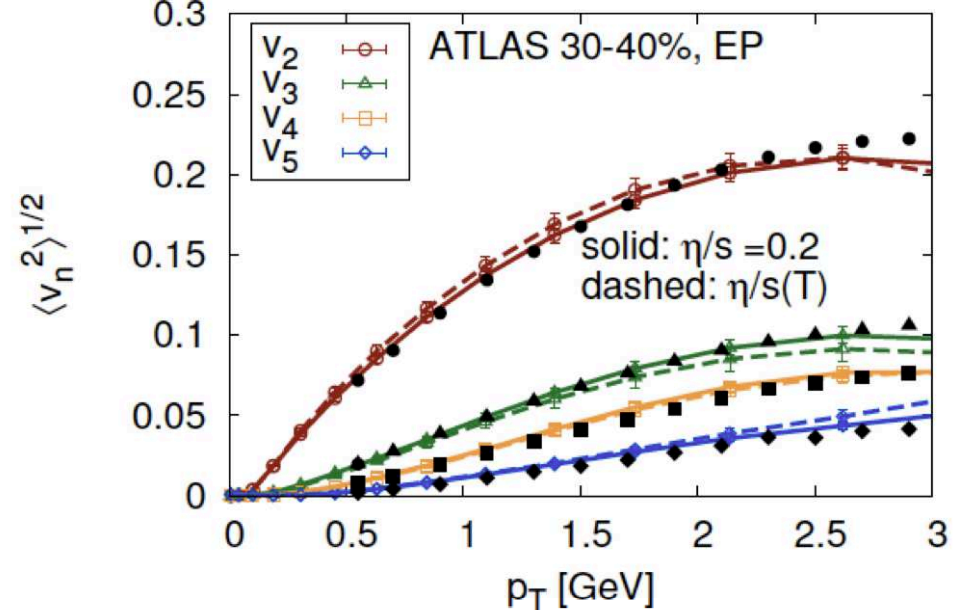
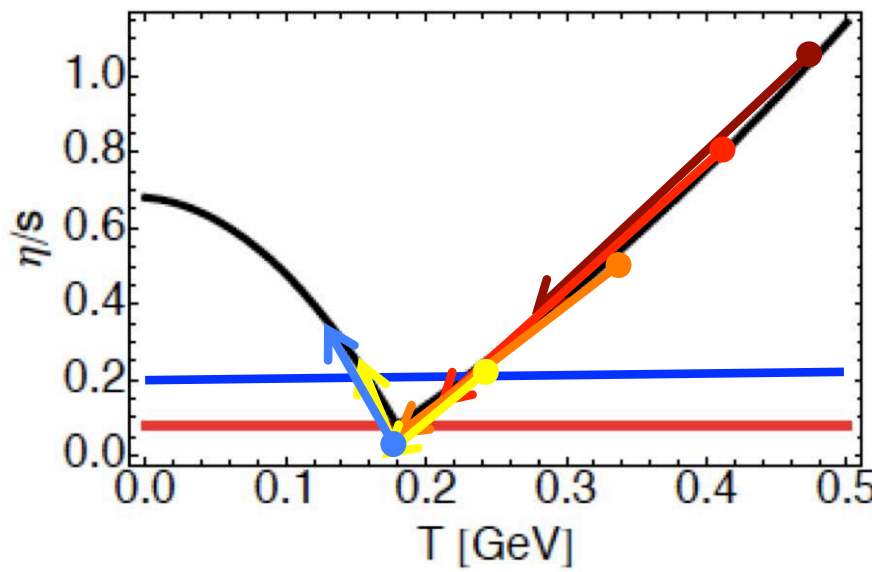
Rapid convergence on a standard model of the Little Bang!

Perfect liquidity reveals in the final state initial-state gluon field correlations
of size $1/Q_s$ (sub-hadronic)!

Schenke, Tribedy, Venugopalan,
Phys.Rev.Lett. 108:25231 (2012)

What We Don't Know

B. Schenke: QM2012

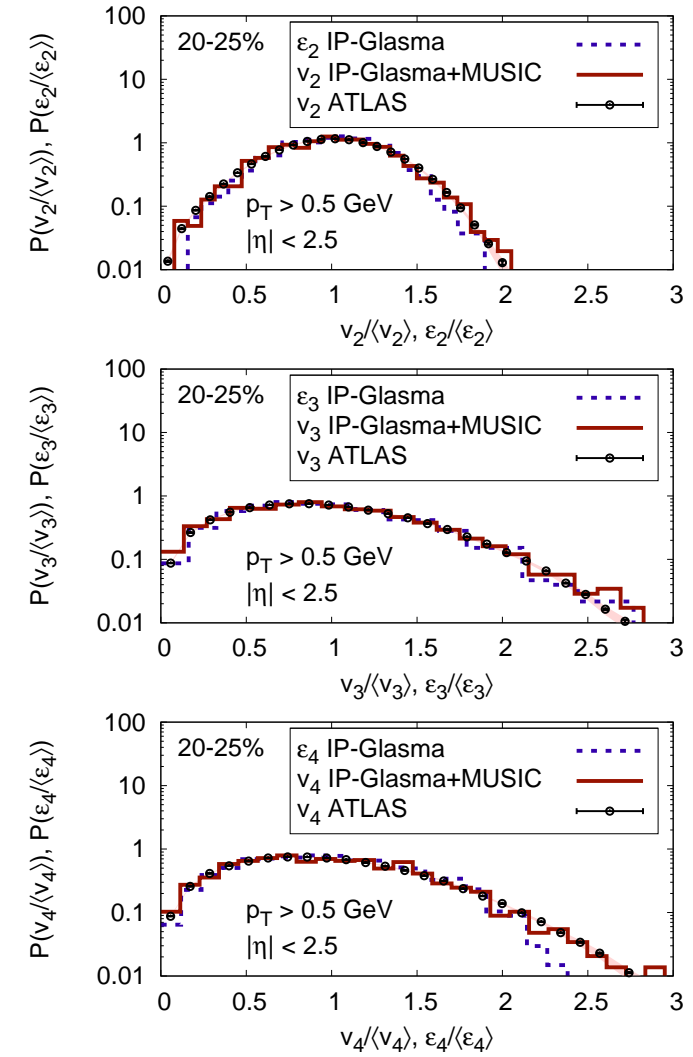
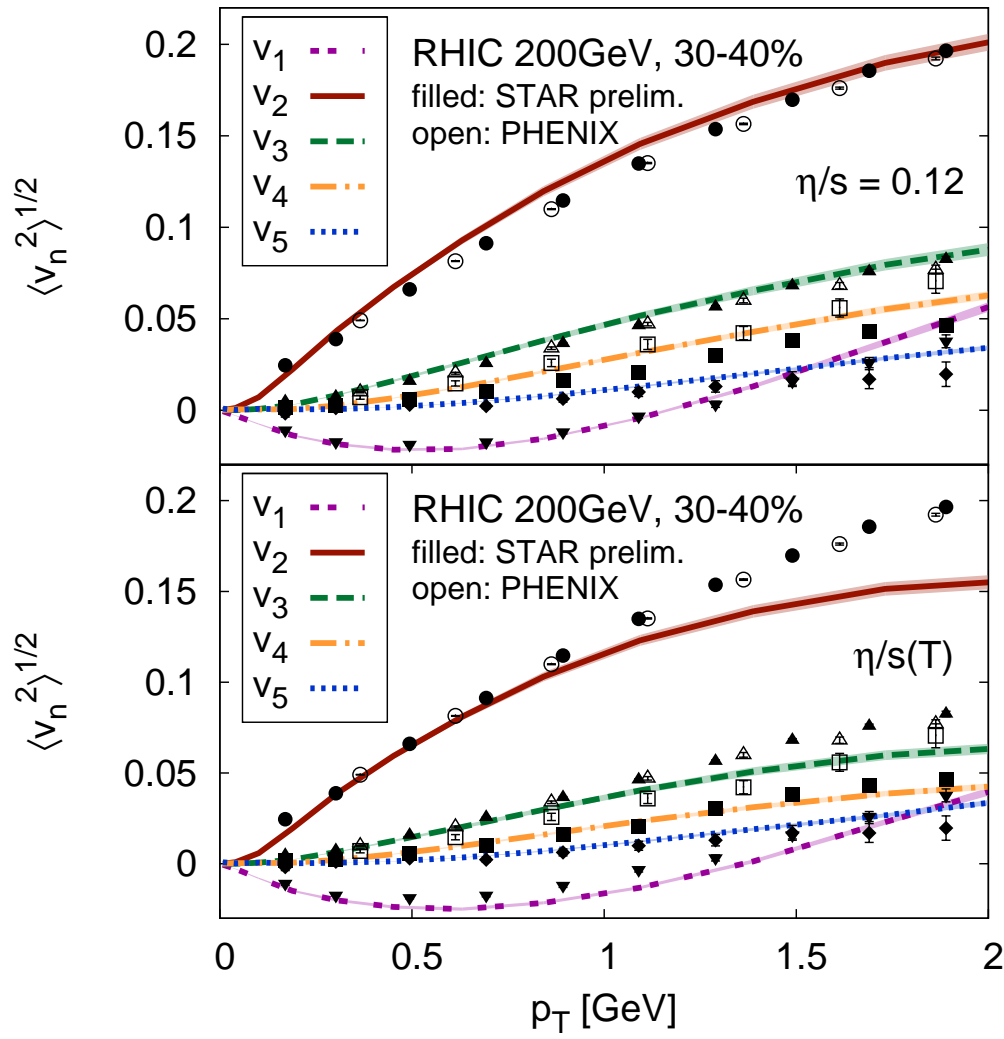


Model doesn't distinguish between a constant η/s of 0.2 or a temperature dependent η/s with a minimum of $1/4\pi$

Need both RHIC and LHC to sort this out!

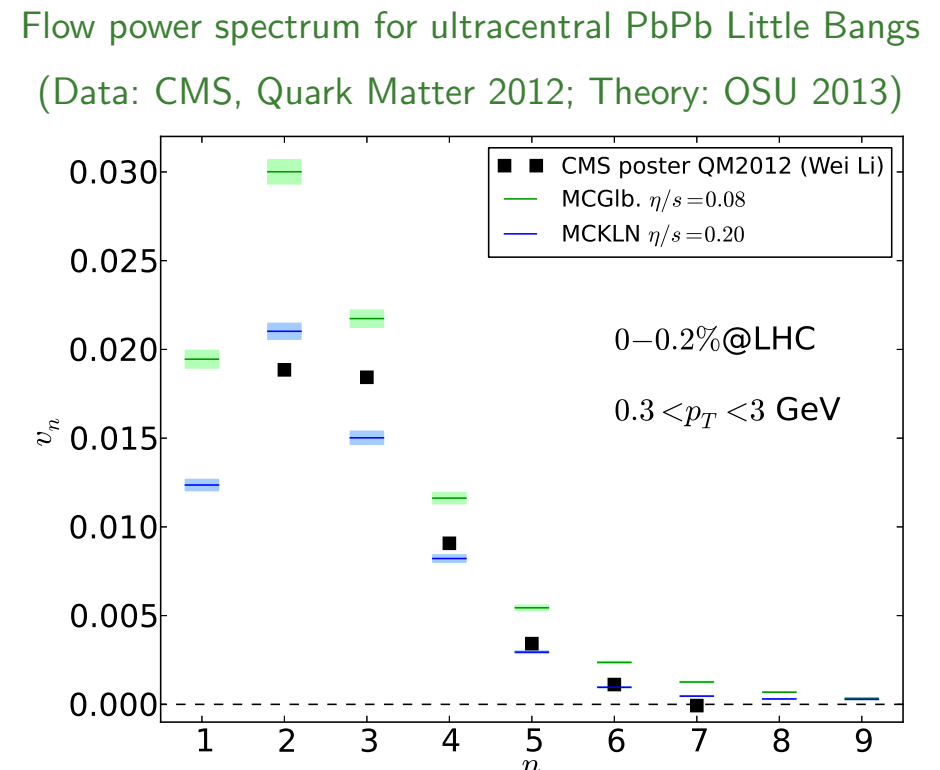
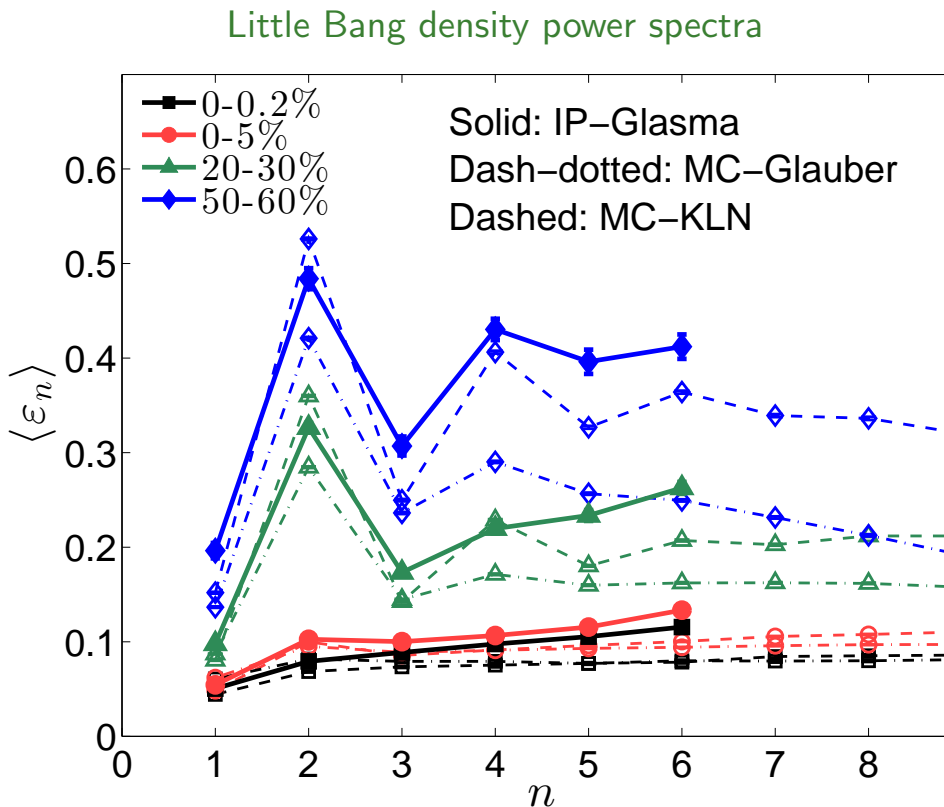
Other successes of the Little Bang Standard Model

Gale, Jeon, Schenke, Tribedy, Venugopalan, arXiv:1209.6330 (PRL 2012)



- Model describes RHIC data with lower effective specific shear viscosity $\eta/s = 0.12$
- In contrast to MC-Glauber and MC-KLN, IP-Sat initial conditions correctly reproduce the final flow fluctuation spectrum, generated from initial shape fluctuations by viscous hydrodynamics

The Little Bang fluctuation power spectrum: initial vs. final



Higher flow harmonics get suppressed by shear viscosity

Neither MC-Glauber nor MC-KLN gives the correct initial power spectrum! † R.I.P.

A detailed study of fluctuations is a powerful discriminator between models!

Single event anisotropic flow coefficients

In a single event, the specific initial density profile results in a set of complex, y - and p_T -dependent flow coefficients (we'll suppress the y -dependence):

$$V_n = \textcolor{red}{v}_n e^{in\Psi_n} := \frac{\int p_T dp_T d\phi e^{in\phi} \frac{dN}{dy p_T dp_T d\phi}}{\int p_T dp_T d\phi \frac{dN}{dy p_T dp_T d\phi}} \equiv \{e^{in\phi}\},$$

$$V_n(p_T) = \textcolor{red}{v}_n(p_T) e^{in\Psi_n(p_T)} := \frac{\int d\phi e^{in\phi} \frac{dN}{dy p_T dp_T d\phi}}{\int d\phi \frac{dN}{dy p_T dp_T d\phi}} \equiv \{e^{in\phi}\}_{p_T}.$$

Together with the azimuthally averaged spectrum, these completely characterize the measurable single-particle information for that event:

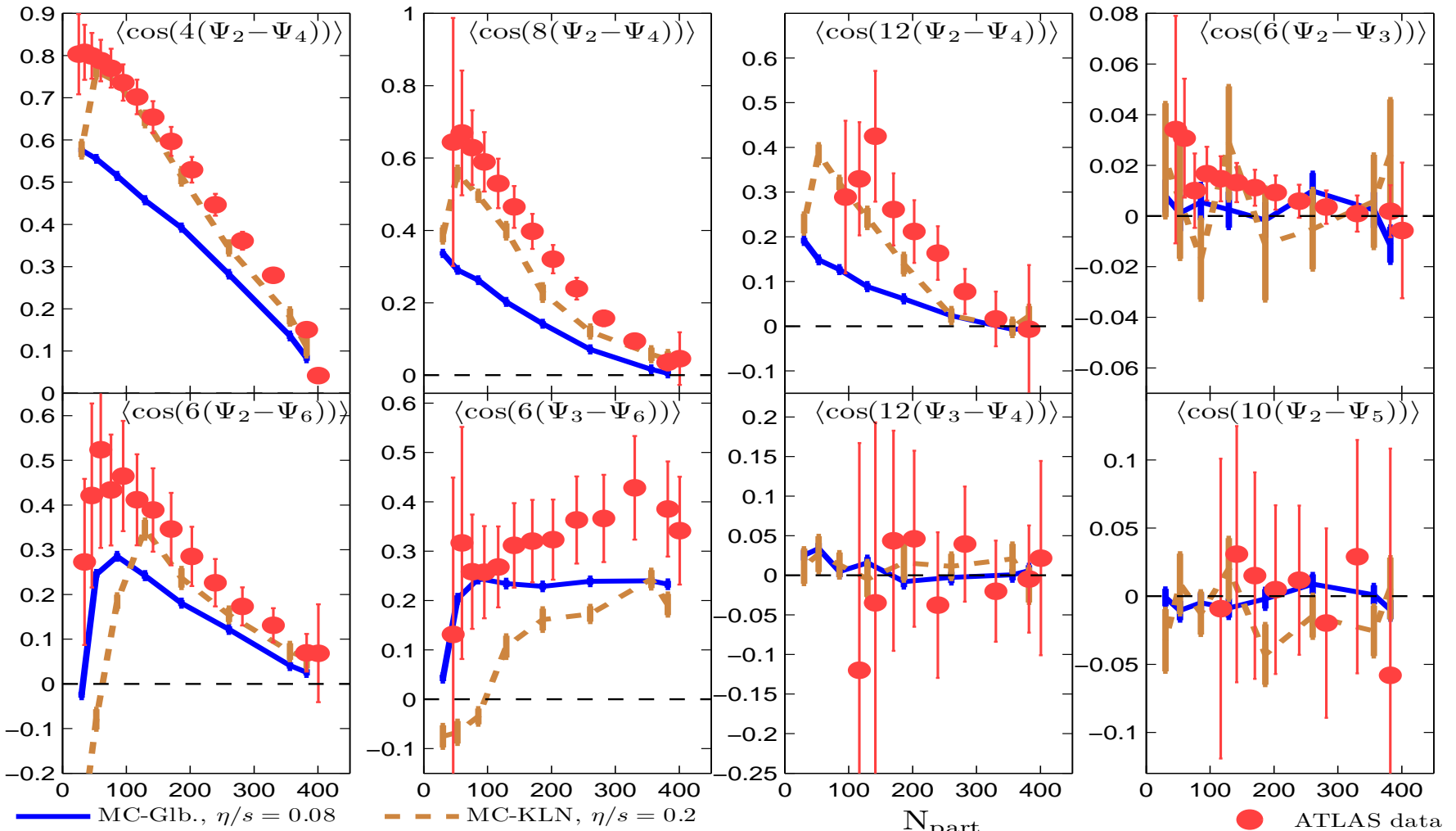
$$\begin{aligned} \frac{dN}{dy d\phi} &= \frac{1}{2\pi} \frac{dN}{dy} \left(1 + 2 \sum_{n=1}^{\infty} \textcolor{red}{v}_n \cos[n(\phi - \Psi_n)] \right), \\ \frac{dN}{dy p_T dp_T d\phi} &= \frac{1}{2\pi} \frac{dN}{dy p_T dp_T} \left(1 + 2 \sum_{n=1}^{\infty} \textcolor{red}{v}_n(p_T) \cos[n(\phi - \Psi_n(p_T))] \right). \end{aligned}$$

- Both the magnitude $\textcolor{red}{v}_n$ and the direction Ψ_n ("flow angle") depend on p_T .
- $\textcolor{red}{v}_n$, Ψ_n , $\textcolor{red}{v}_n(p_T)$, $\Psi_n(p_T)$ **all fluctuate from event to event**.
- $\Psi_n(p_T) - \Psi_n$ fluctuates from event to event.

Higher order event plane correlations in PbPb@LHC

Data: ATLAS Coll., J. Jia et al., Hard Probes 2012

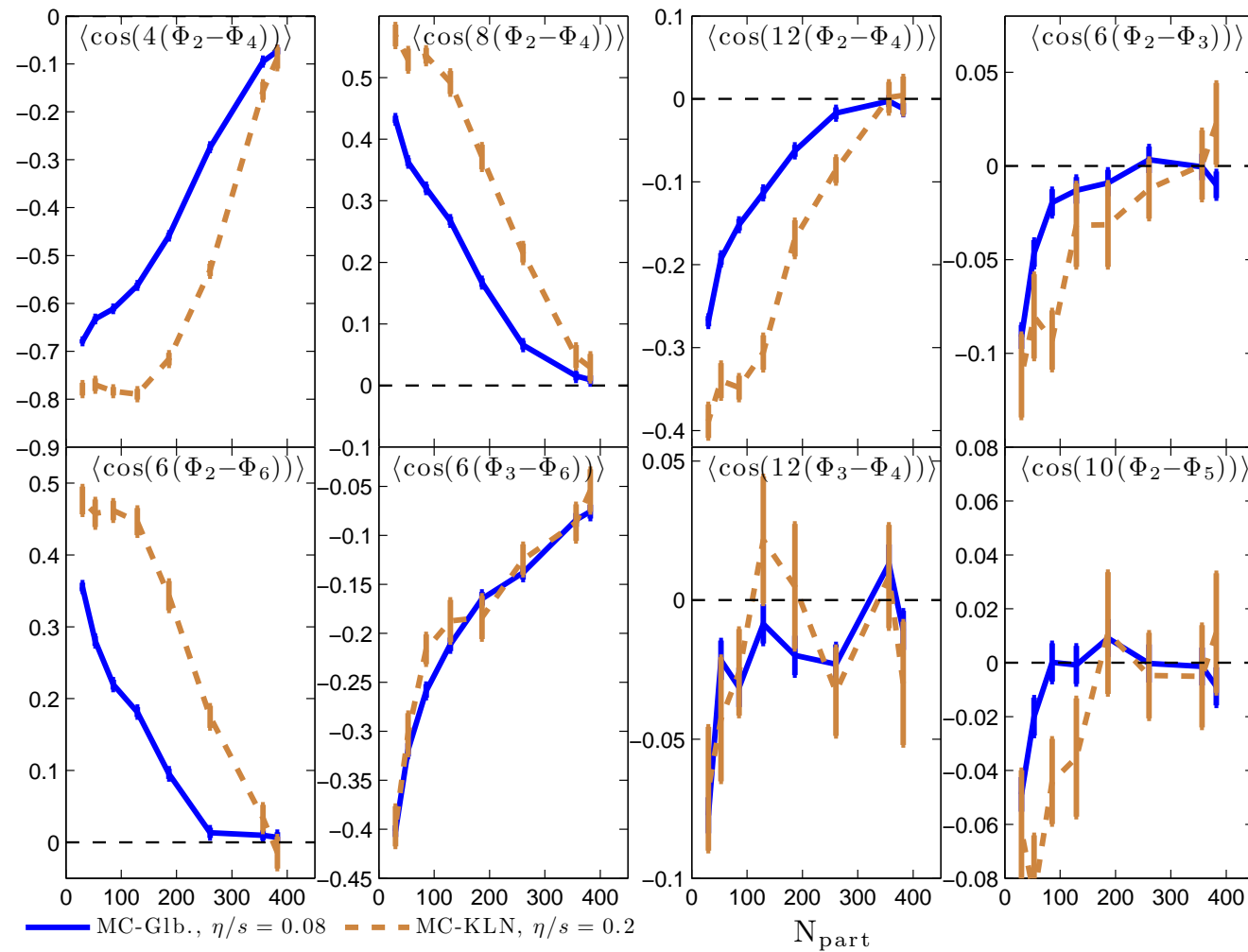
Event-by-event hydrodynamics: Zhi Qiu, UH, PLB 717 (2012) 261 ([VISH2+1](#))



VISH2+1 reproduces qualitatively the centrality dependence of all measured event-plane correlations

Higher order event plane correlations in PbPb@LHC

Zhi Qiu, UH, PLB 717 (2012) 261

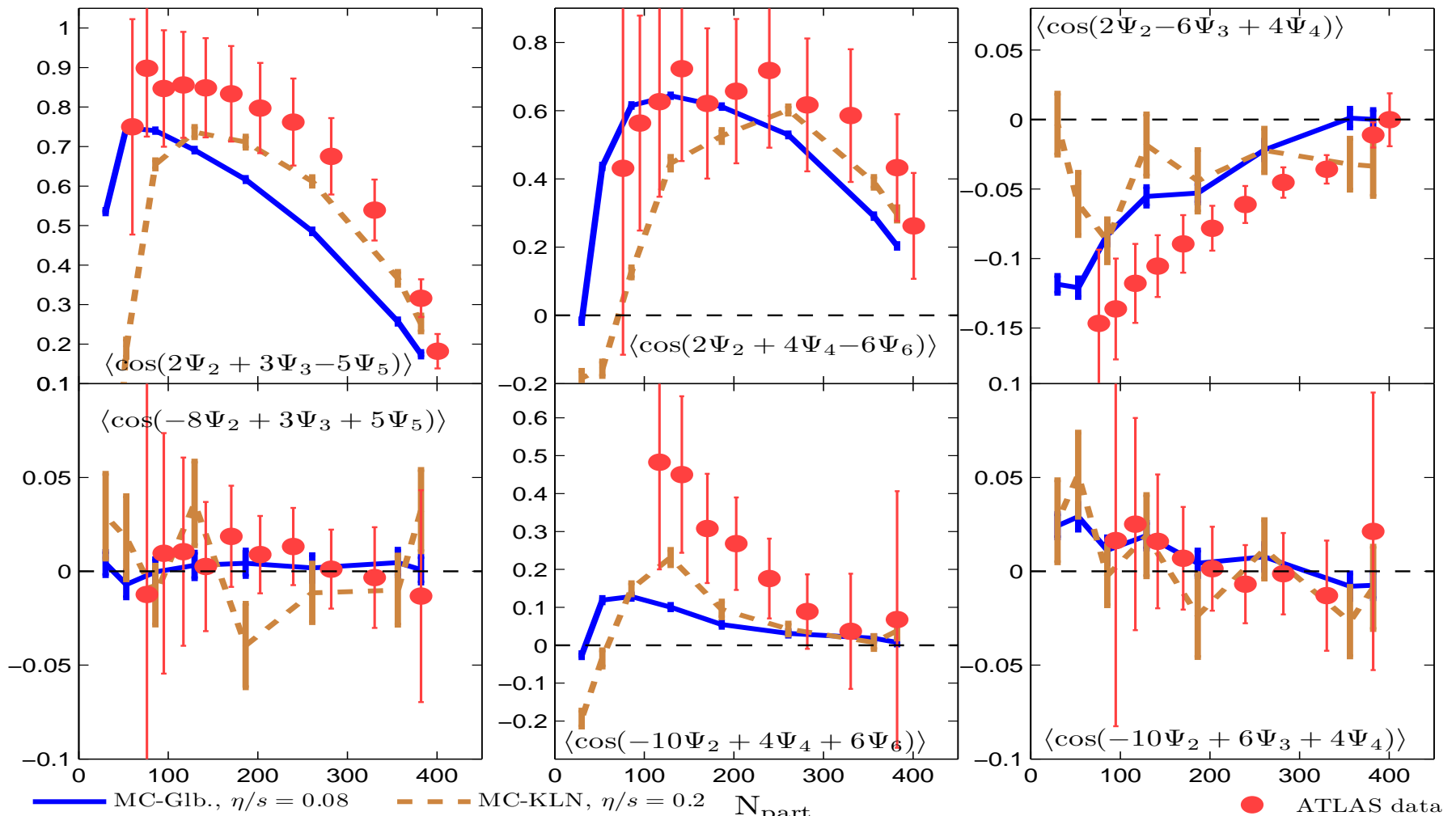


Initial-state participant plane correlations disagree with final-state flow-plane correlations
⇒ Nonlinear mode coupling through hydrodynamic evolution essential to describe the data!

Higher order event plane correlations in PbPb@LHC

Data: ATLAS Coll., J. Jia et al., Hard Probes 2012

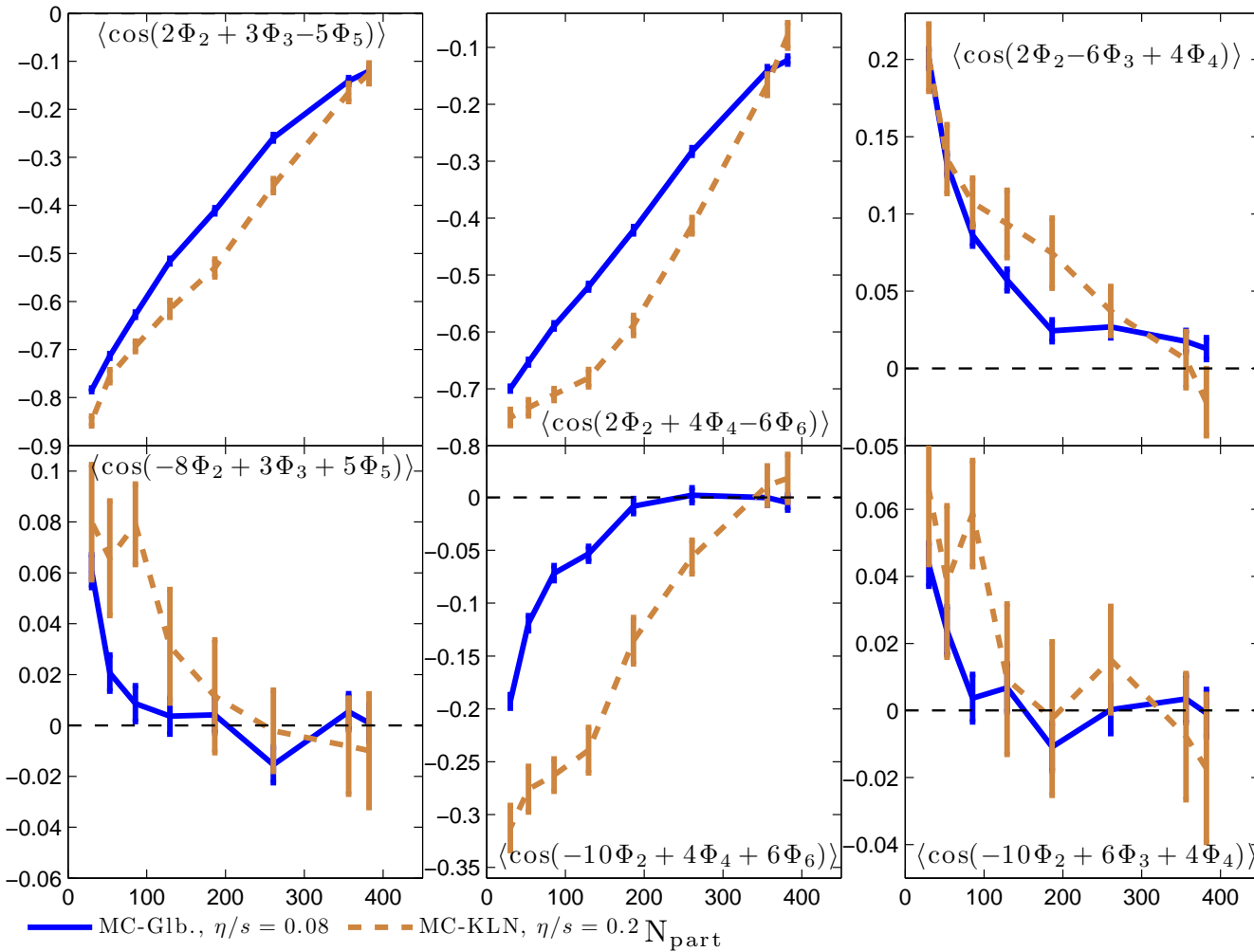
Event-by-event hydrodynamics: Zhi Qiu, UH, PLB 717 (2012) 261 ([VISH2+1](#))



VISH2+1 reproduces qualitatively the centrality dependence of all measured event-plane correlations

Higher order event plane correlations in PbPb@LHC

Zhi Qiu, UH, PLB 717 (2012) 261



Initial-state participant plane correlations disagree with final-state flow-plane correlations
⇒ Nonlinear mode coupling through hydrodynamic evolution essential to describe the data!

Test of factorization of two-particle spectra

Factorization $V_{n\Delta}(p_{T1}, p_{T2}) := \langle \{\cos[n(\phi_1 - \phi_2)]\}_{p_{T1}p_{T2}} \rangle \approx "v_n(p_{T1}) \times v_n(p_{T2})"$ was checked experimentally as a test of hydrodynamic behavior, and found to hold to good approximation.

Gardim et al. (PRC87 (2013) 031901) pointed out that event-by-event fluctuations break this factorization even if 2-particle correlations are exclusively due to flow.

They proposed to study the following ratio:

$$r_n(p_{T1}, p_{T2}) := \frac{V_{n\Delta}(p_{T1}, p_{T2})}{\sqrt{V_{n\Delta}(p_{T1}, p_{T1})V_{n\Delta}(p_{T2}, p_{T2})}} = \frac{\langle v_n(p_{T1})v_n(p_{T2})\cos[n(\Psi_n(p_{T1}) - \Psi_n(p_{T2}))] \rangle}{v_n[2](p_{T1})v_n[2](p_{T2})}.$$

Even in the absence of flow angle fluctuations, this ratio is < 1 due to v_n fluctuations (Schwarz inequality), except for $p_{T1} = p_{T2}$. But it additionally depends on flow angle fluctuations.

To assess what share of the deviation from 1 is due to flow angle fluctuations, we can compare with

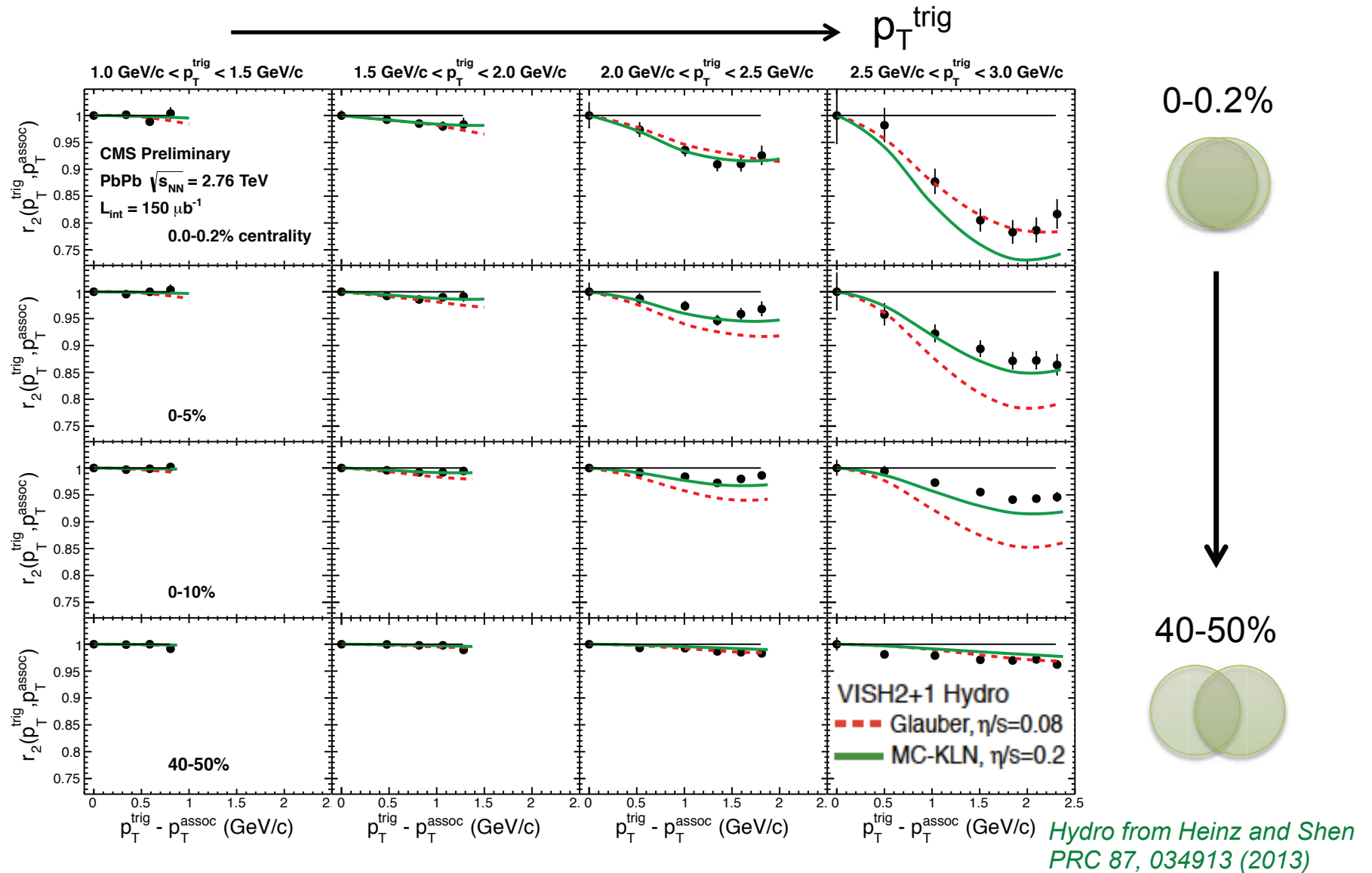
$$\tilde{r}_n(p_{T1}, p_{T2}) := \frac{\langle v_n(p_{T1})v_n(p_{T2})\cos[n(\Psi_n(p_{T1}) - \Psi_n(p_{T2}))] \rangle}{\langle v_n(p_{T1})v_n(p_{T2}) \rangle}$$

which deviates from 1 **only** due to flow angle fluctuations. Again, this ratio approaches 1 for $p_{T1} = p_{T2}$.

Gardim et al. studied r_n for ideal hydro; we have studied r_n and \tilde{r}_n for viscous hydro (UH, Z. Qiu, C. Shen, PRC87 (2013) 034913) and found that about half of the factorization breaking effects are due to flow angle fluctuations.

Breaking of factorization by e-by-e fluctuations: v_2

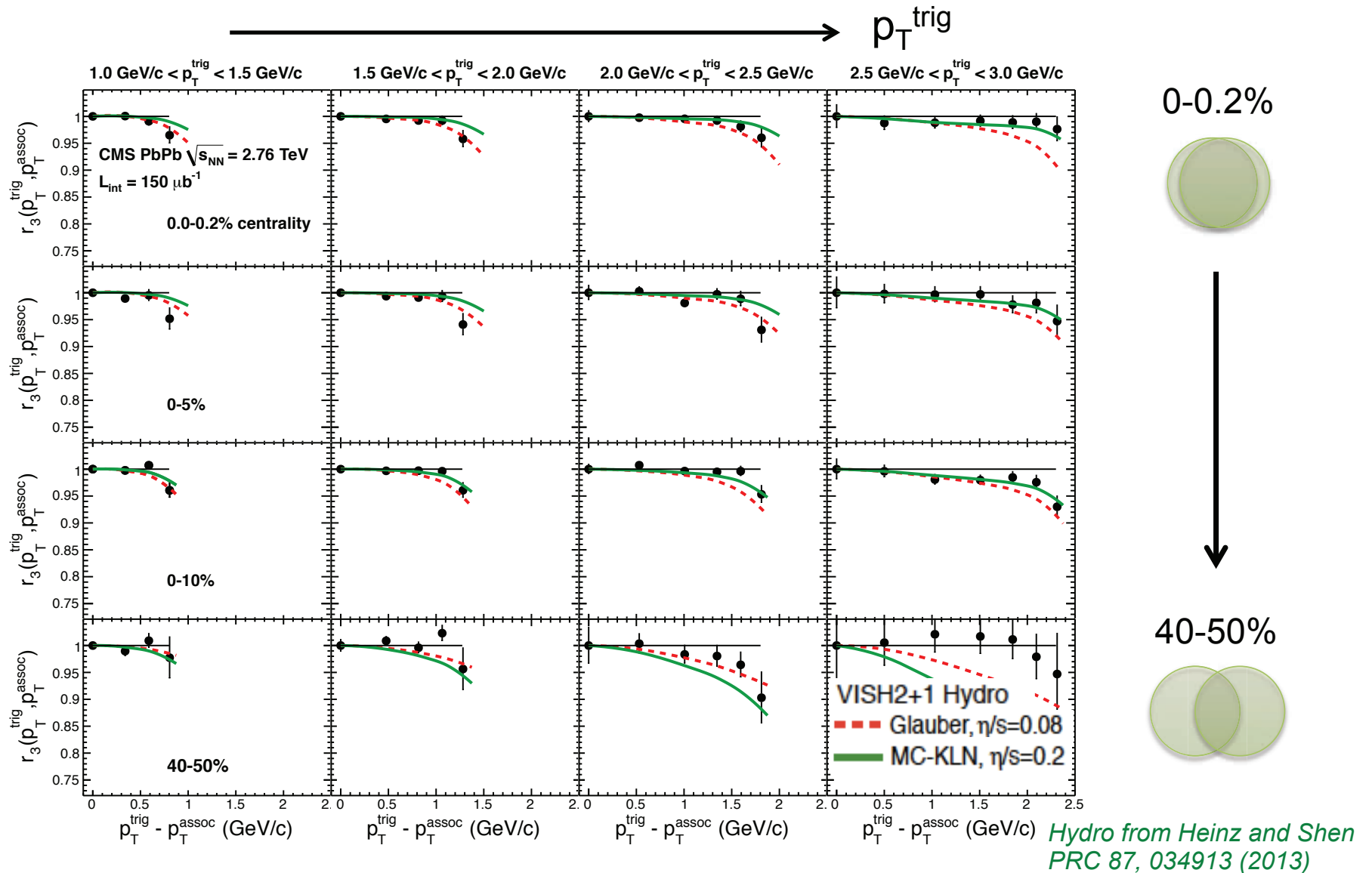
Data: Wei Li (CMS), Hard Probes 2013; Theory (prediction!): UH, Z. Qiu, C. Shen, PRC87 (2013) 034913



Factorization breaking effects appear to be suppressed by shear viscosity.

Breaking of factorization by e-by-e fluctuations: v_3

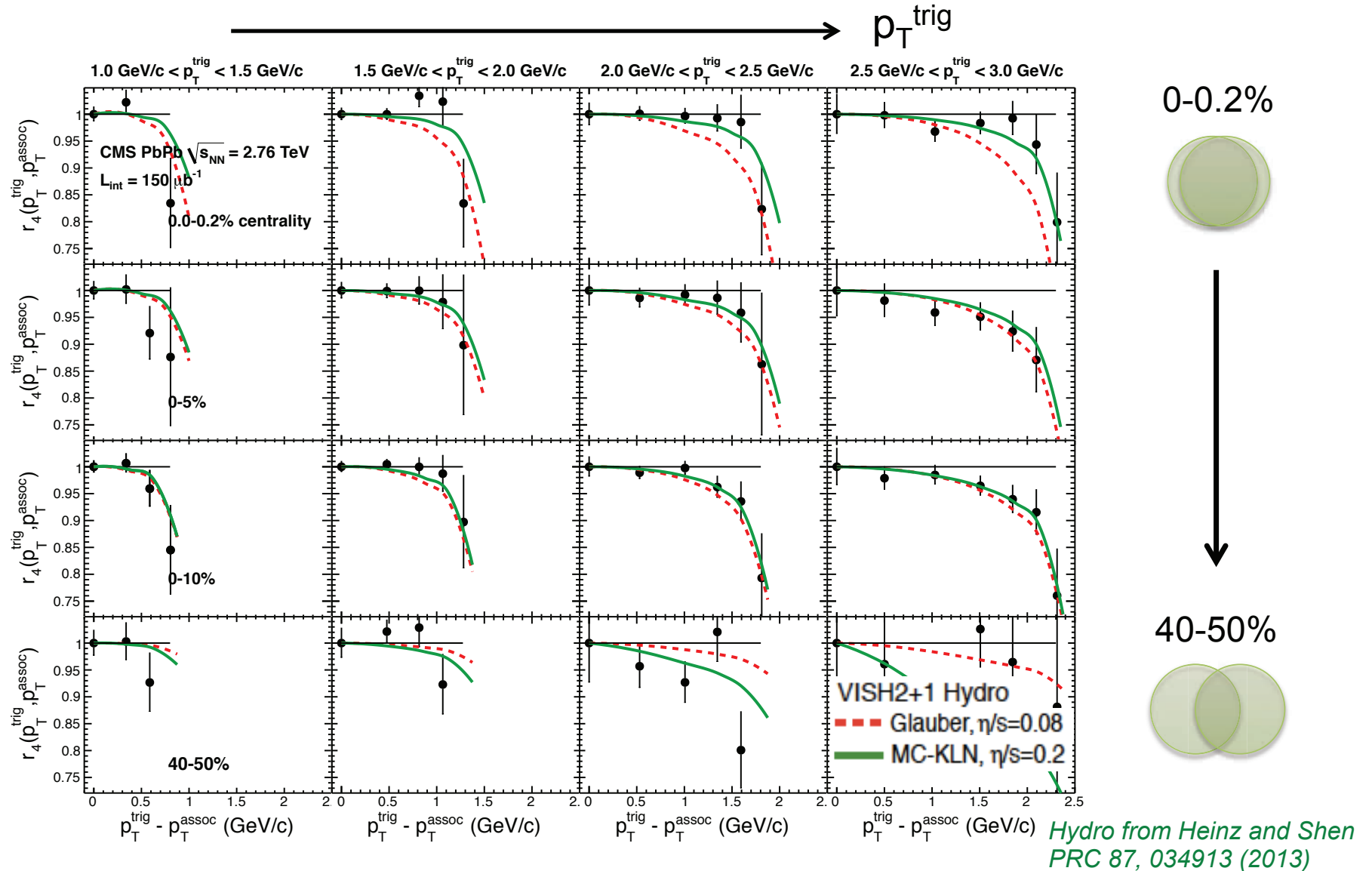
Data: Wei Li (CMS), Hard Probes 2013; Theory (prediction!): UH, Z. Qiu, C. Shen, PRC87 (2013) 034913



Factorization breaking effects appear to be larger for fluctuation dominated flow harmonics.

Breaking of factorization by e-by-e fluctuations: v_4

Data: Wei Li (CMS), Hard Probes 2013; Theory (prediction!): UH, Z. Qiu, C. Shen, PRC87 (2013) 034913



Hydrodynamics qualitatively, and even semi-quantitatively, predicts all observed factorization breaking effects below $p_T \sim 2.5 - 3$ GeV.

vaHydro: Viscous Anisotropic Hydrodynamics

D. Bazow, UH, M. Strickland, 1311.6720

Viscous Hydrodynamics Expansion

$$f(\tau, \mathbf{x}, \mathbf{p}) = \underbrace{f_{\text{eq}}(\mathbf{p}, T(\tau, \mathbf{x}))}_{\substack{\text{Isotropic in momentum space}}} + \delta f$$

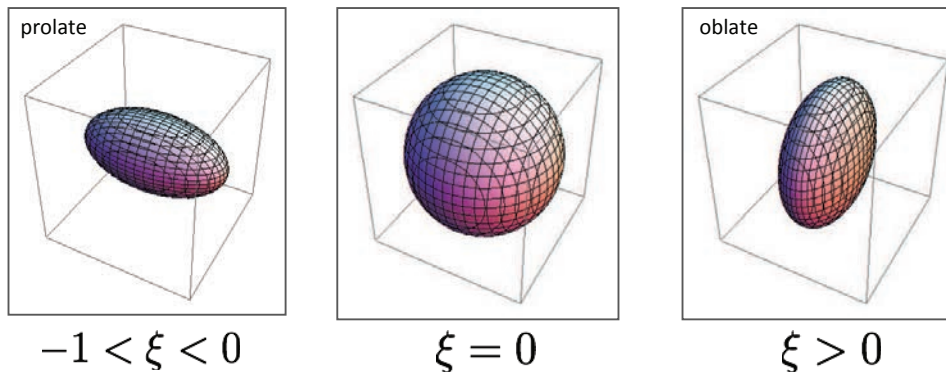
Anisotropic Hydrodynamics Expansion

$$f(\tau, \mathbf{x}, \mathbf{p}) = f_{\text{aniso}}(\mathbf{p}, \underbrace{\Lambda(\tau, \mathbf{x})}_{T_{\perp}}, \underbrace{\xi(\tau, \mathbf{x})}_{\text{anisotropy}}) + \tilde{\delta f}$$

→ “Romatschke-Strickland” form in LRF

$$f_{\text{aniso}}^{\text{LRF}} = f_{\text{iso}} \frac{\sqrt{\mathbf{p}^2 + \xi(\mathbf{x}, \tau)p_z^2}}{\Lambda(\mathbf{x}, \tau)}$$

$$\xi = \frac{\langle p_T^2 \rangle}{2\langle p_L^2 \rangle} - 1$$



Anisotropic hydrodynamics (AHYDRO) was developed by Strickland and Martinez, 1007.0889. It treats non-equilibrium (viscous) effects arising from a spheroidal deformation of the local momentum distribution exactly (i.e. non-perturbatively), but ignores other viscous corrections. vaHYDRO adds the remaining viscous corrections $\sim \tilde{\delta f}$ perturbatively, as usually done in other viscous hydrodynamic frameworks.

vaHydro Equations

Skipping over the gory details the final 14-moment approximation result is

$$\dot{\mathcal{N}} = -\mathcal{N}\theta - \boxed{\partial_\mu \tilde{V}^\mu} + \mathcal{C}.$$

[D. Bazow, U. Heinz, and MS, 1311.6720]

$$\begin{aligned} \dot{\mathcal{E}} + (\mathcal{E} + \mathcal{P}_\perp + \tilde{\Pi})\theta + (\mathcal{P}_L - \mathcal{P}_\perp) \frac{u_0}{\tau} + \boxed{u_\nu \partial_\mu \tilde{\pi}^{\mu\nu}} &= 0, \\ (\mathcal{E} + \mathcal{P}_\perp + \tilde{\Pi})\dot{u}_x + \partial_x(\mathcal{P}_\perp + \tilde{\Pi}) + u_x(\dot{\mathcal{P}}_\perp + \tilde{\Pi}) + (\mathcal{P}_\perp - \mathcal{P}_L) \frac{u_0 u_x}{\tau} - \boxed{\Delta^{1\nu} \partial^\mu \tilde{\pi}_{\mu\nu}} &= 0, \\ (\mathcal{E} + \mathcal{P}_\perp + \tilde{\Pi})\dot{u}_y + \partial_y(\mathcal{P}_\perp + \tilde{\Pi}) + u_y(\dot{\mathcal{P}}_\perp + \tilde{\Pi}) + (\mathcal{P}_\perp - \mathcal{P}_L) \frac{u_0 u_y}{\tau} - \boxed{\Delta^{2\nu} \partial^\mu \tilde{\pi}_{\mu\nu}} &= 0, \end{aligned}$$

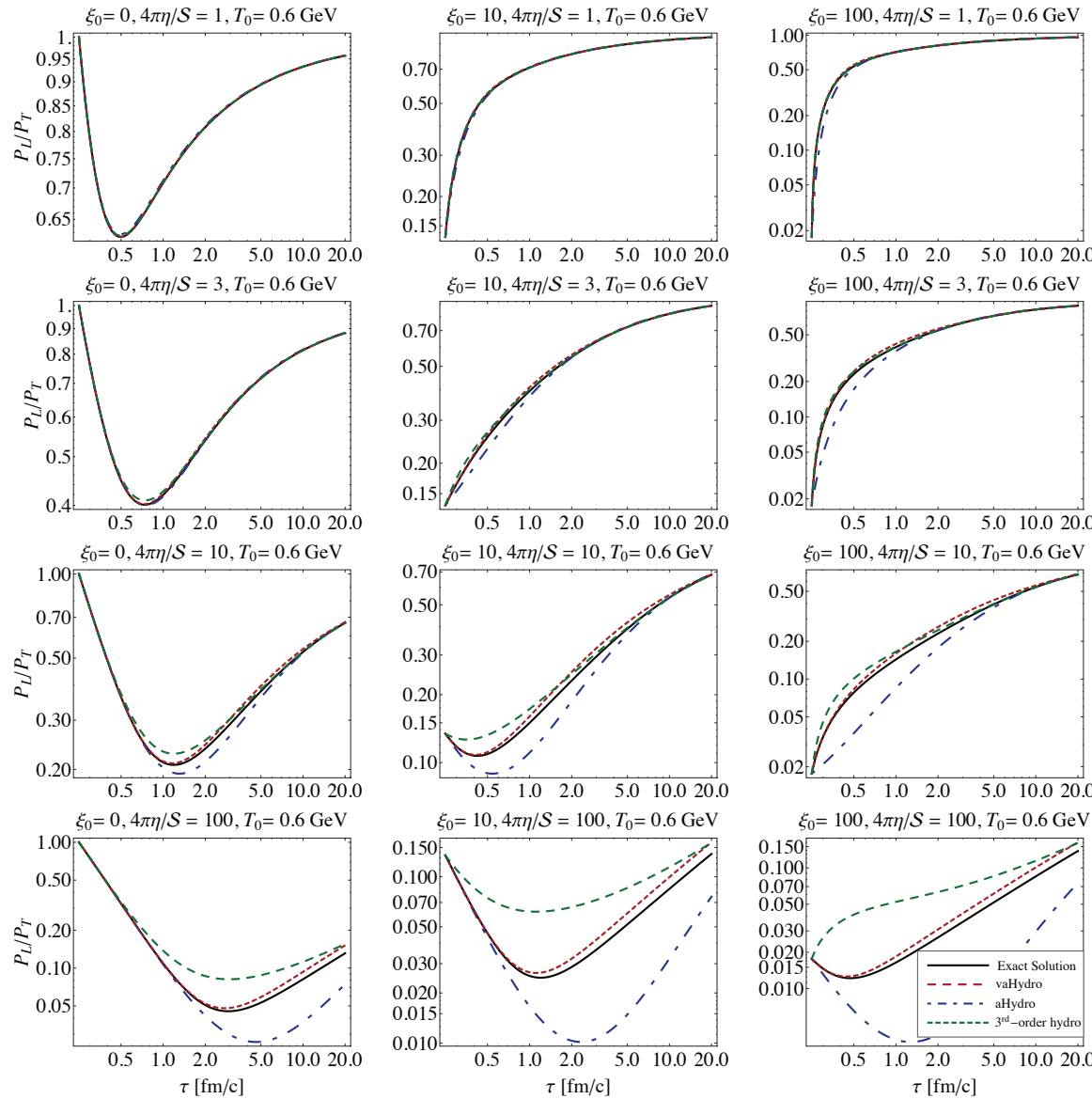
$$\begin{aligned} \dot{\tilde{\Pi}} &= -\frac{\dot{\tilde{\gamma}}_r^\Pi}{\tilde{\gamma}_r^\Pi} \tilde{\Pi} + \frac{1}{\tilde{\gamma}_r^\Pi} \mathcal{C}_{r-1} + \mathcal{W}_r + \mathcal{U}_r^{\mu\nu} \nabla_\mu u_\nu \\ &\quad + \lambda_{\Pi\pi}^r \tilde{\pi}^{\mu\nu} \sigma_{\mu\nu} + \tau_{\Pi V}^r \tilde{V}^\mu \dot{u}_\mu - \frac{1}{\tilde{\gamma}_r^\Pi} \nabla_\mu \left(\tilde{\gamma}_{r-1}^V \tilde{V}^\mu \right) - \delta_{\Pi\Pi}^r \tilde{\Pi} \theta \\ \dot{\tilde{V}}^{\langle\mu\rangle} &= -\frac{\dot{\tilde{\gamma}}_r^V}{\tilde{\gamma}_r^V} \tilde{V}^\mu + \frac{1}{\tilde{\gamma}_r^V} \mathcal{C}_{r-1}^{\langle\mu\rangle} + \mathcal{Z}_r^\mu - \tilde{V}^\nu \omega_\nu^\mu + \delta_{VV}^r \tilde{V}^\mu \theta - \Delta_\lambda^\mu \frac{1}{\tilde{\gamma}_r^V} \nabla_\nu \left(\tilde{\gamma}_{r-1}^\pi \tilde{\pi}^{\nu\lambda} \right) \\ &\quad + \tau_{q\Pi}^r \tilde{\pi}^{\mu\nu} \dot{u}_\nu + \lambda_{VV}^r \tilde{V}_\nu \sigma^{\nu\mu} + \tau_{q\Pi}^r \tilde{\Pi} \dot{u}^\mu + \ell_{q\Pi}^r \nabla^\mu \tilde{\Pi} + \tilde{\Pi} \mathcal{O}^\mu, \\ \dot{\tilde{\pi}}^{\langle\mu\nu\rangle} &= -\frac{\dot{\tilde{\gamma}}_r^\pi}{\tilde{\gamma}_r^\pi} \tilde{\pi}^{\mu\nu} + \mathcal{T}^{\langle\mu V^\nu\rangle} + \frac{1}{\tilde{\gamma}_r^\pi} \mathcal{C}_{r-1}^{\langle\mu\nu\rangle} + \mathcal{K}_r^{\mu\nu} + \mathcal{L}_r^{\mu\nu} + \mathcal{H}_r^{\mu\nu\lambda} \dot{z}_\lambda + \mathcal{Q}_r^{\mu\nu\lambda\alpha} \nabla_\lambda u_\alpha + \mathcal{X}_r^{\mu\nu\lambda} u^\alpha \nabla_\lambda z_\alpha \\ &\quad - 2\lambda_{\pi\pi}^r \tilde{\pi}_\alpha^{\langle\mu} \sigma^{\nu\rangle\alpha} + 2\tilde{\pi}^{\lambda\langle\mu} \omega_\lambda^{\nu\rangle} + 2\lambda_{\pi\Pi}^r \tilde{\Pi} \sigma^{\mu\nu} + 2\lambda_{\pi V}^r \nabla^{\langle\mu} \tilde{V}^{\nu\rangle} + 2\tau_{\pi V}^r \tilde{V}^{\langle\mu} \dot{u}^{\nu\rangle} - 2\delta_{\pi\pi}^r \tilde{\pi}^{\mu\nu} \theta. \end{aligned}$$

- Orange-boxed terms are new
- Dot indicates a convective derivative
- Complicated bits in last two equations correspond to dissipative “forces” and anisotropic transport coefficients

In 1311.6720 we simplified these equations for massless particles and (0+1)-d expansion with longitudinal boost-invariance and no transverse expansion. For this case the theory can be tested against an exact solution of the Boltzmann equation (Florkowski, Ryblewski, Strickland, PRC88 (2013) 024903).

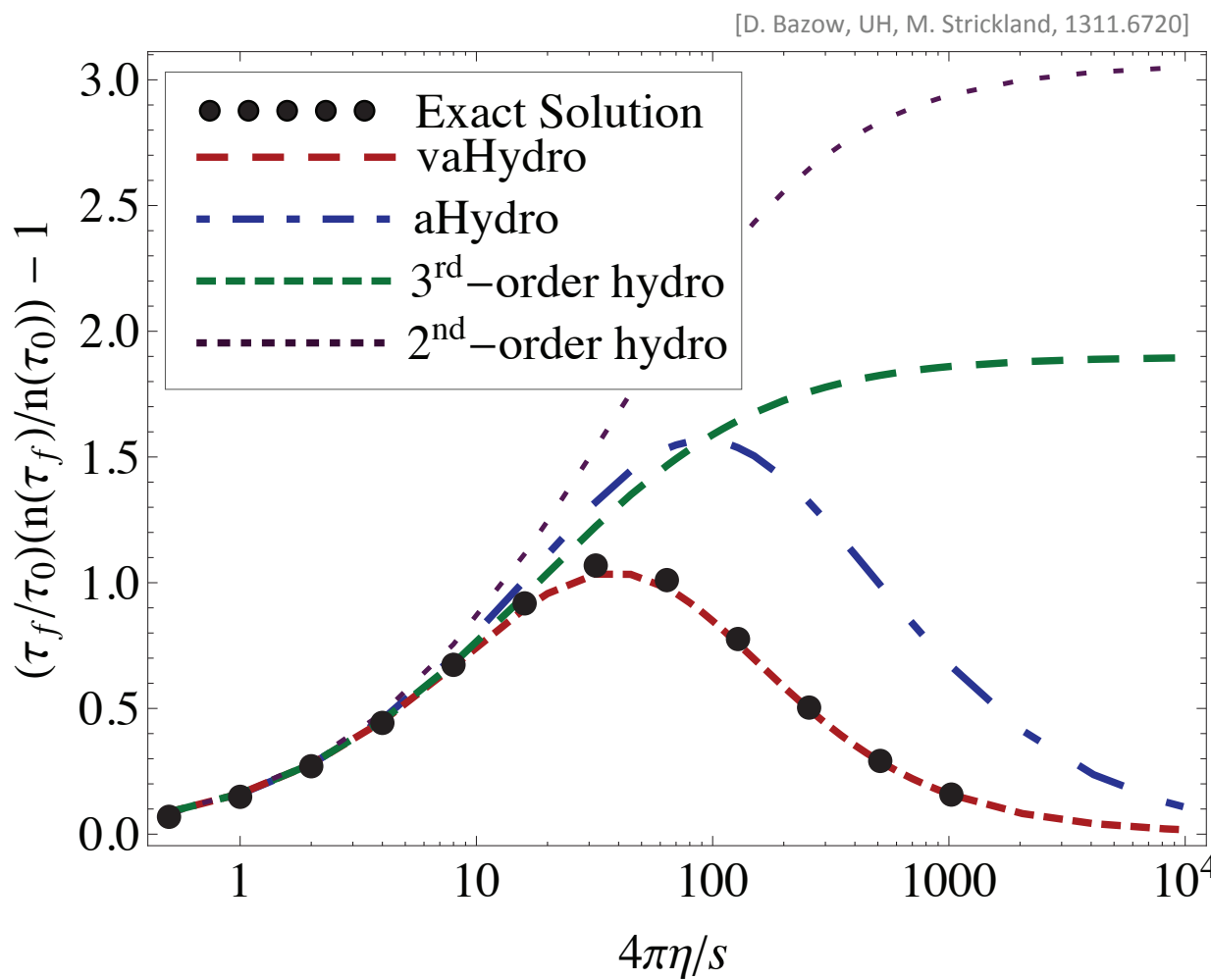
Pressure Ratio Comparisons

[D. Bazow, UH, M. Strickland, 1311.6720]



- Panels show ratio of longitudinal to transverse pressure
 - $T_0 = 600 \text{ MeV} @ \tau_0 = 0.25 \text{ fm/c}$
 - Left to right is increasing initial momentum-space anisotropy
 - Top to bottom is increasing η/S
 - Black line is the exact solution
 - Red dashed line is the aHydro approximation
 - Blue dot-dashed line is the vaHydro approximation
 - Green dashed line is a third-order Chapman-Enskog-like viscous hydrodynamics approximation
 - As we can see from these plots vaHydro does quite well indeed!
- [A. Jaiswal, 1305.3480]

Entropy Generation



- Entropy production vanishes in two limits: ideal hydrodynamics and free streaming
- For massless particles, number density is proportional to entropy density

In the (0+1)-d case, which maximizes the difference between longitudinal and transverse expansion rates and thus the P_T/P_L pressure anisotropy, VAHYDRO outperforms all other available approaches. We expect it to improve the validity of viscous hydrodynamics for heavy-ion collisions at early times.

Conclusions

- Quark-Gluon Plasma is by far the hottest and densest form of matter ever observed in the laboratory. Its properties and interactions are controlled by QCD, not QED.
- It is a **liquid** with almost **perfect fluidity**. Its specific shear viscosity at RHIC and LHC energies is

$$(\eta/s)_{QGP}(T_c < T < 2T_c) = \frac{2}{4\pi} \pm 50\%$$

This is significantly below that of any other known real fluid.

Precision comparison of harmonic flow coefficients at RHIC and LHC provides first serious indications for a moderate increase of the specific QGP shear viscosity between $2T_c$ and $3T_c$.

- **Viscous relativistic hydrodynamics** provides a quantitative description of QGP evolution.
- By coupling viscous fluid dynamics for the QGP stage to microscopic evolution models of the dense early pre-equilibrium and dilute late hadronic freeze-out stages, a **complete dynamical description** of the strongly interacting matter created in ultra-relativistic heavy-ion collisions has been achieved. This dynamical theory has made successful predictions for the first Pb+Pb collisions at the LHC that were quantitatively precise and non-trivial (in the sense that they disagreed with other predictions that were falsified by the data).
- The **Color Glass Condensate** theory (IP-Sat model) appears to give the correct spectrum of initial-state gluon field fluctuations.
- A **large set of flow fluctuation observables**, so far only partially explored, (over)constrains this initial fluctuation spectrum.

⇒ We are rapidly converging on the Standard Model for the Little Bang

Thanks to:

Dennis Bazow, Steffen Bass,
Scott Moreland, Zhi Qiu, Chun Shen,

Huichao Song, Mike Strickland

for their collaboration, to

Gabriel Denicol, Matt Luzum,

Bjoern Schenke, Jean-Yves Ollitrault

for many in-depth discussions, and to

Paul Sorensen

for letting me use some of his beautiful slides

Supplements

Single event anisotropic flow coefficients

In a single event, the specific initial density profile results in a set of complex, y - and p_T -dependent flow coefficients (we'll suppress the y -dependence):

$$V_n = \textcolor{red}{v}_n e^{in\Psi_n} := \frac{\int p_T dp_T d\phi e^{in\phi} \frac{dN}{dy p_T dp_T d\phi}}{\int p_T dp_T d\phi \frac{dN}{dy p_T dp_T d\phi}} \equiv \{e^{in\phi}\},$$

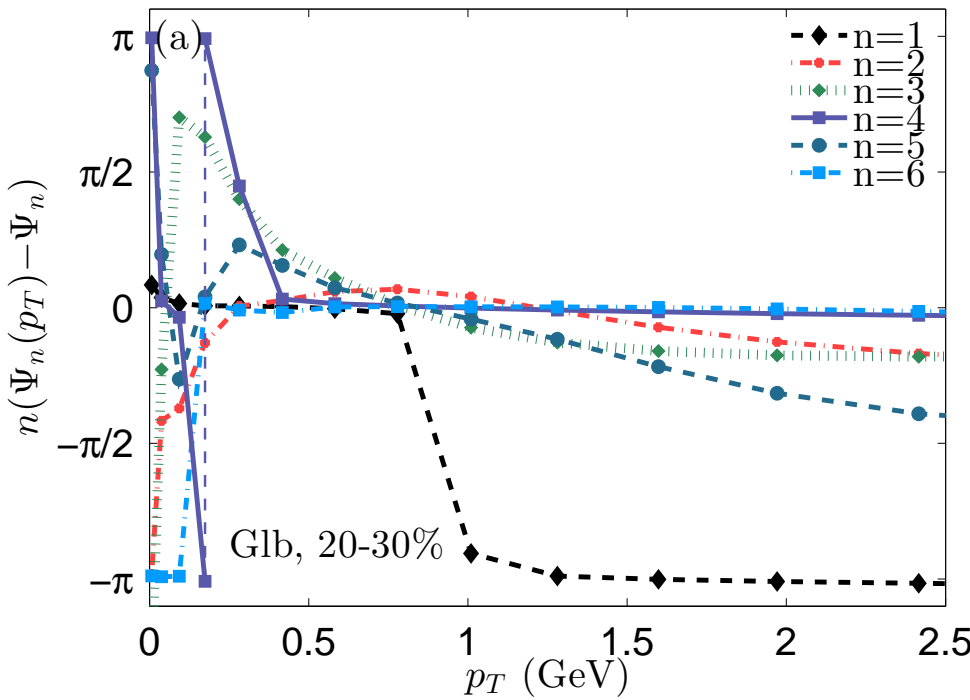
$$V_n(p_T) = \textcolor{red}{v}_n(p_T) e^{in\Psi_n(p_T)} := \frac{\int d\phi e^{in\phi} \frac{dN}{dy p_T dp_T d\phi}}{\int d\phi \frac{dN}{dy p_T dp_T d\phi}} \equiv \{e^{in\phi}\}_{p_T}.$$

Together with the azimuthally averaged spectrum, these completely characterize the measurable single-particle information for that event:

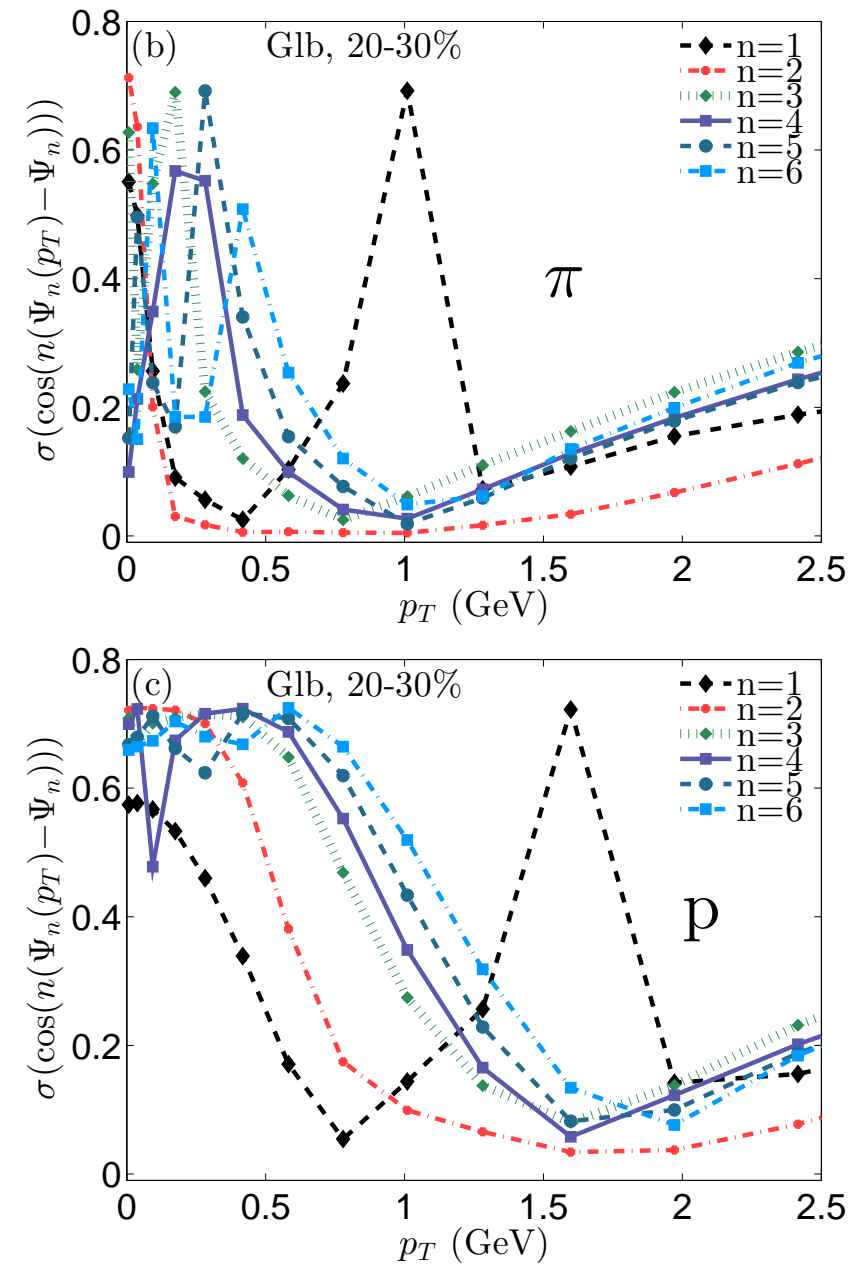
$$\begin{aligned} \frac{dN}{dy d\phi} &= \frac{1}{2\pi} \frac{dN}{dy} \left(1 + 2 \sum_{n=1}^{\infty} \textcolor{red}{v}_n \cos[n(\phi - \Psi_n)] \right), \\ \frac{dN}{dy p_T dp_T d\phi} &= \frac{1}{2\pi} \frac{dN}{dy p_T dp_T} \left(1 + 2 \sum_{n=1}^{\infty} \textcolor{red}{v}_n(p_T) \cos[n(\phi - \Psi_n(p_T))] \right). \end{aligned}$$

- Both the magnitude $\textcolor{red}{v}_n$ and the direction Ψ_n ("flow angle") depend on p_T .
- $\textcolor{red}{v}_n, \Psi_n, \textcolor{red}{v}_n(p_T), \Psi_n(p_T)$ **all fluctuate from event to event.**
- $\Psi_n(p_T) - \Psi_n$ fluctuates from event to event.

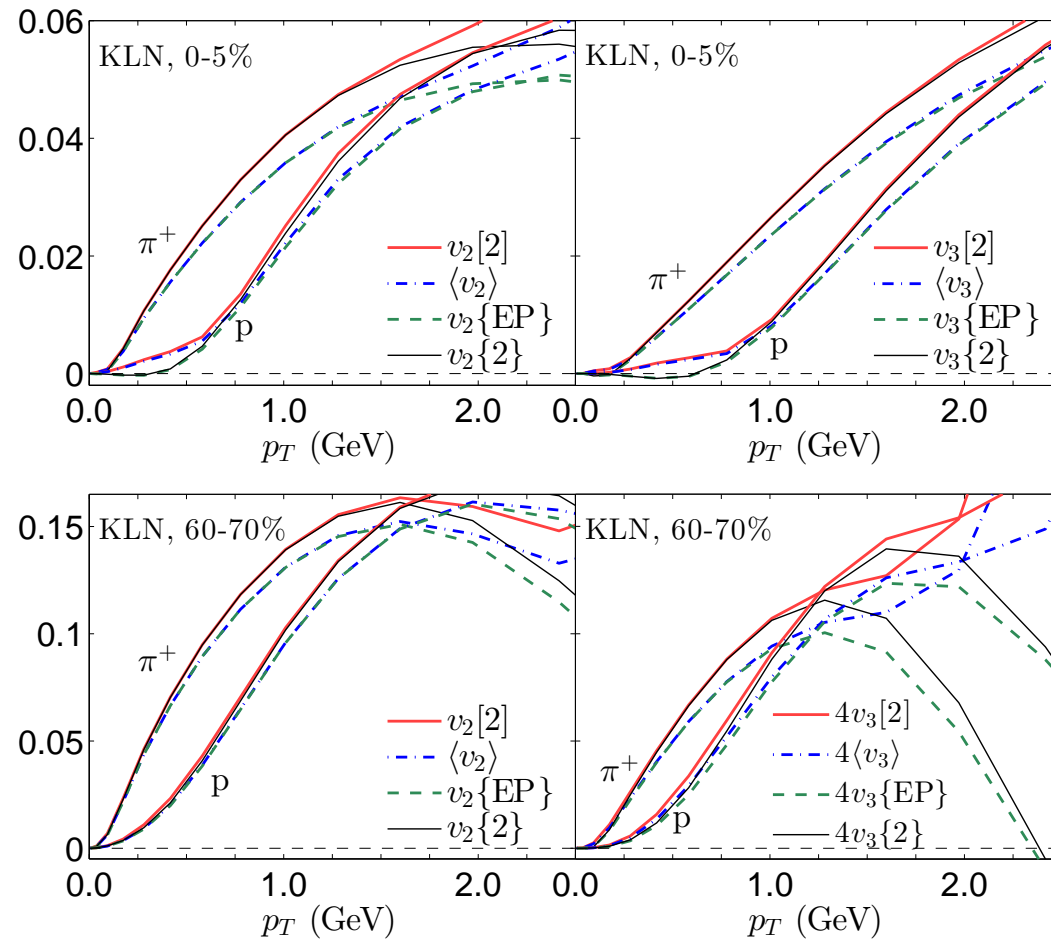
p_T -dependent flow angles and their fluctuations



- Except for directed flow ($n=1$), $\Psi_n(p_T) - \Psi_n$ fluctuates most strongly at low p_T
- Directed flow angle $\Psi_1(p_T)$ flips by 180° at $p_T \sim 1$ GeV for charged hadrons (pions) and at $p_T \sim 1.5$ GeV for protons (momentum conservation)



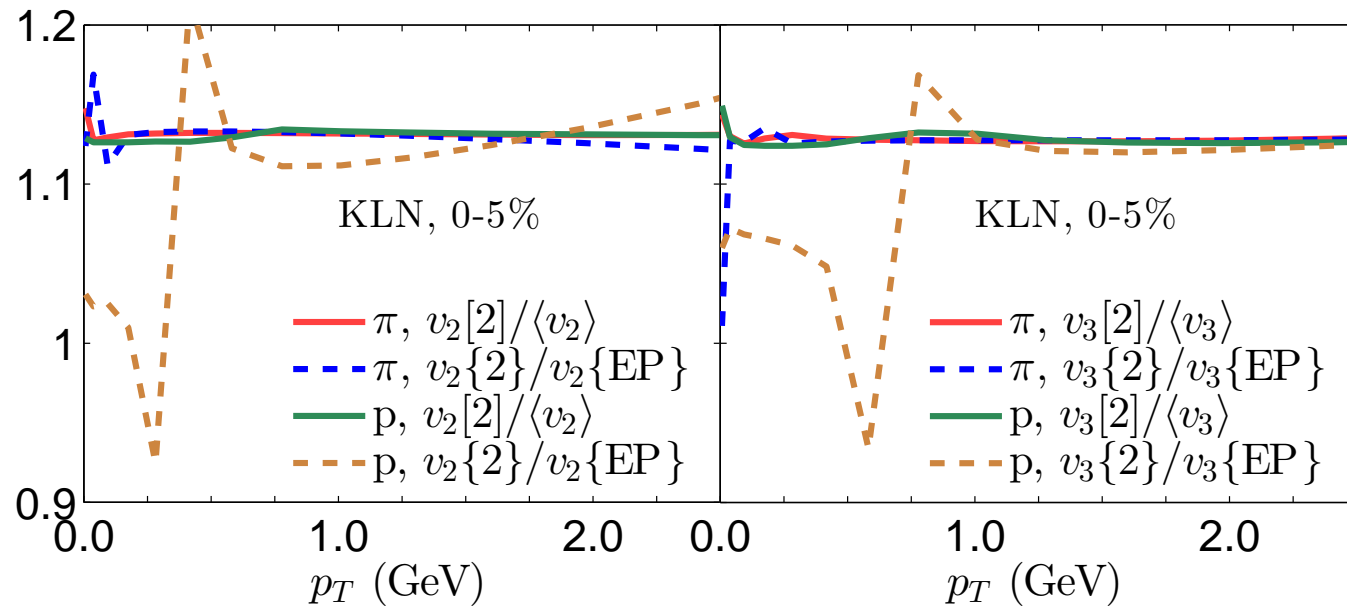
Elliptic and triangular flow comparison (I)



In central collisions, angular fluctuations suppress $v_n\{\text{EP}\}(p_T)$ and $v_n\{2\}(p_T)$ below the mean and rms flows at low p_T (clearly visible for protons)

This effect disappears in peripheral collisions, but a similar effect then takes over at higher p_T , for both pions and protons.

Elliptic and triangular flow comparison (II): v_n ratios



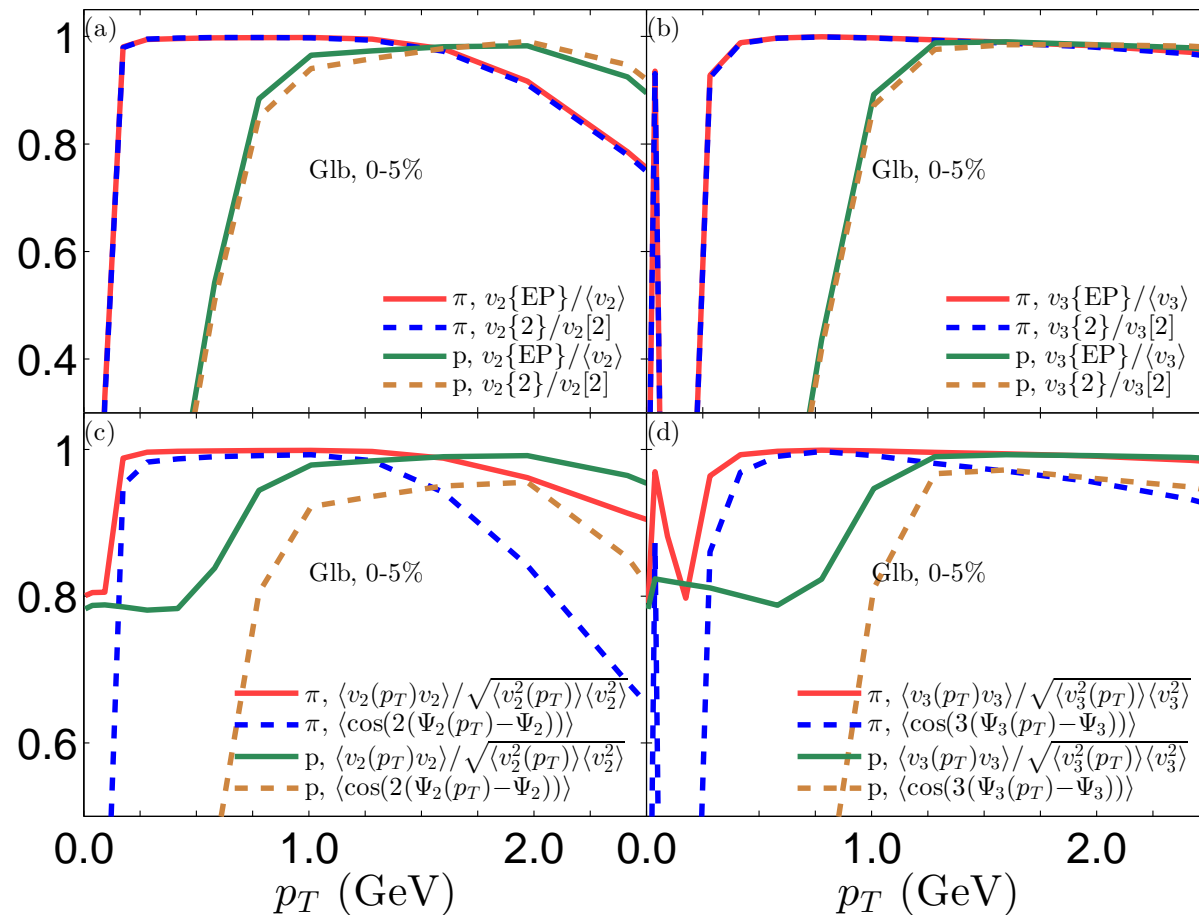
Except for where the numerator or denominator goes through zero, for central collisions these ratios are equal to $2/\sqrt{\pi} \approx 1.13$, independent of p_T . Expected if flow angles are randomly oriented (Bessel-Gaussian distribution for v_n , see Voloshin et al., PLB 659, 537 (2008)).

Not true in peripheral collisions, especially not for v_2 (Gardim et al., 1209.2323)

That this works even for $v_n\{2\}/v_n\{\text{EP}\}$ suggests an approximate factorization of angular fluctuation effects!

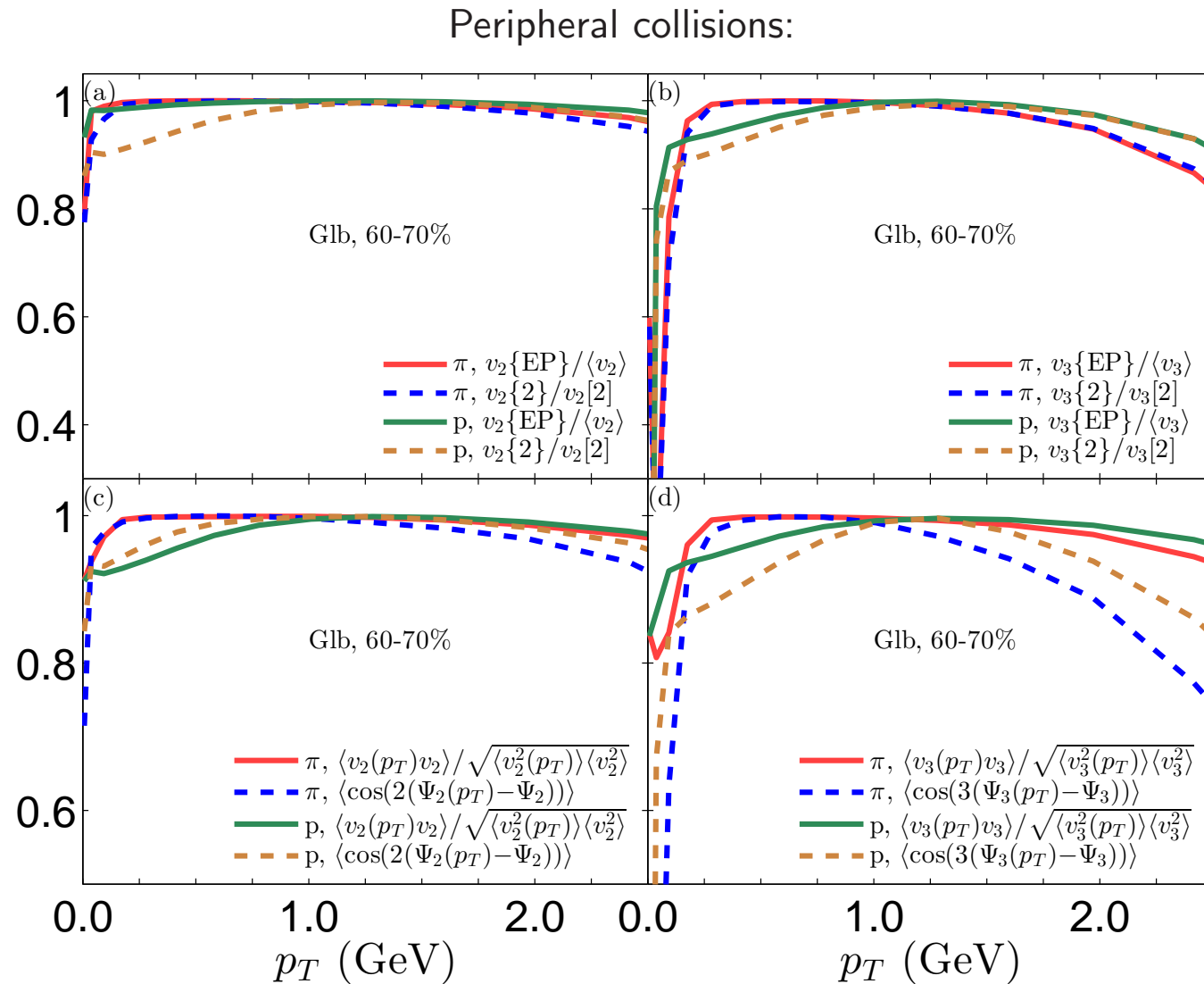
Elliptic and triangular flow comparison (III): v_n ratios

Central collisions:



- The angular fluctuation factor $\langle \cos[n(\Psi_n(p_T) - \Psi_n)] \rangle$ completely dominates the p_T -dependence of these ratios!
- Angular fluctuations have similar effect as poor event-plane resolution: they reduce v_n .
- Angular fluctuations are effective both at low and high p_T , but not at intermediate p_T .
- The window for seeing flow angle fluctuation effects at low p_T is smaller for pions than for protons.

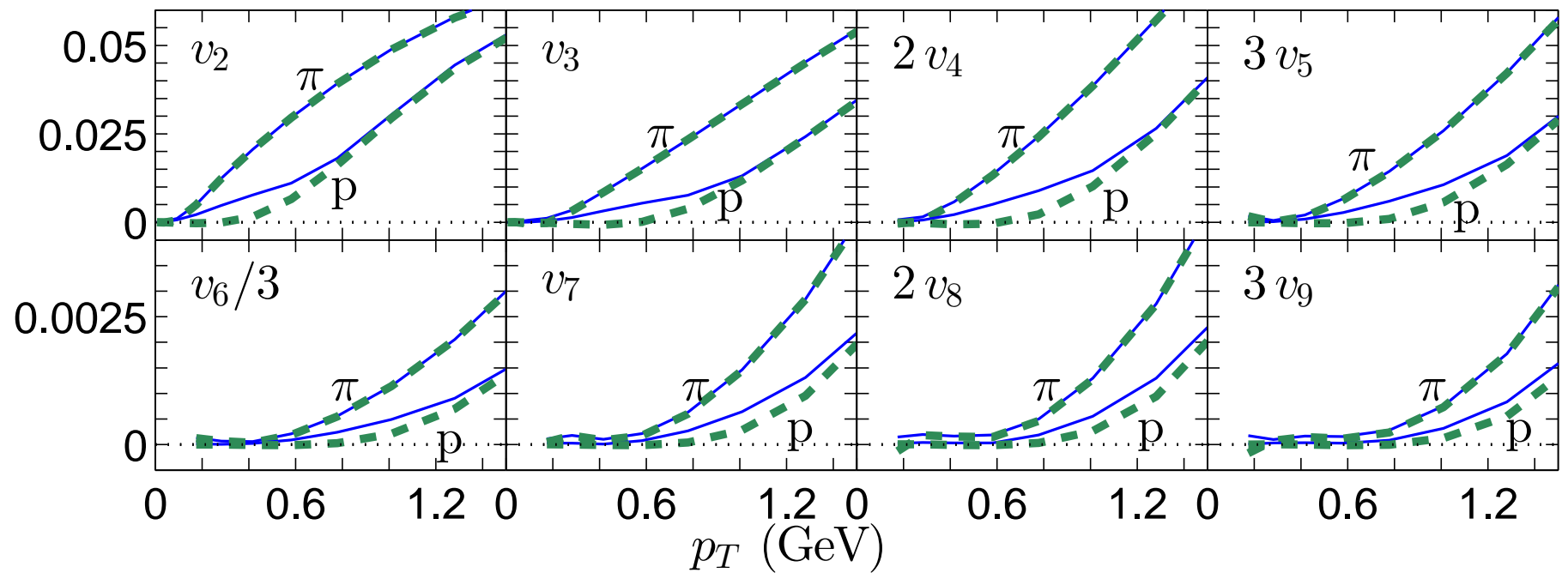
Elliptic and triangular flow comparison (IV): v_n ratios



The window for seeing flow angle fluctuation effects at low p_T closes in peripheral collisions.

Flow angle fluctuation effects for higher order $v_n(p_T)$

Central collisions; solid: $\langle v_n(p_T) \rangle$; dashed: $v_n\{\text{EP}\}(p_T)$:



As harmonic order n increases, suppression of $v_n\{\text{EP}\}(p_T)$ (or $v_n\{2\}(p_T)$) from flow angle fluctuations for protons gets somewhat weaker but persists to larger p_T .

Conclusions

- Both the magnitudes v_n and the flow angles Ψ_n depend on p_T and fluctuate from event to event.
- In each event, the “ p_T -averaged” (total-event) flow angles Ψ_n are identical for all particle species, but their p_T distribution differs from species to species.
- The mean v_n values and their p_T -dependence at RHIC and LHC have already been shown to put useful constraints on the QGP shear viscosity and its temperature dependence (see next talk by B. Schenke)
- **The effects of v_n and Ψ_n fluctuations can be separated experimentally by studying different V_n measures based on two-particle correlations.**
- Flow angle correlations are a powerful test of the hydrodynamic paradigm and will help to further constrain the spectrum of initial-state fluctuations and QGP transport coefficients.
- Studying event-by-event fluctuations of the anisotropic flows v_n and their flow angles Ψ_n as functions of p_T , as well as the correlations between different harmonic flows (both their magnitudes and angles), provides a rich data base for identifying the **“Standard Model of the Little Bang”**, by pinning down its initial fluctuation spectrum and its transport coefficients.